CUKUROVA UNIVERSITY

INSTITUTE OF NATURAL AND APPLIED SCIENCES

MSc THESIS

Design and Power Quality Improvement of a Grid Connected Hybrid PV System

Batuhan GÜZEY

Electrical and Electronics Engineering Department

December, 2023

CUKUROVA UNIVERSITY

INSTITUTE OF NATURAL AND APPLIED SCIENCES

MSc THESIS APPROVAL

Design and Power Quality Improvement of a Grid Connected Hybrid PV System

---

Batuhan GÜZEY

Electrical and Electronics Engineering Department

This Master's Thesis was evaluated by the following Jury Members on 29/12/2023 and was approved by unanimity / majority of votes.

Jury : Prof. Dr. Ahmet TEKE (Advisor) ……

: Asst. Prof. Dr. Oğuzhan TİMUR ……

: Asst. Prof. Dr. Özgür ÇELİK ……

This Thesis was written in the Department of Electrical and Electronics Engineering, Institute of Natural and Applied Sciences.

Thesis Number:

Prof. Dr. Sadık DİNÇER
Director
Institute of Natural and Applied Sciences

Note: The usage of the presented specific declarations, tables, figures, and photographs either in this thesis or in any other reference without citation is subject to "The law of Arts and Intellectual Products" number of 5846 of Turkish Republic

CONTENTS

ABSTRACT I
ÖZ II
GENİŞLETİLMİŞ ÖZET III
ACKNOWLEDGEMENTS VII
LIST OF TABLES VIII
LIST OF FIGURES IX
SYMBOLS AND ABBREVIATIONS XII
1. INTRODUCTION 1
1.1. Statement of Problem and Research Motivation 1
1.2. Objective and Outline of the Thesis 4
1.3. Contributions of Thesis 6
1.4. Summary 6
2. LITERATURE REVIEW 7
2.1. Renewable Energy 7
2.2. Overview of Photovoltaic Technologies 13
2.2.1. First Generation PV Cells 15
2.2.2. Second Generation PV Cells 16
2.2.3. Third Generation PV Cells 17
2.2.4. Fourth Generation PV Cells 19
2.2.5. Equivalent Circuit and Mathematical Expression 20
2.3. Grid Connection Standards 23
2.4. Switched Mode DC-DC Converter 24
2.4.1. Classification of DC-DC Converter 25
2.4.2. Boost Converter 27
2.4.3. Bidirectional Buck Boost Converter 29
2.5. Maximum Power Point Tracking Methodologies 32
2.5.1. Perturb and Observe Method 34
2.5.2. Incremental Conductance Method 36
2.5.3. Artificial Neural Network Method 39
2.6. DC/AC Inverter 41
2.7. LCL Filter 44
2.8. Phase Locked Loop 46
2.9. Summary 46
3. DESIGN STAGE FOR OVERALL SYSTEM 47
3.1. PV Array Parameters 48

3.2. Boost Converter and Parameter Calculation 50
3.3. Configuration of MPPT Algorithms 52
3.3.1. Design of a P&O MPPT 52
3.3.2. Design of an INC MPPT 53
3.3.3. Design of an ANN MPPT 53
3.3.4. Recommended Technique Hybrid MPPT: Combination of P&O, INC and ANN 55
3.4. Battery Energy Storage System 57
3.5. Energy Management System 61
3.6. Grid Connected Inverter and Control 61
3.7. Harmonic Mitigation with Two Mode LCL Filter 64
3.8. Summary 65
4. RESULTS AND DISCUSSIONS 67
4.1. Simulation Outcomes at 1000 W/m2 with P&O 67
4.2. Simulation Outcomes at 1000 W/m^2 with INC 70
4.3. Simulation Outcomes at 1000 W/m^2 with ANN 73
4.4. Simulation Outcomes at 800 W/m^2 with P&O 75
4.5. Simulation Outcomes at 800 W/m^2 with INC 78
4.6. Simulation Outcomes at 800 W/m^2 with ANN 80
4.7. Simulation Outcomes at 600 W/m^2 with P&O 83
4.8. Simulation Outcomes at 600 W/m^2 with INC 85
4.9. Simulation Outcomes at 600 W/m^2 with ANN 88
4.10. Recommended Model: Using Hybrid Mode MPPT to Increase Efficiency 90
4.11. Summary 92
5. CONCLUSIONS 93
REFERENCES 95
CURRICULUM VITAE 105

CUKUROVA UNIVERSITY

INSTITUTE OF NATURAL AND APPLIED SCIENCES

MSc THESIS

Design and Power Quality Improvement of a Grid Connected Hybrid PV System

Batuhan GÜZEY

Advisor: Prof. Dr. Ahmet TEKE

Department of Electrical and Electronics Engineering

ABSTRACT

Renewable energy sources (RES) are critical to meet energy demand in the changing and developing world. Among these resources, one of the most invested areas is solar energy. Photovoltaic (PV) panels are devices that convert radiation from the sun into electricity. Temperature and radiation parameters are used to generate electricity. Therefore, the produced power varies under bad weather conditions. Maximum power point tracking (MPPT) algorithms are used with the PV system to prevent power variability. In addition, battery-supported designs are utilized to ensure power continuity at night and keep the system running. The aim of this study is to design a hybrid PV system with grid connected and battery-supported. Moreover, in this thesis has been selected the most efficient method among the implemented tracking algorithms. Perturb&Observe (P&O), Incremental Conductance (INC), Artificial Neural Network (ANN) methods are applied respectively. The ranges in which these three tracking algorithms perform the best results are combined and the hybrid MPPT is designed. The system outcomes is tested at 1000-800-600 W/m^2 irradiance levels in MATLAB/SIMULINK program. Moreover, the battery energy storage system (BESS) has been developed to ensure power continuity. Since the powers of PV and BESS are different from each other, it has been determined that total harmonic distortion (THD) increases when the system is in night mode. To solve this problem and improve power quality, two mode LCL filter design has been performed. The system charges the battery while in daytime mode, and the daytime mode LCL filter is activated. When the system is in night mode, the battery is discharged and the night mode LCL filter is activated. Thanks to these designs, the THD value has been significantly reduced and the most efficient MPPT algorithm has been proposed. When the results are compared, the THD value obtained at 4.8% level while using single mode LCL filter. This value is decreased to 3.2% in two mode LCL filter application. In addition, according to the test results, when ANN MPPT is operated, 97.5% efficiency is observed at low irradiance. In the circuit operated with high efficiency, the DC link voltage has been become more uniform, smoothness.

Keywords: Grid Connected PV System, Battery Energy Storage System, MPPT with ANN, Power Quality Improvement.

ÇUKUROVA ÜNİVERSİTESİ
FEN BİLİMLERİ ENSTİTÜSÜ

YÜKSEK LİSANS TEZİ

Şebeke Bağlantılı Hibrit Fotovoltaik bir Sistemin Tasarımı ve Güç Kalitesinin İyileştirilmesi

Batuhan GÜZEY

Danışman: Prof. Dr. Ahmet TEKE

Elektrik Elektronik Mühendisliği Anabilim Dalı

ÖZ

Değişen ve gelişen dünyada enerji talebini karşılamak için yenilenebilir enerji kaynakları kritik öneme sahiptir. Bu kaynaklar arasında en çok yatırım alanlardan biri ise güneş enerjisidir. Fotovoltaik (FV) paneller güneşten gelen ışınımı elektriğe dönüştüren cihazlardır. Elektrik üretmek için sıcaklık ve ışınım parametreleri kullanılır. Bu yüzden, kötü hava şartlarında üretilen güç, değişkenlik gösterir. Güçte oluşan değişkenliği önlemek için FV sistemi ile maksimum güç noktası izleme (MGNİ) algoritmaları kullanılmaktadır. Ayrıca, gece vaktinde güç sürekliliğini sağlamak ve sistemleri devam ettirmek için batarya destekli tasarımlar kullanılmaktadır. Bu çalışmanın amacı, şebeke bağlantılı ve batarya destekli bir hibrit FV sistem tasarlamak ve uygulanan MGNİ algoritmaları arasında en verimli olanı seçmektir. Çalışmada sırasıyla Dürt & Gözle, Artımlı İletkenlik, Yapay Sinir Ağı (YSA) metotları uygulanmıştır. Sonrasında bu üç yöntemin en iyi performans gösterdikleri aralıklar birleştirilip Hibrit MGNİ yöntemi tasarlanmıştır. Sistem sonuçları sırasıyla 1000-800-600 W/m^2 ışınım seviyelerinde ve MATLAB/SIMULINK programında test edilmiştir. Bunların yanı sıra, güç sürekliliğini sağlamak için batarya enerji depolama sistemi (BEDS) geliştirilmiştir. FV ve BEDS'nin güçleri birbirlerinden farklı olduğundan sistem gece modundayken toplam harmonik bozulmasının (THB) yükseldiği tespit edilmiştir. Problemi çözümlemek ve güç kalitesini arttırmak amacıyla iki modlu LCL filtre tasarımı yapılmıştır. Sistem gündüz modundayken bataryayı şarj eder, gündüz modu için tasarlanan LCL filtre aktif olur. Sistem gece modundayken batarya deşarj olur ve gece modu LCL filtresi aktif olur. Bu tasarımlar sayesinde THB değeri oldukça azalmış ve en verimli MGNİ yöntemi önerilmiştir. Sonuçlar karşılaştırıldığında tek modlu LCL filtre kullanılırken THB değerinin 4.8% seviyelerinde elde edildiği görülmektedir. Bu değer iki modlu LCL filtre uygulamasında 3.2%'ye düşürülmüştür. Ek olarak, test sonuçlarına göre, YSA MGNİ kullanıldığında, düşük ışımalarda 97.5% verim gözlemlenmiştir. Yüksek verimle çalıştırılan devrede, DC bağlantı voltajı daha düzgün, pürüssüz hale getirilmiştir.

Anahtar Kelimeler: Şebeke Bağlantılı FV Sistem, Batarya Enerji Depolama Sistemi, YSA ile MGNİ, Güç Kalitesi Arttırma.

GENİŞLETİLMİŞ ÖZET

Geçmişten günümüze kadar gelen sürede enerjiye olan talep toplumların en temel ihtiyaçlarında biri haline gelmiştir. İhtiyaç olan enerji eskiden yenilenemeyen enerji türlerinden karşılanmaktaydı. Bu türler, fosil yakıtlar olarak da adlandırılabilir. Kömür, petrol, doğalgaz kullanarak enerji üretmek yenilenemeyen enerji kaynaklarına örnek olarak verilebilir.

Fosil yakıtlarda enerji üretirken çevreye zararlı gazlar yayılır bu durum küresel ısınmaya yol açar, doğada bulunan karbondioksit oranı arttır, oksijen oranının azalmasına neden olur, uzun vadede iklim değişikliklerine yol açar, asit yağmurları oluşturur ve daha bunun gibi birçok zararlı faaliyete sebep olur. Ayrıca doğada bulunan yenilenemeyen enerji kaynakları rezervi her geçen gün tükenmektedir. Bu durum, toplumları yenilenebilir enerji kaynakları kullanımına yöneltmektedir. Yenilenebilir enerji türlerine güneş enerjisi, rüzgar enerjisi, biyokütle enerjisi, jeotermal enerji, hidroelektrik enerji gibi kaynaklar örnek olarak verilebilir.

Günümüzde, teknolojinin sürekli gelişmesiyle birlikte enerjiye olan ihtiyaç büyük oranda artmaktadır. Hem artan talebi karşılamak hem de daha çevreci, sağlıklı bir kaynak kullanmak adına yenilenebilir enerji uygulamaları, hükümetler ve yatırımcılar için bir odak noktası haline gelmiştir. Bu kaynakların avantajları örnek olarak: bitmeyen, sürdürülebilir bir enerji üretimi sağlaması, zehirli gaz yaymayıp çevreci bir yol sunması, ozon gazına kötü bir etki yapmadığı için sağlıklı bir yöntem olması, enerji verimliliğinin artmasına yardımının dokunması, karbon emisyonunu azaltması verilebilir. Olumlu etkilerinin çok olması sebebiyle, artan enerji talebini karşılamak için geleneksel fosil yakıtların kullanımı yerini temiz enerji kaynaklarına bırakmaktadır. Ancak, bu süreç beraberinde bazı zorlukları da getirmektedir. Güç verimliliğini ve sürekliliğini sağlamak, güç kaybı yaşamadan üretilen seviyeyi maksimumda tutmak, şebeke ile entegrasyonunu gerçekleştirmek, harmonik bozulmalarını önlemek bu zorluklara örnek olarak verilebilir.

Geleneksel enerji üretim tesislerinin aksine, yenilenebilir enerji kaynaklı üretim, hava koşullarına bağlı olarak değişebilir. Bu durum, üretilen voltaj ve akım üzerinde anlık dalgalanmalara sebep olabilir. Örneğin güneş enerjisinden faydalanarak elektrik üretirken panel çıkarttığı güce iki parameter etki etmektedir. Bunlardan ilki ışınım seviyesi, diğeri ise sıcaklık parametresidir. Güneş paneline gelen ışınların geliş açıları, çevrede olan gölge durumu, yağmur ve bulut gibi etkiler ana parametreleri etkiler.

Üretimi etkileyen tüm faktörleri sınırlandırıp güneşten elde edilen gücü hep maksimumda tutmak için maksimum güç noktası izleme algoritmaları kullanılmaktadır. Bu algoritmaların amacı, güç elektroniği devresinin transistörünü tetikleyecek bir darbe genişlik modülasyonu üretmektir. Güç elektroniği devresi olarak sistemlerde yükseltici DA DA dönüştürücüler kullanılabilir. MGNİ algoritmaları sayesinde panelden üretilen güç en yüksek seviyede ve sabit bir şekilde tutulabilir. Kullanılan yöntemle birlikte panelden özütlenen DA voltajı düz bir çizgi haline yani saf DA formuna

benzer ve dalgalanmaları azaltmaktadır. Literatürde birçok farklı tip MGNİ algoritmaları bulunmaktadır.

Bu tez çalışmasında MATLAB/SIMULINK uygulaması kullanılarak dört farklı güç izleme algoritması kullanılarak şebeke bağlantılı batarya destekli FV sistemi tasarlanmıştır. Sistemin ana gücünü sağlayan FV panel 12.45kW güç üretecek şekilde belirlenmiştir. Uygulamada kullanılan hücre 1Soltech-1Sth-Frl-4H-260-M60'dir. FV içerisinde dörtlü seri bloklar halinde oniki paralel modül birleştirilip dizi oluşturulmuştur. Tasarlanan dört yöntemin ilk ikisi INC ve P&O metotlarıdır. Belirtilen bu algoritmalar geleneksel yöntemler kategorisine girmektedir. Sistemleri birbirine benzemektedir. P&O algoritmasında güç, voltaj ve akımın şimdiki değeri ve bir önceki değeri sürekli olarak fark alınır ve elde edilen veriye bakılarak görev döngüsü ayarlanır. INC algoritmasında ise voltaj ve akım için şimdiki değer, bir önceki değer farkı hesaplanır. Ardından bu iki parameter birbirine bölünerek özindüktans hesaplanır. Hesaplanan bu özindüktans değerine bakılarak görev döngüsü arttırılır veya azaltılır.

Geleneksel metotlardan farklı olarak tasarlanan bir yöntem YSA algoritmasıdır. Bu izleme yöntemi, zeki tip algoritma olarak da adlandırılabilir. YSA metotunun tepki süresi diğer metotlara göre daha hızlı ve başarılı olmaktadır. Bu üç algoritmanın performans analizleri 1000, 800 ve 600 W/m^2 ışınım seviyesinde test edilmiştir. En yüksek verimlilik seviyesi düşük ışımalarda 97.5% elde edilmiştir. Tüm test değerlendirme sonuçlarına göre verimi en yüksek çıktılar notlandırılmıştır.

Tüm yöntemler karşılaştırılıp bir yöntem önerilmiştir. Öncelikle en güzel çıktılar farklı farklı algortimalardan geldiği tespit edilmiştir. Yüksek ışınım seviyelerinde geleneksel yöntemlerle YSA metotunun çok farkı olmadığı görülmüştür. Fakat düşük ışınım seviyesinde YSA metot, verimlilik açısından diğer tasarımlardan daha iyi bir performans sergilemiştir. Bu sebeple tüm metotların en iyi olduğu durum grafikleri birleştirilip hibrit bir güç izleme algoritma fonksiyonu tasarlanmıştır ve yeni çalışmalar için önerilmiştir. Önerilen bu tasarım, hem yüksek ışımalarda hem de düşük ışımalarda iyi performans sağlamıştır. Diğer metotlardan farklı olarak önerilen algoritma, 1000 ile 0 W/m^2 arasındaki tüm ışımalar için değerlendirilmiş olup her seviyenin verimlilik çıktıları test simülasyon sonuçları kısmında belirtilmiştir.

Gerçekleştirilen bu tasarımda, izleme algoritmalarından başka birçok uygulama da yapılmıştır. Bunlardan biri güç sürekliliğini sağlamak için kontrol edilebilen bir batarya tasarımıdır. Bu batarya için kullanılan pil lityum iyon tipidir. Ayrıca bataryanın şarj ve deşarj durumunu, FV'nin moduna göre ayarlamak için bir batarya enerji yönetim sistemi senaryosu tasarlanmıştır. Bu senaryoya göre simülasyon 0-1 saniye arasında gündüz modunda olacaktır. Gündüz modundayken FV güç üretir. Üretilen bu gücün bir kısmı invertera giderken bir kısmı da bataryaya aktarılıp pili besler. Yani simülasyon zamanı 0-1 saniye aralığındayken batarya şarj modunda çalışmaktadır. Sistem birinci saniyeye geldiği an değişir ve gündüz modundan gece moduna geçer. Bu modda FV panel güç üretemez ve devreye herhangi bir şekilde iletemez. Batarya tam bu anda kendini otomatik olarak şarj modundan deşarj moduna alarak içinde biriken enerjiyi sisteme aktarmaya başlar. Bu

system sayesinde şebekeye hem gündüz hem de gece güç akışı sağlanmaktadır. Ek olarak, batarya enerji depolama sistemi tasarımı 10kWh olarak alımıştır. Devrede DA bağlantı noktası üzerinden gücün her iki yönde de iletilebilmesi için çift yönlü alçaltıcı-yükseltici dönüştürücü tasarlanmıştır. 0-1 saniye aralığında batarya şarj edilirken dönüştürücü alçaltıcı modda çalışır. Batarya DA bara voltajı bağlantı noktası üzerinden beslenir. 1-2 saniye aralığında batarya deşarj edilirken dönüştürücü yükseltici modda çalışır ve DA bara voltajı bağlantı hattına güç aktarılır. Lityum iyon pilin başlangıç şarj değeri yüzde 50 olarak alınmıştır.

Devrede yer alan bir diğer sistem ise üç fazlı DA-AA eviricidir. DA-DA yükseltici dönüştürücüden gelen akım ve voltajın şebekeye bağlanabilmesi için üç fazlı sinüzoidal dalga formuna getirilmesi gerekmektedir. Bu işlemi DA-AA evirici gerçekleştirir. Yapılan modelde kullanılan evirici geleneksel 6 transistörlü 6 darbe genişlik modülasyonu üreten tip tercih edilmiştir. Ayrıca bu evirici tasarımıyla beraber şebekenin fazlarla uyumlu olabilmesi için bir faz kilitlemeli döngü ve aktif reaktif güç kontrolü yapılmıştır.

Tasarım aşamasında güç kalitesini belirleyen en önemli faktörlerden biri de filtredir. Eviriciden çıkan akım ve gerilim, belirli bir miktarda harmonik bozulmaları içerir. Bu harmonik bozulmalarının giderilmesi için filtre kullanılır. Bu tez çalışmasında üç faz eviricinin çıkış gücündeki harmonik bozulmalarını süzmek için LCL filtre kullanılmıştır. Ayrıca test sırasında devrenin THD seviyesinin gündüz modundan gece moduna geçerken yükseldiği fark edilmiştir. FV ve bataryadaki güç farklılıklarından dolayı filtre yalnızca FV ye uyumlu değerler için hesaplanmıştır. Gece modu batarya geçişi sonrasında bir güç düşümü yaşandığı için harmonik seviyesi yükselmiştir. Sonrasında hem literatüre katkı yapıp yenilik eklemek hem de THD oranını düşürmek için bu konu üzerinde çalışılmıştır. Yapılan çalışmanın ardından tek bir LCL filtre devresi üzerinden iki modlu tasarım geliştirilmiştir. Geliştirilen bu tasarımda gündüz modunda ilk filtre aktif ikinci filtre pasif durumdayken sistem durumu değiştiğinde yani gece modunda ilk filtre pasif konuma geçerken ikinci filtre aktif konuma geçecektir. Bu çalışma sayesinde 5%'e yakın olan THD değerleri gece modunda 3.2%'ye düşürülmüştür. Literatür detaylı bir şekilde incelenmiş olup, bu tip iki modlu LCL filtre tasarımı yapısı geliştirilen herhangi bir teze rastlanılmamıştır.

Geliştirilen bu simülasyon en son noktada şebekeye bağlanmış olup, sistemin ürettiği gücü şebekeye aktarabilmesi açısından verimli bir yol izlenilmiştir. Bu şebeke bloğu, Türkiye regülasyonlarına uygun olarak 3 faz, 400V AA ve 50 hz frekansa sahip olacak şekilde ayarlanmıştır.

Sonuç olarak, önerilen FV-BESS hibrit maksimum güç izleme algoritması yenilenebilir enerji sistemi, şebekeye güç sağlayarak enerji talebine çözüm sunmaktadır. Aynı zamanda harmonik bozulmalarının derinlemesine incelenmesi, bununla ilgili akademik katkı yapılması da ilerde yapılacak çalışmalara bir öngörü niteliği de sunmaktadır. Tasarlaanan sistemin ışımaya bağlı tepki kabiliyetlerinden maksimum fayda sağlanacak biçimde hibrit güç izleme metotu kullanılmış ve sistemin en verimli hale gelmesine çalışılmıştır. Gelecekte yapılacak çalışmalar, güç elektroniği devrelerinin anahtar tetik sürelerini azaltmaya yönelik olabilir. Daha verimli bir güç izleme yolu

geliştirilebilir. Geleneksel olarak tasarlanan evirici yerine, daha karmaşık olup net sonuçlar veren eviriciler entegre edilebilir. Yüksek voltajlı ve iç verimliliği daha yüksek olan bir güneş paneliyle elektrik üretimi üzerinde çalışılabilir. Batarya algoritmalarında lityum iyon yerine geliştirilecek son teknolojik mimariler üzerinde çalışılabilir. Toplam maliyet düşürme kapsamında yapılan tüm devre ve kontrolcü uygulamalarını sadeleştirmek üzerine çalışmalar yapılabilir.

ACKNOWLEDGEMENTS

Foremost, I would like to express my deepest gratitude to Prof. Dr. Ahmet TEKE for his continuous support, immense knowledge, invaluable expertise, and patience throughout the journey of this thesis. His scientific approach has enabled me to accomplish this study. I could not have imagined having a better advisor and mentor for my MSc study.

Besides my advisor, I would like to extend my sincere gratitude to members of the jury Asst. Prof. Dr. Özgür ÇELİK and Asst. Prof. Dr. Oğuzhan TİMUR for providing encouragement to me, helpful suggestions, and insightful comments.

I am extremely grateful to Prof. Dr. Metin Sabuncu for broadening my horizons, ensuring limitless support and encouraging me when I was an undergraduate student.

I would be remiss in not mentioning Mr. Kürşat SAYILGAN who gave me an engineering perspective, vaccinated continuous improvement and strongly recommended the MSc journey with thesis. I am also thankful to him for precious support.

Last but not least, I would like to thank my family especially mother Dilek GÜZEY, my father Süha GÜZEY and my uncle Prof. Dr. Hasan Murat GÜNDÜZ for never withholding their material aid and spiritual support from me throughout my life. Words cannot express my gratitude to them.

LIST OF TABLES

Table 2.1. Benefits and Deficiencies of First Generation Solar Cells 16
Table 2.2. Benefits and Deficiencies of Second Generation Solar Cells 17
Table 2.3. Benefits and Deficiencies of Third Generation Solar Cells 18
Table 2.4. Benefits and Deficiencies of Fourth Generation Solar Cells 19
Table 2.5. Operating Time in Frequency Range 23
Table 2.6. Current Harmonic Distortion Limits 24
Table 2.7. Benchmark of Non-Isolated DC-DC Converter Topologies 26
Table 2.8. Literature Review of Perturb and Observe Algorithm 35
Table 2.9. Literature Review of Incremental Conductance MPPT 38
Table 2.10. Literature Review of ANN MPPT 40
Table 2.11. Literature Review of Inverter for PV System 43
Table 3.1. Technical Features of 1Soltech-1Sth-Frl-4H-260-M60 Cell 48
Table 3.2. Technical Features of 1Soltech-1Sth-Frl-4H-260-M60 Array 49
Table 3.3. Boost Converters Design Parameters 51
Table 3.4. Chosen Battery Parameters for Designing Criteria 57
Table 3.5. Chosen Bidirectional Buck Boost Converter Parameters 58
Table 3.6. Daytime Mode LCL Filter 65
Table 3.7. Nighttime Mode LCL Filter 65
Table 4.1. Summary of Simulation Results 92

LIST OF FIGURES

Figure 1.1. Classification of Energy Sources 1
Figure 1.2. I-V and P-V Characteristic Curves 3
Figure 1.3. Basic Block Diagram of a Double Stage PV to Grid System 4
Figure 2.1. The World and Republic of Turkey Energy Consumption Graphs 1965-2022 7
Figure 2.2. Global Electricity Generation Source by Source in 2022 8
Figure 2.3. Distribution of Electricity Generation Worldwide in 2022 9
Figure 2.4. Global Investments in Renewable Energy from 2004 to 2022 10
Figure 2.5. Pioneer Countries of Installed Renewable Energy Capacity 11
Figure 2.6. Solar Radiation Map of Turkey 13
Figure 2.7. PV Cell Representation Including Both Layers (p-type and n-type) 15
Figure 2.8. Four Different Generation Types and Inside Structures 19
Figure 2.9. Double Diode Solar Cell Equivalent Circuit 20
Figure 2.10. Single Diode Solar Cell Equivalent Circuit 21
Figure 2.11. Fill Factor in I-V Characteristic Curve 22
Figure 2.12. Different Topologies of DC-DC Converter 26
Figure 2.13. Circuit Analogy of Boost Converter 27
Figure 2.14. Circuit Analogy of Non-Isolated Bidirectional Buck Boost Converter 29
Figure 2.15. Current Flowing When S2 is On 30
Figure 2.16. Current Flowing When D1 is Forward Biased 30
Figure 2.17. Current Flowing When S1 is ON 31
Figure 2.18. Current Flowing When D2 is Forward Biased 31
Figure 2.19. Classification Diagram of MPPT Methodologies 33
Figure 2.20. Flowchart of Conventional P&O Algorithm 34
Figure 2.21. P-V Curve of INC Methodology 36
Figure 2.22. Flowchart of Incremental Conductance Algorithm 37
Figure 2.23. Structure of ANN 39
Figure 2.24. Load Connected PV System with ANN MPPT Controller 40
Figure 2.25. Classification of Inverters 41
Figure 2.26. Three Phase Full Bridge Voltage Source Inverter 42
Figure 2.27. Three Phase Grid Connected Inverter with LCL Filter 44
Figure 2.28. Block Diagram of PLL Circuit 46
Figure 3.1. Proposed PV&BESS to Grid System 47
Figure 3.2. Chosen PV Cell and I-V, P-V Curves 49
Figure 3.3. PV Array Output Graphs I-V and P-V 50
Figure 3.4. Simulation Circuit of Boost Converter 50

Figure 3.5. Implementation of P&O MPPT 52
Figure 3.6. Implementation of INC MPPT 53
Figure 3.7. Neural Network Training Tool 54
Figure 3.8. Implementation of ANN MPPT 55
Figure 3.9. Function Block of Hybrid MPPT 55
Figure 3.10. Flowchart of Hybrid MPPT 56
Figure 3.11. Block Diagram of BESS 58
Figure 3.12. Charging Process of the BESS 59
Figure 3.13. Discharging Process of the BESS 59
Figure 3.14. Setting the Status Switch for Charge or Discharge Operation 60
Figure 3.15. Gate Pulse Controller Diagram 60
Figure 3.16. Energy Management System Scenario 61
Figure 3.17. Power Control of the Three Phase Inverter 63
Figure 3.18. Designed PLL Circuit for Inverter Control and Grid Synchronization 63
Figure 3.19. Representation of Three Phase LCL Filter 64
Figure 4.1. The Inverter Output Voltage and Current Waveform at 1000 W/m^2 with P&O 67
Figure 4.2. The Graphs of Battery Outcomes and DC Link Voltage with P&O at 1000 W/m 68
Figure 4.3. Efficiency of Power with P&O at 1000 W/m^2 69
Figure 4.4. The THD of Daytime Mode LCL Filter with P&O at 1000 W/m^2 69
Figure 4.5. The THD of Two Mode LCL Filter with P&O at 1000 W/m^2 70
Figure 4.6. The Inverter Output Voltage and Current Waveform at 1000 W/m^2 with INC 70
Figure 4.7. The Graphs of Battery Outcomes and DC Link Voltage with INC at 1000 W/m^2 71
Figure 4.8. Efficiency of Power with INC at 1000 W/m^2 71
Figure 4.9. The THD of Daytime Mode LCL Filter with INC at 1000 W/m^2 72
Figure 4.10. The THD of Two Mode LCL Filter with INC at 1000 W/m^2 72
Figure 4.11. The Inverter Output Voltage and Current Waveform at 1000 W/m^2 with ANN 73
Figure 4.12. The Graphs of Battery Outcomes and DC Link Voltage with ANN at 1000 W/ 73
Figure 4.13. Efficiency of Power with ANN at 1000 W/m^2 74
Figure 4.14. The THD of Daytime Mode LCL Filter with ANN at 1000 W/m^2 74
Figure 4.15. The THD of Two Mode LCL Filter with ANN at 1000 W/m^2 75
Figure 4.16. The Inverter Output Voltage and Current Waveform at 800 W/m^2 with P&O 75
Figure 4.17. The Graphs of Battery Outcomes and DC Link Voltage with P&O at 800 W/m^2 76
Figure 4.18. Efficiency of Power with P&O at 800 W/m^2 76
Figure 4.19. The THD of Daytime Mode LCL Filter with P&O at 800 W/m^2 77
Figure 4.20. The THD of Two Mode LCL Filter with P&O at 800 W/m^2 77
Figure 4.21. The Inverter Output Voltage and Current Waveform at 800 W/m^2 with INC 78
Figure 4.22. The Graphs of Battery Outcomes and DC Link Voltage with INC at 800 W/m^2 78

Figure 4.23. Efficiency of Power with INC at 800 W/m^2 79
Figure 4.24. The THD of Daytime Mode LCL Filter with INC at 800 W/m^2 79
Figure 4.25. The THD of Two Mode LCL Filter with INC at 800 W/m^2 80
Figure 4.26. The Inverter Output Voltage and Current Waveform at 800 W/m^2 with ANN 80
Figure 4.27. The Graphs of Battery Outcomes and DC Link Voltage with ANN at 800 W/m^2 81
Figure 4.28. Efficiency of Power with ANN at 800 W/m^2 81
Figure 4.29. The THD of Daytime Mode LCL Filter with ANN at 800 W/m^2 82
Figure 4.30. The THD of Two Mode LCL Filter with ANN at 800 W/m^2 82
Figure 4.31. The Inverter Output Voltage and Current Waveform at 600 W/m^2 with P&O 83
Figure 4.32. The Graphs of Battery Outcomes and DC Link Voltage with P&O at 600 W/m^2 83
Figure 4.33. Efficiency of Power with P&O at 600 W/m^2 84
Figure 4.34. The THD of Daytime Mode LCL Filter with P&O at 600 W/m^2 84
Figure 4.35. The THD of Two Mode LCL Filter with P&O at 600 W/m^2 85
Figure 4.36. The Inverter Output Voltage and Current Waveform at 600 W/m^2 with INC 85
Figure 4.37. The Graphs of Battery Outcomes and DC Link Voltage with INC at 600 W/m^2 86
Figure 4.38. Efficiency of Power with INC at 600 W/m^2 86
Figure 4.39. The THD of Daytime Mode LCL Filter with INC at 600 W/m^2 87
Figure 4.40. The THD of Two Mode LCL Filter with INC at 600 W/m^2 87
Figure 4.41. The Inverter Output Voltage and Current Waveform at 600 W/m^2 with ANN 88
Figure 4.42. The Graphs of Battery Outcomes and DC Link Voltage with ANN at 600 W/m^2 88
Figure 4.43. Efficiency of Power with ANN at 600 W/m^2 89
Figure 4.44. The THD of Daytime Mode LCL Filter with ANN at 600 W/m^2 89
Figure 4.45. The THD of Two Mode LCL Filter with ANN at 600 W/m^2 90
Figure 4.46. Irradiance Level for Hybrid Mode MPPT 91
Figure 4.47. Efficiency Result of Hybrid Mode MPPT 91

SYMBOLS AND ABBREVIATIONS

AC	:	Alternating Current
AH	:	Ampere Hour
ANN	:	Artificial Neural Network
A-SI	:	Amorphous Silicon
BEV	:	Battery Electric Vehicle
BESS	:	Battery Energy Storage System
CCM	:	Continuous Conduction Mode
CDS	:	Cadmium Sulfide
CDTE	:	Cadmium Telluride
CIGS	:	Copper Indium Gallium Selenide
CSI	:	Current Source Inverter
DC	:	Direct Current
DDM	:	Double Diode Model
DQ0	:	Direct Quadrature Zero
DSSC	:	Dye-Sensitized Solar Cell
EMRA	:	Electricity Market Regulatory Authority
FF	:	Fil Factor
FLC	:	Fuzzy Logic Control
FLE	:	Fuzzy Logic Estimator
GAAS	:	Gallium Arsenide
G2V	:	Grid to Vehicle
GW	:	Gigawatt
IEA	:	International Energy Agency
IEC	:	International Electrotechnical Commission
IEEE	:	Institute of Electrical and Electronics Engineers
IGBT	:	Insulated Gate Bipolar Transistor
INC	:	Incremental Conductance
IRENA	:	International Renewable Energy Agency
KW	:	Kilowatt
M-SI	:	Monocrystalline Silicon
MJC	:	Multi Junction Cell
MOSFET	:	Metal Oxide Field Effect Transistor
MPP	:	Maximum Power Point
MPPT	:	Maximum Power Point Tracker

NASA : National Aeronautics and Space Administration

NPC : Neutral Point Clamped

NZE : Net Zero Emission

OPSC : Organic and Polymer Solar Cell

P&O : Perturb and Observe

P-SI : Polycrystalline Silicon

PHEV : Plug-in Hybrid Electric Vehicle

PI : Proportional Integral

PLL : Phase Locked Loop

PTC : PV USA Test Conditions

PV : Photovoltaic

PVSC : Perovskite Cell

PWM : Pulse Width Modulation

QDS : Quantum Dot Cell

RAD : Radian

RES : Renewable Energy Sources

SDM : Single Diode Model

SMC : Sliding Mode Control

SOC : State of Charge

STC : Standard Test Condition

THD : Total Harmonic Distortion

TWH : Terawatt Hours

UPS : Uninterruptible Power Supply

USD : United States Dollar

VCO : Voltage Controlled Oscillator

VSI : Voltage Source Inverter

V2G : Vehicle to Grid

1. INTRODUCTION

1.1. Statement of Problem and Research Motivation

The demand of energy is increasing day by day due to many factors. These factors can be shown as rapid development of technology, population growth in every area and migration of people to developed countries. To meet this increasing demand, energy resources are used. Basically, energy resources can be classified into two different types. The first of these types is called Traditional or Conventional Sources. It is a type of energy produced and released using fossil fuels such as oil, coal, natural gas. Although it is not suitable and the main cause of many health problems, energy production methodology from fossil fuels still makes the main contribution to this sector (Olabi and Abdelkareem, 2022). Conventional fuels release high amount of greenhouse gases during the combustion process such as methane, carbon dioxide, nitrogen oxide etc. The release greenhouse gases expose humanity to serious dangers such as weather changes, global warming, health problems, rising of sea level, melting of glaciers and extinction of species (Olabi and Abdelkareem, 2022). In order not to face such things and to protect our world, Renewable Energy Sources (RES) offer more environmentally, friendly, reliable, healthy and sustainable energy production way. RES also known as non-traditional energy sources can be classified as solar energy, wind energy, tidal energy, bioenergy, geothermal energy. Figure 1.1. shows the classification of energy sources.

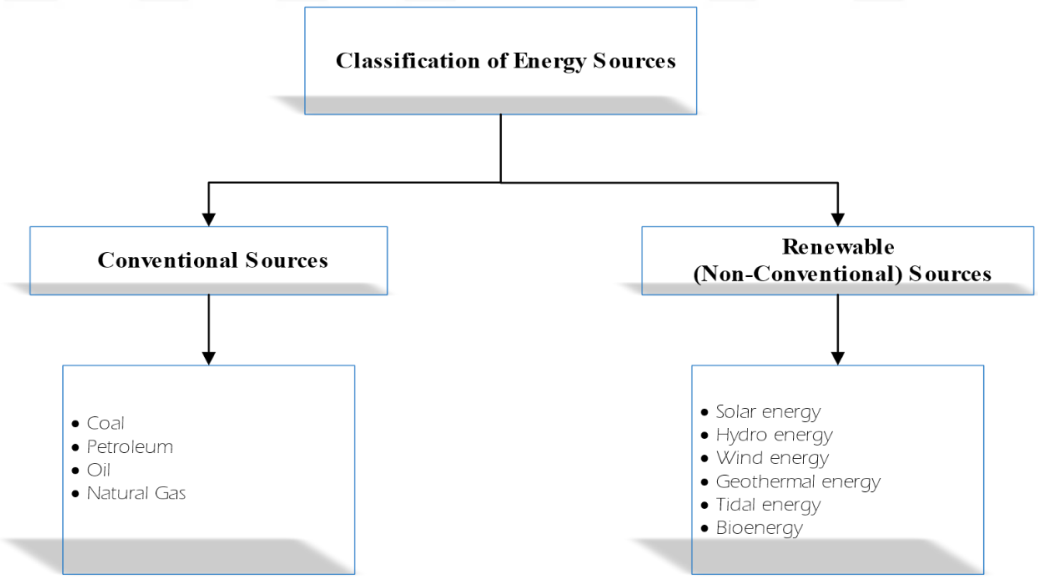


Figure 1.1. Classification of Energy Sources

On a global scale, conventional energy sources are replaced by RES. Technological developments and investments are increasing in this field day by day. Especially Solar energy is one of these sources.

Solar energy is very convenient compared with other sources. Besides other resources, it does not require high maintenance costs, it can be easily applied even in narrow spaces such as the roofs of houses, it provides energy in a sustainable way because sunlight does not run out. It is a perfect way to reduce carbon footprint, it does not emit any gas that pollutes nature. For the this kind reasons, solar energy is preferred (Vo et al., 2021). In addition, the energy obtained from solar can be used in almost any area where it is needed. Despite the many advantages this type of energy, there are also some disadvantages The high investment cost makes it difficult to commission large-scale industrial applications. Moreover, it is completely dependent on the angle of incidence the sun's rays and the ambient temperature, the energy that can be produced can vary under these conditions. However, it cannot be implementable to the roof of every house, if the roof does not face the sun, sufficient solar energy will not be captured and production part will not be possible. Sun-facing roofs are more favorable than flat roofs. The limitation of the ground on which it will be applied can be described as another disadvantage. In addition, semiconductor device technologies, which should be used together in solar energy extract system, availability becomes difficult due to the chip crisis should be disadvantage.

Solar energy is basically the conversion of the radiation from sun directly into electrical energy with the help of Photovoltaic (PV) panels. This system can also be called as a solar panel system. The PV module is the most critical component of an energy conversion system that uses semiconductor technology to convert light energy into electrical energy for use as a power source. It consists of the combination of multiple PV cells and includes different type of materials. Cadmium telluride (CdTe) Gallium Arsenide (GaAs), mono and polycrystalline silicon materials can be shown as a most commonly used materials inside structure of PV (Khan and Arsalan, 2016). A solar panel cell can be characterized as a small electricity generation device. Solar cells on a larger scale can be combined to from a module in order to generate electricity. Modules consist of more than one cell can be mounted in a PV array up to the desired production capacity.

PV panel efficiency is quite an important factor in solar energy production. Due to advances technology within this scope in recent years, the average panel conversion efficiency rise from 14% to over 22%. This big development in efficiency leads to increase power values of panels produced with the latest technology. Panel efficiency is determined by two main factors are called design and silicon type. As a result of technological improvements made on these factors, the panel efficiency is increasing every day. The voltage and current generated from the PV panel vary depending on the incoming sunlight and temperature level. The graph of output voltage and current of the panel is called the I-V characteristic curve. This curve is a crucial graph for system verification and determination of given values clearly.

Indicated in Figure 1.2, the point where x equal to zero on the y axis is called the short circuit current (I_{sc}) and the point where y is equal to zero on the x axis is called the open circuit voltage (V_{oc}). As can be seen below, the place where current is corresponds to maximum is specified as

maximum power point of the current (I_{MP}) and the place where the voltage is maximum is called the maximum power point of the voltage (V_{MP}). The location at which both components are maximum is namely as maximum power point (P_{MP}).

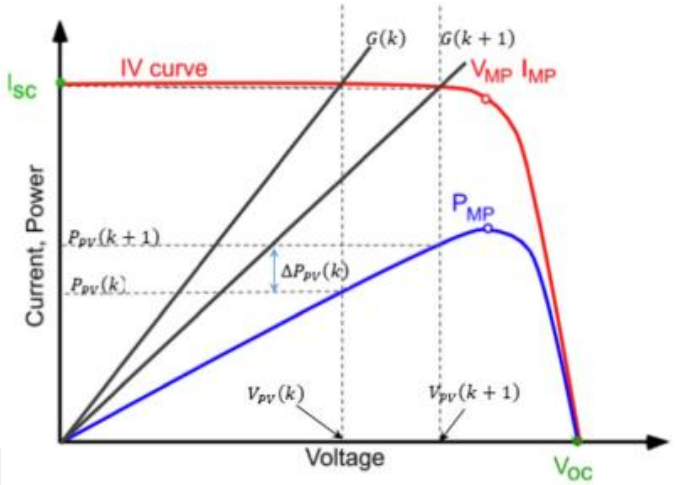


Figure 1.2. I-V and P-V Characteristic Curves (Eldessouky et al., 2023)

In order to reduce paying off time of the investment costs for PV systems, it is extremely important to keep to power to be drawn from PV at the maximum level. Various algorithms are used to track the power status and keep the power at maximum. The algorithms following MPP are generally referred as Maximum Power Point Tracking (MPPT). Applied MPPT method basically generate a control signal and the produced signal is sent to the Direct Current (DC) – Direct Current (DC) Converter as a trigger signal. The DC-DC converter is controlled by the Pulse Width Modulation (PWM) signal coming from MPPT. This is an important way for system continuity. Besides traditional MPPT algorithms, there are also different variants supported by artificial intelligence. Selected type of algorithm also plays an active role for determining system efficiency. MPPT not only ensures the power maximization from PV module, but also increases the operating life of PV system. (Reisi et al., 2012). According to design procedure, the power drawn from module can be connected to the grid or the load at the end point of system If design includes DC-DC Converter and DC-Alternative Current (AC) Inverter, this is called as a two stage or double stage system. If there is only DC-AC inverter in design, it is also called as a single stage system.

A robust control algorithm is also needed for the inverter. This algorithm transmit the PWM signal to the inverter as a trigger and ensures control operation to be performed. A wide variety of inverter control algorithms can be used according to design.

The output voltage and current of inverters are usually different from pure sine waves. The difference is due to the high level of harmonics. The harmonics have a disturbing effect on the sine wave form of signals. Collection of all harmonic effects on a system is called Total Harmonic Distortion (THD). Filters are used to increase the wave roughness and bring it closer to the sine

waveform. Depending on the type of filter and parameter quality is used in circuit, signal can resemble the sine waveform

Phase Locked Loop (PLL) method is a necessary issue for synchronization of the grid with the inverter in grid connected power electronics applications. When method is used into the grid synchronization, should not be affected from worse conditions such as voltage fluctuations, harmonics, phase shifts and frequency changes. The system includes some parts such as feedback line, Voltage Controlled Oscillator(VCO), phase detector, low pass filter in loop. The PLL is called a control system. It locks the frequency and inhibit phase shift between input and output

Figure 1.3 shows a block diagram of the entire design from the PV to grid. Generated current and voltage with help of semiconductors in PV are sent as input to MPPT algorithm, and the output of MPPT goes to the DC-DC converter either as a reference voltage or as a duty cycle. Test results of different methods are mentioned. Particular kinds of MPPT algorithms are tried one by one and their outputs are compared in terms of efficiency. Moreover, when the other part is examined, an algorithm is used to control the Inverter as well. Vary algorithms can be used in order to control inverter. Generally, since the system includes both a converter and an inverter, the desired design is called double-stage.

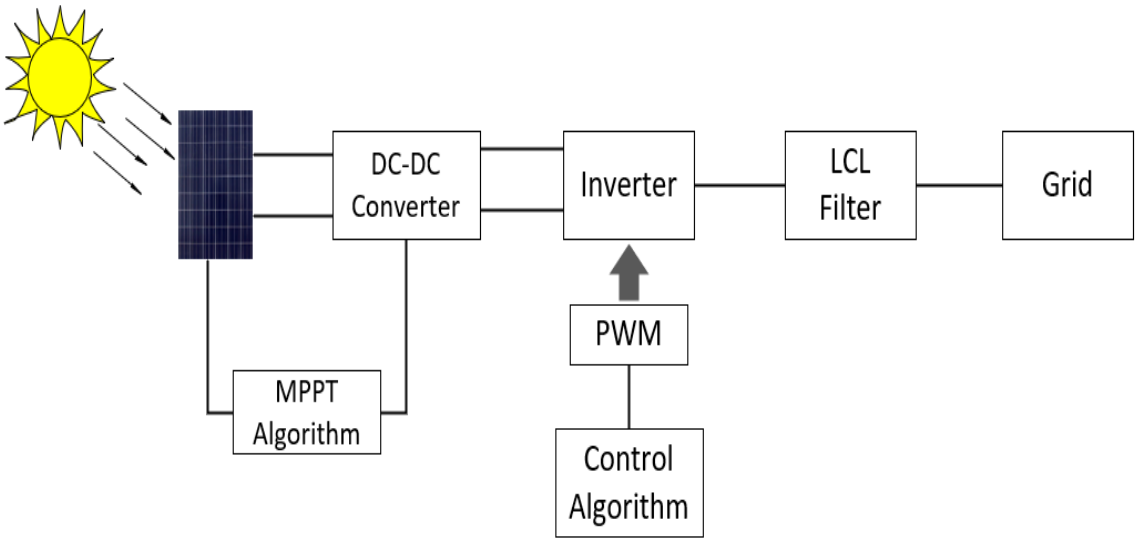


Figure 1.3. Basic Block Diagram of a Double Stage PV to Grid System

1.2. Objective and Outline of the Thesis

The aim of this thesis is designing a system that can transmit energy from the PV to the grid. Moreover, it is to provide battery support and realize power continuity when energy cannot be transmitted from PV to the grid. Especially in night mode, PV does not produce any electricity, battery takes an action to provide energy. Thus, Battery Energy Storage System (BESS) contributes for feeding electrical grid at night. In addition to these design purposes, it is aimed to make separate

LCL filter designs in daytime mode and night mode to regulate the power quality and to reduce harmonic effects. Moreover, the main aim is to provide a single LCL filter in two separate mode. This structure allows for the simplification of the circuit. This design is discussed on the MATLAB/SIMULINK platform. Furthermore, the system should always keep the power produced by the PV panel at maximum level against changing irradiation levels. In order not to reduce from this power level, it is aimed to use various MPPT algorithms and to determine the most efficient one. The types of algorithms are Perturb and Observe (P&O), Incremental Conductance (INC) and Artificial Neural Network (ANN). Furthermore, an additional input will be placed in the ANN algorithm used to increase efficiency according to the temperature level and its differences with the traditional ANN will be examined. In the last case, it is targeted to determine the type of algorithm that brings the energy waves closest to the pure sine wave form and gives the best results in terms of both THD and efficiency. Thanks to be detected model, the system's response to changing conditions will be earlier and properly, and it will make it easier to become stable for the system. Besides the parts which is mentioned, DC-AC inverter, DC-DC converter, LCL filter, battery, bidirectional buck boost converter and grid also are used in the circuit design.

After this introductory chapter where the statement of problem, research motivation and contribution of the study are introduced, the structure of this thesis is as follows:

In Chapter 2, the global status of renewable energy especially solar energy, the investments made in this field in recent years, the leading countries of world for renewable area, Turkey's position of renewable energy sector, the recent studies have summarized in this scope are explained. Detailed literature reviews were prepared and academic studies were compiled on the main components used in the design such as PV panel, DC-DC converter, bidirectional buck boost converter, DC-AC inverter. MPPT control algorithms are described widely for P&O, INC, ANN and were given with their flowcharts. Literature review outcomes of LCL filter and PLL system are mentioned. Moreover, the formulas of parameters used are specified in this section. The standards of grid connection which play an important role of designing criteria in the system were summarized.

In Chapter 3, the materials used in circuit design and their parameter values are shown in detail. The applied MPPT control algorithms P&O, INC and ANN were specified together. In addition, the hybrid method in which all MPPT algorithms are used, is also described in this section. To ensure energy continuity, the battery design, parameter values and the energy management system to connect it with the entire circuit have been mentioned. Moreover, the DC-DC converter used in the design and two mode LCL filter design to reduce harmonics were indicated.

In Chapter 4, the design results were examined for different MPPT algorithms and compared each other. The results have taken from the MATLAB/SIMULINK platform were interpreted. According to the output graphs, it was determined which method gave best results. The effect of temperature input was observed for the ANN method. The most efficient method was proposed among all modeled of algorithms.

In Chapter 5 the consequences of all these studies are described in a comprehensive way. The studies and technologies expected to be carried out in the future have been indicated.

1.3. Contributions of Thesis

The importance of this thesis study and its contributions to the literature can be explained as follows:

(i) A detailed literature review was performed on PV panels. The compiled information about the latest technologies in panel production stage was explained.

(ii) Related with all important components in the PV to grid system such as DC-DC converter, DC-AC inverter, LCL filter were examined and a comparison was made about the differences between single stage system with double stage system.

(iii) Academic studies on traditional MPPT algorithms used to maximize power are compiled. Disadvantages of traditional methods compared to innovative MPPT methods were remarked. Studies on ANN MPPT, which is used to increase system efficiency and reduce harmonics, were indicated and its advantages according to other methods were mentioned.

(iv) Two separate LCL filters are designed for PV to grid mode and battery supported mode. The producing current passes through first LCL filter in PV to grid mode, in battery support mode first filter becomes cut off position and second LCL filter becomes active position. Due to this double mode filter structure, total harmonic distortions have been suppressed. The filter designed for the battery lead to cost reduction

(v) Two separate parameter blocks were executed via a single LCL filter for the simulation to work more effectively.

(vi) According to the irradiance levels, the MPPT types that provide the highest efficiency have been determined and the hybrid MPPT design has been applied. In this way, high efficiency has been achieved at low power levels.

1.4. Summary

In this section, the objectives of the research, the main lines of this thesis, the contributions to academic literature are explained. Renewable energy sources were briefly explained. The purpose and importance of solar energy was mentioned. Additionally, the information to be explained in other parts of the thesis is briefly stated.

2. LITERATURE REVIEW

2.1. Renewable Energy

Rapid development of global economy, technology, research and education, growth, trading have brought about to rise energy consumption. Resource utilization is also increasing to meet demand same ratio. Therefore, the value and importance of energy resources has increased considerably. Being independent and self-sufficient in energy sector has become the goal of countries (Randelovic et al., 2020). The world and Republic of Turkey energy consumption graphs between 1965-2022 is shown below in Figure 2.1.

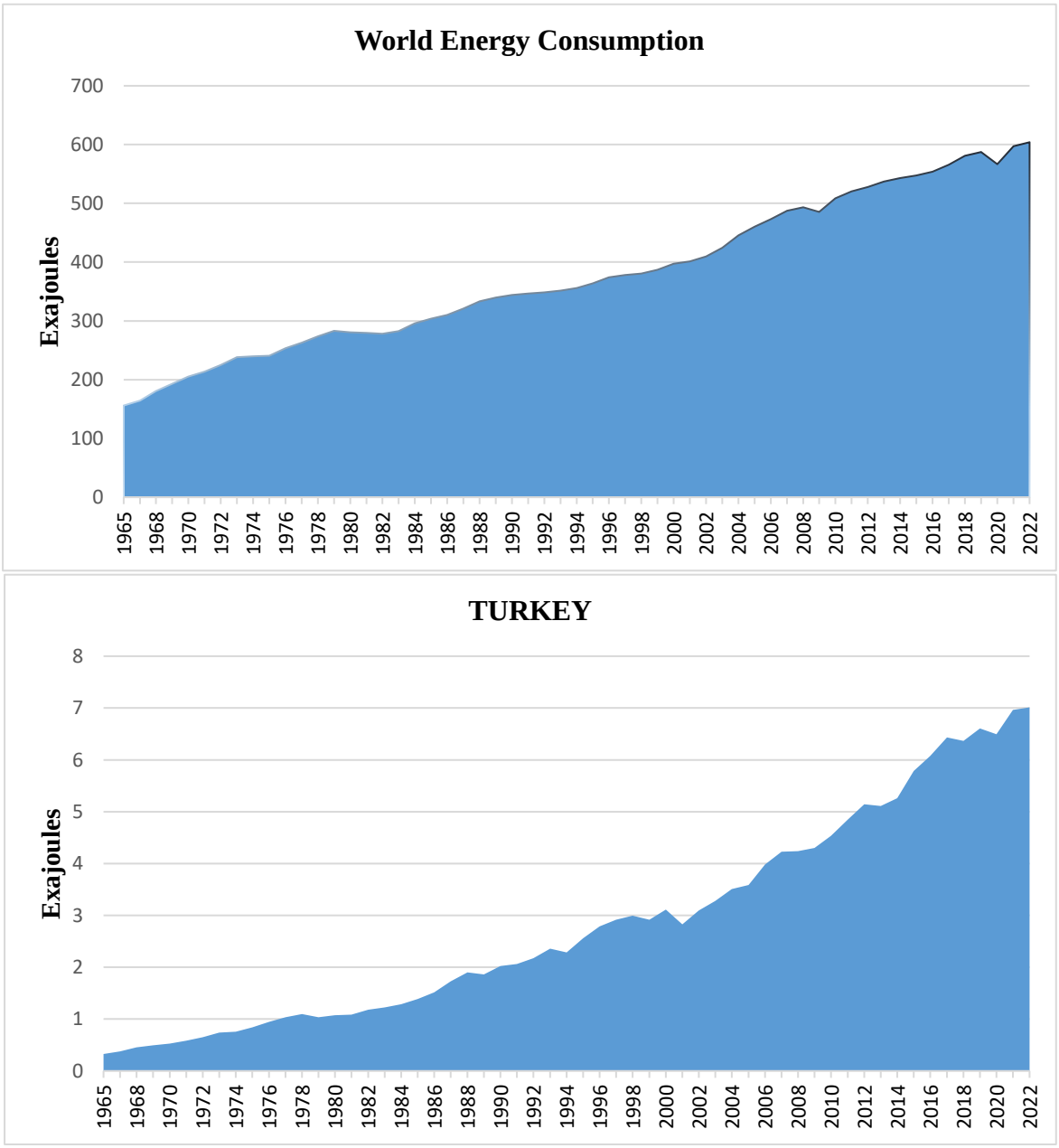


Figure 2.1. The World and Republic of Turkey Energy Consumption Graphs 1965-2022

The first type of energy production sources is called fossil fuel, conventional, traditional or non-renewable energy resource. It includes coal, natural gas, oil and nuclear energy. Running out of resources is accelerating, while their accessibility is decreasing. Besides facing with the depletion of conventional resources, it leads to global warming of the planet, environmental pollution, being unreliable, consumes a lot of time and labor power in order to produce energy. In order to combat all these situations, some academic studies have mentioned that the transition to RES which is described the second type of energy production resource should be accelerated (Giannakopoulos et al., 2009). RES involve solar energy, wind energy, geothermal energy, bioenergy. These resources provide sustainable, reliable, inexhaustible, clean, low carbon emission levels, saving money and health, eco-friendly and more technological energy production (Aman et al., 2015). The global electricity production is led by conventional fuels which ensured 61% of electricity generation in 2022. Electricity is acquired from coal 10186 Terawatthours (TWh), by natural gas 6336 TWh, from other traditional resources 850 TWh of total generation. Based on hydro energy for electricity manufacture corresponds 4311 TWh. Using wind and solar sources together, achieved 3444 TWh, the wind energy equal to 2160 TWh, remain source is match 1284 TWh nuclear source contributed 2611 TWh, in addition bioenergy supported to produce around 672 TWh. (EMBER, 2023). These stated electricity generation source by source are shown in a figure in 2.2.

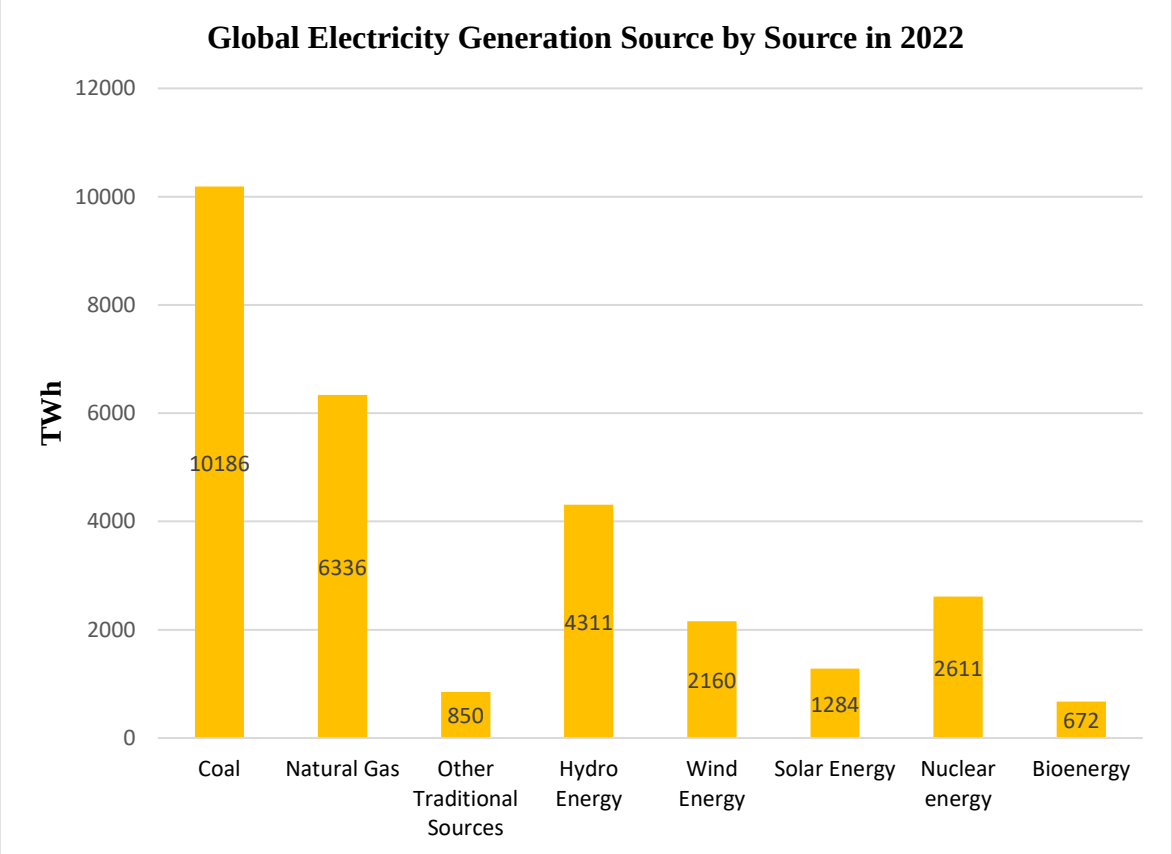


Figure 2.2. Global Electricity Generation Source by Source in 2022 (EMBER, 2023)

The Figure 2.3. is shown the percentage distribution of electricity generation sources in the world in 2022.

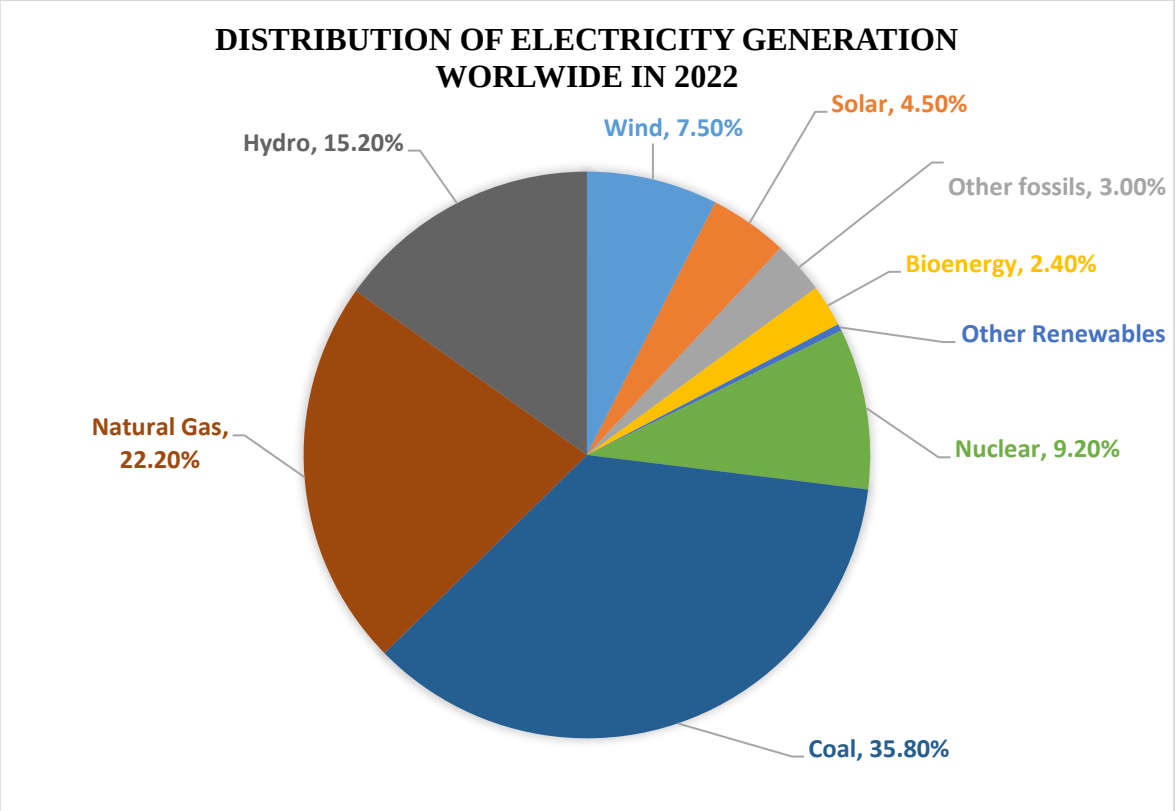


Figure 2.3. Distribution of Electricity Generation Worldwide in 2022 (EMBER, 2023)

Considering figure 2.3 it shows that the most used source for electricity generation is coal. While the usage rate of coal in this sector is 35.8% in 2022, it is seen as 35.98% in 2021 (BP-Statistics, 2022). The another type of energy source which is called as nuclear source, has a rate of 10.01% in 2020, 9.83% in 2021 and 9.2% in 2022 (BP-Statistics, 2022). The same situation as in coal also exists in natural gas. While the electricity production from natural gas was 23.69% in 2020, it decreased to %22.91 in 2021 and the rate in 2022 was 22.20% (BP-Statistics, 2022). This indicates that the conversion to green energy will increase every year and the utilizing rate of fossil fuel will decrease. Based on the specified production rates, it is understood that the investment in renewable energy sources is higher than others. Thanks to the investments which was made before, solar and wind electricity generation totally percentage were 12% between global electricity sources. According to International Energy Agency (IEA) report, this percentage is predicted to reached 41% by 2030 and the biggest change in electricity production in 2022 was growth of solar rising 24%, wind increasing 17% compare to previous year. (IEA, 2023). This situation expresses that the amount of money which is spent in RES will enhance rapidly every year.

Investments of this field are a good opportunity to quickly strengthen the country's economy and to create a sustainable source of money for entrepreneurs. China, United States of America and Europe

countries are the main investors. Furthermore, the incentives are given by governments for these area with both cash support and tax exemptions are becoming the focus of interest for companies. Figure 2.4. expresses the amount of global investments in renewable energy between 2004 and 2022.

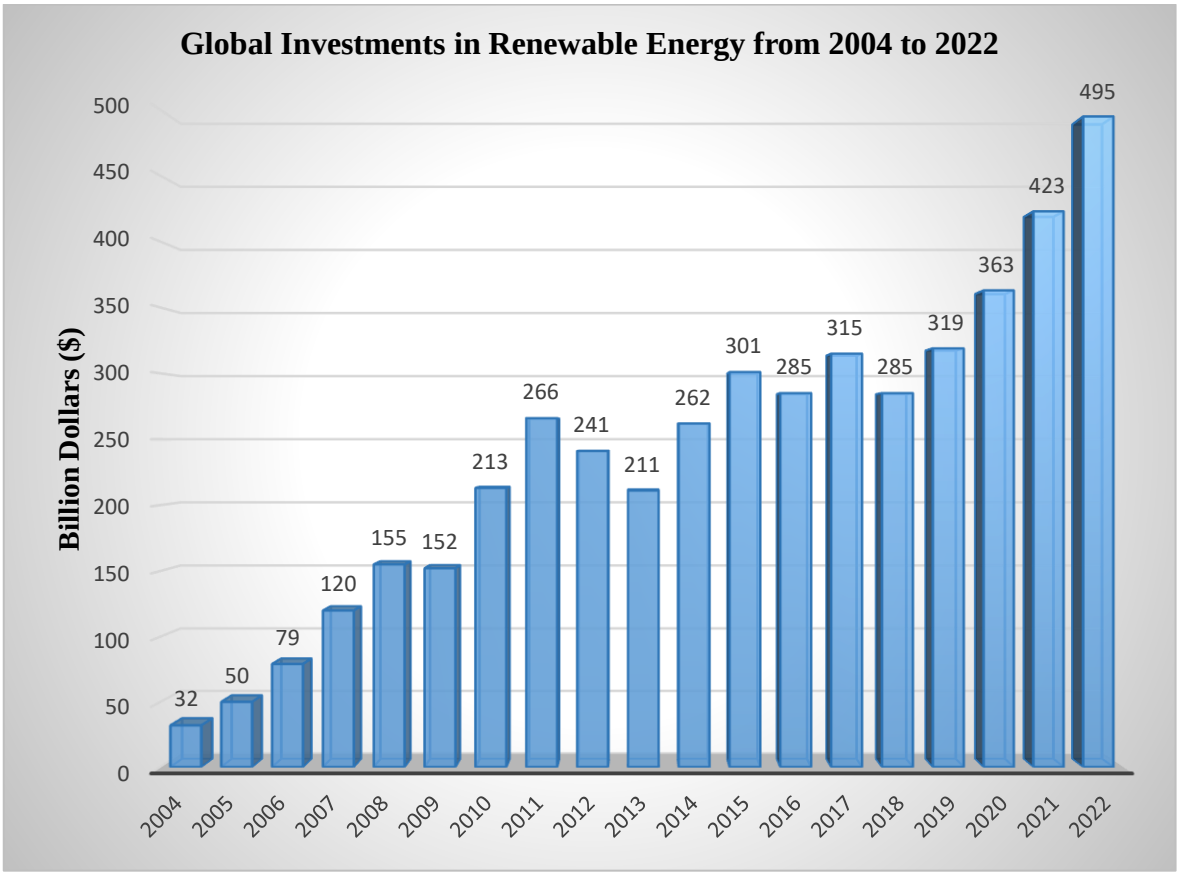


Figure 2.4. Global Investments in Renewable Energy from 2004 to 2022 (Statista, 2023)

When the graph is examined, it is clearly seen that the volume of 32 billion dollars in 2004 increased approximately 15.5 times in 2022. Basically, by looking at this Figure 2.4., it can be easily understood in which direction energy investments are evolving. Compared to the previous year, there was a growth around of 17%. Payments which were 423 billion United States Dollar (USD) in 2021, reached 495 billion USD level in 2022. The vital enhancement in RES funding specify that the industry has extended greatly. Thanks to giving policy support for renewable sources has accelerated exponentially. According to special roadmap report which was called Net Zero Emissions by 2050 Scenario (NZE) published by IEA indicates as in 2050 RES investments will grow 4 times compare with 2020 (IEA, 2021). If the aim is achieved, more than 85% of buildings will in zero carbon status, more than 90% of heavy industrial companies will low emission level and almost 70% of electricity generation will provide from solar PV and wind turbines globally. It will prevent rising of global temperature around 1.5 °C. Some countries have made great evolution in generating renewable energy. Iceland leads the area with 86.87% of its energy manufactured from renewable sources. Norway is the other country coming after Iceland with the most renewable energy percentage of

71.56% its energy coming from renewable sources. 46.22% of the total energy produced by Sweden is from renewable sources. Most of countries have realized that reducing carbon emission and descending climate change is mandatory by turning to clean and green energy sources. Developments in technology for this scope, public awareness have contributed to the growth of worldwide (Anonymous1, 2023). When viewed from a different perspective, the sorting changes. Installed renewable energy capacity datas of the countries are shown in figure 2.5.

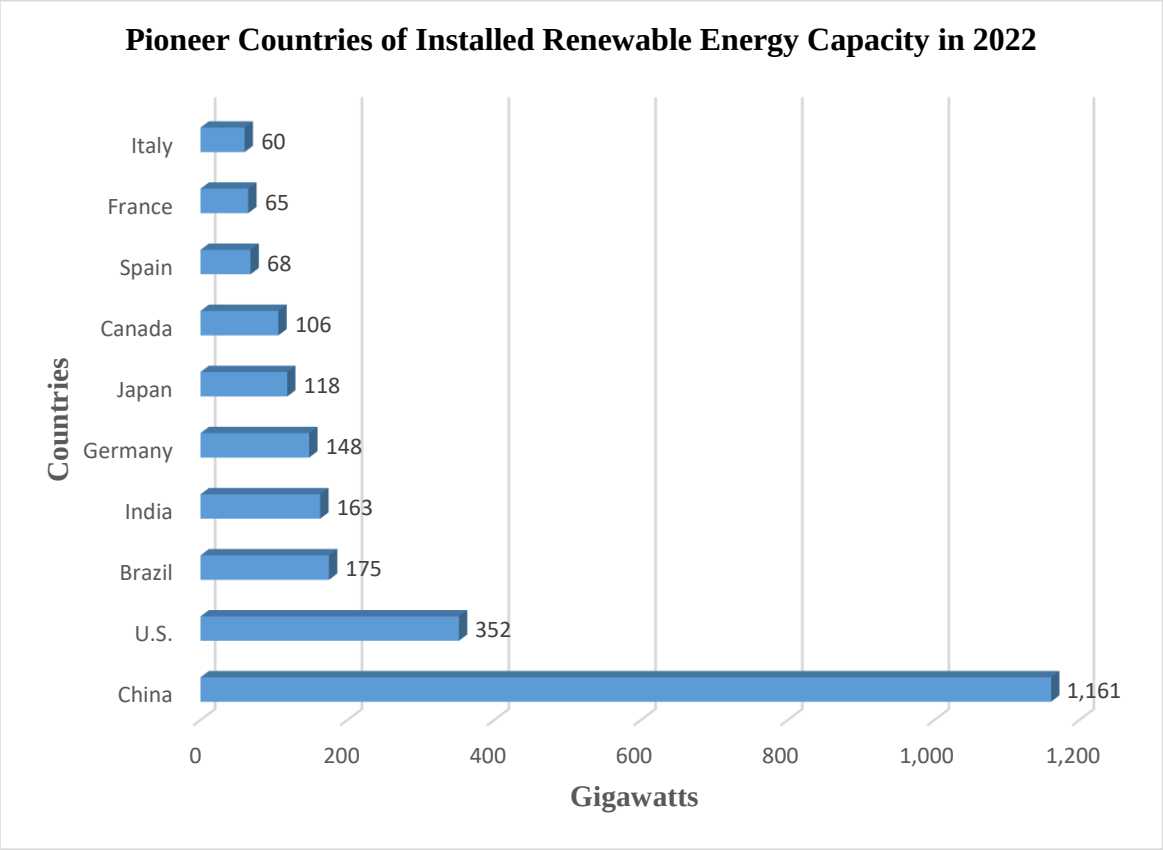


Figure 2.5. Pioneer Countries of Installed Renewable Energy Capacity (IRENA, 2023)

As can be seen from the figure 2.5, Republic of China is the leader in installed power capacity in 2022. It is understood that China is far ahead of other countries in terms of installed capacity in the renewable energy field. Thanks to both increasing its production capacity and support they provide to technological development through research project. After that, America comes with a capacity of 352 GW. Brazil and India also have important initiatives in this scope. In addition, the potential case of European countries and Japan were also mentioned in figure 2.5. It can be said that the countries of the world are in a robust competition for establishing a renewable energy zone in terms of sustainability and commissioning it as soon as possible.

In this study, solar energy will be used as the energy source. Solar energy is one of the best choice for clean, sustainable energy source and can be found in abundance everywhere. The Earth receives enough irradiation in 90 minutes to meet the planet's energy demand for 1 year from the

sun (Guangul et al., 2019). The source to be used has many advantages and some disadvantages compared to other sources. In theory, approximately four million exajoules (1 EJ = 10^{18} J) of solar energy reaches the Earth annually, $5x10^{4}$ EJ of which is considered to be easily extractible (Kabir et al., 2018). Around 885 million TWh collect in the earth's surface in a year which is equal to 4200 times the energy that humankind would consume in 2035. If 1 percent of this energy coming from sun can be captured with the help of PV, the energy supply problem will be eliminated without requiring additional sources in the world (H.Weldekidan et al., 2018). Solar energy can differ everywhere in the world. This situation is directly reflected in the irradiation levels. In other words, the irradiation levels of different place are also separated. Another advantage is to eco-friendly. Utilizing of solar energy quite descends the negative impact of carbon emissions. Moreover, this type of energy does not release detrimental gases that could devastation the environment. PV panels are suitable for recycling. It shows that harvesting energy type from sun is a non-polluting, reliable and clean source of energy (Weldekidan et al., 2018) . Although the initial investment cost for the system is high, it almost does not require maintenance for about 10-15 years. This source is used either directly or indirectly for various implementation that are not only restricted to industry processes but also feasible other areas such as, drying of agricultural parts, battery electric vehicle, solar powered refrigerator, water heating and pumping, solar cooking. Cooking with solar energy can often be used in areas where there is plenty of radiation and no electricity (Sansaniwal et al., 2017). Numerous kind of solar cookers invented such as box cookers, parabolic reflector, solar vacuum tube cooker, spherical reflector. In addition to all the advantages are mentioned, every new investment brings with it a new business opportunity for humanity. Thousands of people are employed in sales, quality, maintenance and repair, fault detection and production departments in companies producing in this scope all over the world. Although generating electricity using the sun has many advantages some of which are mentioned, it also has some disadvantages. Producing power from solar is only available in day time because of solar irradiations have only come in day time. PV panels and other components can only convert solar energy when there is sunlight. If consumer wants to Uninterruptible Power Supply (UPS), battery applications have to use with solar systems. However, the UPS systems ensure additional cost that rise the installation cost of the system (Anonymous2, 2018). This makes the system more expensive than before. The another disadvantage of this system is solar panel efficiency. The rate of efficiency is so low compared with other energy resources. PV efficiencies are generally in the range of 14-22% depend on quality of producion company. Together with technological and academic developments, the ratio of efficiency is tried to be increased (Abd-Elhady et al., 2016). Since panel efficiency is low, investors require empty and large areas for producing solar energy. Air temperature factor is also crucial in area selection. The efficiency of PV panels may decrease at so high temperatures. This will cause a reduction in energy manufacturing (Moharram et al., 2013).

In the solar energy sector, Republic of Turkey is also developing in parallel with the world, both on investment side and on the production side every passing year. Besides the funds made, it is

located in a special region that receives plenty of sun as its geographical location, which makes Republic of Turkey a critical player in the market. Figure 2.6. also explains the solar radiation map of Turkey. This map was taken from the Ministry of Energy and Natural Resources.

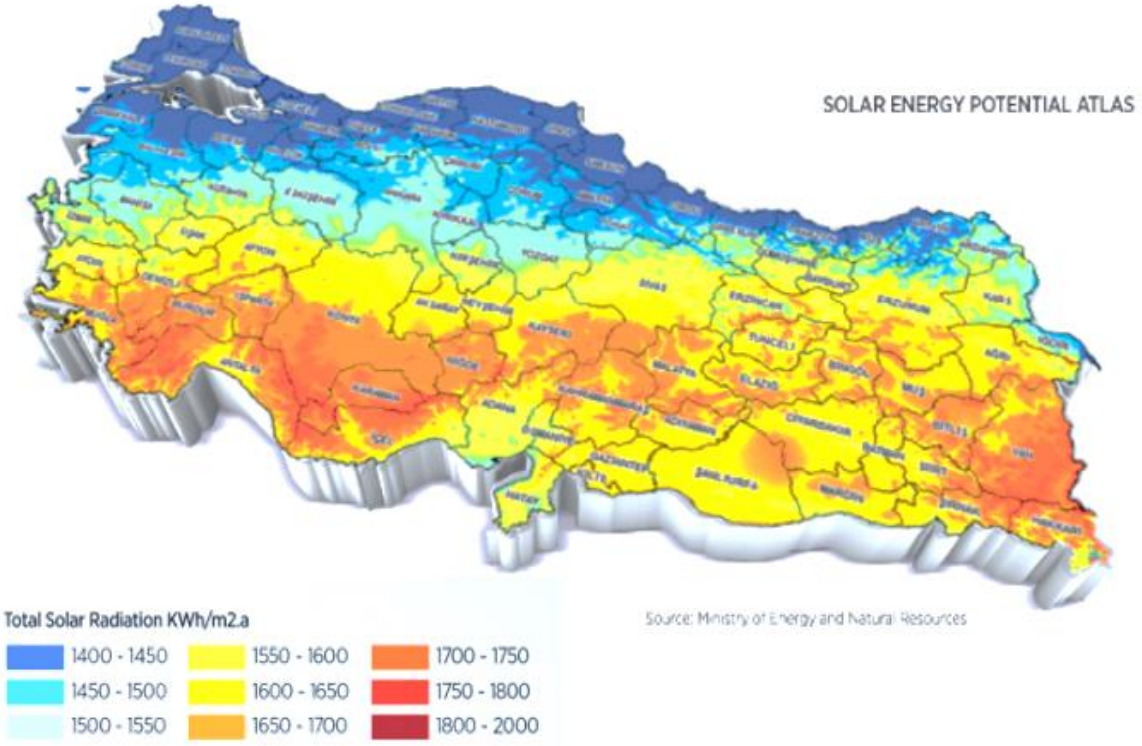


Figure 2.6. Solar Radiation Map of Turkey (Ministry of Energy and Natural Resources, 2023)

Deeply investigating of solar potential for Republic of Turkey, annual average in daylight duration is 7.5 hours and average irradiation is 1527.46kWh/m^2 which is greater than most of Europe (Ministry of Energy and Natural Resources, 2023). Due to the fact that it is a country with a high investment capacity, the installed solar energy is enhancing year to year. The 2023 report of International Renewable Energy Agency (IRENA) clearly expresses the increase in Turkey's installed power capacity for the last 4 years. Installed capacity was 5.9 GigaWatt (GW) in 2019. This situation has ascended to 6.66 GW in 2020 despite the pandemic disaster. Looking at following years, it is seen that the total installed capacity of solar energy reached 7.8 GW at the end of 2021 and finally 9.4 GW in 2022 (IRENA, 2023). When annual changing rates are examined, there was an incrementation of 12.88% in 2020, 17.11% in 2021 and 20.51% in 2022 compared with previous year. Based on these datas, it can be predicted to reach 11.5 GW by the end of 2023.

2.2. Overview of Photovoltaic Technologies

People have been focusing sunlight since ancient times. Reflecting with mirrors to light a fire can be described as an example. In this context, solar energy has been used as a substantial resource for thousands of years. Photovoltaic, is called a way using with solar cell in order to harvest

electrical energy from sun. All of the history began in 1839, together with a French well known scientist Alexandre Edmond Becquerel discovered the photovoltaic effect which was a system that gained a voltage or electric current when exposed to radiation (Mughal et al., 2018). The invention is basically the working system of a solar cell. Researches has been concentrated in this scope. William Grylls Adams and his student Richards Day observed the photovoltaic effect in solidified selenium and released a paper that is related to selenium cell in 1877 (Adams and Day, 1877) . After that, in 1883 Charles Fritts who developed the first solar cell using selenium and the device ensured 1% efficiency. Fritts informed that the selenium module produced continuous current when is exposed sun radiation (Fritts, 1883). In 1905, the photoelectric theory, which would leave its mark on history, was proposed by Albert Einstein. It explained the correlation between photons energy and its frequency. When photons of light are sent to the surfaces of some materials, they show a photoelectric effect. This study brought a revolution on science and Albert Einstein was award Nobel Prize branch of Physics (Lameirinhas et al., 2022). Following these studies, the photovoltaic effect began to be tested on some materials. In 1932, Audobert and Stora used Cadmium Selenide in order to observed photovoltaic effect. This material is currently used in photovoltaic technology (Abbe and Smith, 2016). Since PV cells made with selenium were low efficiency, scientists were investigating for a new more efficient material. In 1954, American physicist Darly Chapin, who was working at Bell Laboratory, invented the first silicon based PV cell. The invention provided approximately 6% efficiency. This rate was the best level achieved until the year of 1954 (Chapin et al., 1954). Thanks to technological developments, America's second satellite, which is called as Vanguard 1 was launched by National Aeronautics and Space Administration (NASA) in 1958. This is the first satellite powered by solar cells and it entered orbit region successfully. It has the ability to capture sunlight (Easton and Votaw, 1959). It contains 0.1 W 100 cm^2 solar panel. After some developments, the first solar panel that gave above the 10% efficiency developed by A. Catalano with amorphous silicon thin film (Catalano et al., 1982). Over the time period to date, efficiency levels have increased year by year and panel installation cost have started to decrease. With the entry of the Republic of China into the sector, panel costs were reduced from 5 dollars to 0.3 dollars per watt rapidly. Looking at recent years, 32.5 efficiency has been achieved with silicon-perovskite tandem solar cells utilizing the single junction doped method from Germany in 2022. Moreover, multi junction method is also used to achieve high efficiency. In 2022, Frank Dimroth designed a four junction solar cell and achieved 47.6% efficiency. It is the most updating world efficiency record for solar energy system (Jacobo, 2022).

Basically, the combined two semiconductor zones represent the inside structure of PV cells in figure 2.7. This type semiconductor can be p-type or n-type. The part type is strictly depending on the direction of electrons. A potential difference occurs in the depletion zone and it is the basis of electricity generation.

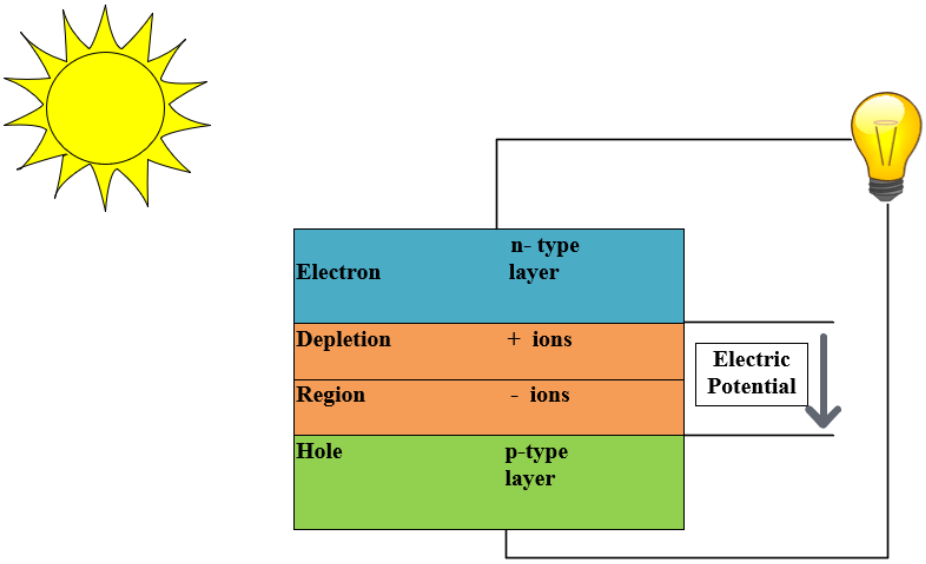


Figure 2.7. PV Cell Representation Including Both Layers (p-type and n-type)

Not only silicon but also different types of materials can be used in the production stage of photovoltaic cells. These materials change according to technological development. Several PV cells can be characterized into four main categories as generation levels. The major target of each generation is to minimize fabrication costs and enhance conversion efficiency.

2.2.1. First Generation PV Cells

The first generation PV cell fabrication were made based on Silicon. It combined technical information and raw materials supplied from industry of microelectronics. Cells were doped with phosphorus and boron. It constructed from p-n junction cells and thick crystalline layers. Nowadays, silicon cells constitute more than 80% of the world's capacity. Due to many reasons, silicon based cells are leader in market such as silicon dioxide is abundant material in earth. It has energy gap of 1.1 eV quite close to ideal solar cell band gap, being non-hazardous to environment, being long life and efficient, no need too much money for maintenance. This type of production is divided into three categories which are called as Monocrystalline Silicon (M-Si), Polycrystalline Silicon (P-Si) and Gallium Arsenide (GaAs) (Suman et al., 2020). The benefits and deficiencies of using these raw materials are widely shown in table 2.1.

Table 2.1. Benefits and Deficiencies of First Generation Solar Cells

Type of Solar Cell	Benefits	Deficiencies
M-Si	Stability High efficiency Long service life It requires minimum amount of space	Loss of material Sensitive to temperature Absorption problem High production cost
P-Si	Fabrication procedure is basic Being profitable Decrease the waste of silicon Higher extraction	Efficiency is less Require a larger place Lower architecture integration Affect their lifespan due to heat Being unaesthetically Average lifespan is low
GaAs	High Stability Robust for temperature sensitivity Better absorption Higher efficiency	High production cost Being rare material (Gallium) More solid compare to Silicon Less thermal conductivity More expensive raw material

In addition to Table 2.1. the average efficiency of M-Si is between 15-24% and their life cycle is approximately 25 years. P-Si type of solar cell has 10-18% efficiency and their lifetime is approximately 14 years. GaAs is the most efficient type with a rate of 28-30% and its average lifespan is around 18 years (Suman et al., 2020).

2.2.2. Second Generation PV Cells

Another step in the development of PV cells is called as second generation types. The main targets of second generation are to reduce material cost by using thin film. These technologies are single junction devices and achieve to utilize less part with same efficiency with first generation. It comprises some of raw material which is referred as Amorphous Silicon (A-Si), Cadmium Telluride (CdTe), Copper Indium Gallium Selenide (CIGS) (Britt and Ferekides, 1993). Second generation PV ensures good pay back times after minimizes commissioning cost with regards to other types.

According to silicon wafer manufacturing, thin film process tools and fabrication lines include deeply exclusively know how. Accessing the special information is both difficult and expensive.
For this reason, the improvement of second generation PV cell technologies is slower than others (Bagnall and Boreland, 2008). The advantages and disadvantages of using these raw materials in second group for PV fabrication are deeply shown in Table 2.2

Table 2.2. Benefits and Deficiencies of Second Generation Solar Cells

Type of Solar Cell	Benefits	Deficiencies
A-Si	Affordable Easy to find Non toxic Strong absorption Light weight	Low efficiency Doped difficulty Poor life time Fast degradation
CdTe/CdS	High absorption Required less material Easy to find for Cd Easy to manufacturing	Less efficient Cd is highly toxic material Sensitive to temperature Rare to find Td
CIGS	Required less material High efficiency Low carbon footprint Being recycled	Very expensive to buy Being unstable Sensitive to temperature Unreliable Rapid degradation

Moreover, the type of A-Si has an average efficiency of 5-12% and 25 years lifespan approximately. In PV cells made from another raw material called as CdTe/CdS, it provides a higher efficiency around of 15-16% compared to A-Si. The lifetime of this product is around 20 years. CIGS, the last raw material type of the second generation, can reach around 20%, which is the highest efficiency level of its type. However, their lifespan is lower than others and they expire in 12 years (Suman et al,2020).

2.2.3. Third Generation PV Cells

Researches are carried out to eliminate the shortcomings of other generations have created a new generation which is called third generation. This type of PV cells are able to exceed the

Schockley-Queisser border of 31-41% for a single bandgap solar cells. It includes new material referred as nanomaterial and chemical compound. The parts are innovative and combine lots of technological developments (Green, 2001). Third generation consists of Dye-Sensitized Solar Cell (DSSC), Quantum Dot Cell (QDS), Organic and Polymer Solar Cell (OPSC), PVSC (Perovskite Cell) and Multi Junction Cell (MJC). It consists of wide range applications from inexpensive low efficient to expensive high efficient. This kind of cells are indicated as emerging concepts because of their poor market diffusion (Dunlap et al., 2019). However, there is a research archive of over 20 years in this scope. The profits and deficiencies of utilizing the type of raw materials are indicated clearly in Table 2.3.

Table 2.3. Benefits and Deficiencies of Third Generation Solar Cells

Type of Solar Cell	**Benefits**	**Deficiencies**
DSSC	Inexpensive Run in low light Operate low internal temperature Robust and long life	Toxic low efficiency Temperature unstability
QDS	Low cost production Require low power	Toxic in high degree Degradable
OPSC	Low processing cost Light weight Flexible Thermally stable	Low efficiency to harvest energy
PVSC	Inexpensive Simple construction Light weight High efficiency Flexible	Being unstable
MJ	High efficiency	Complex Being overpriced

In addition to table 2.3, DSSC type is a low cost but inefficient raw material type. The average efficiency of solar cells which is made from this material is around 5-20%. This efficiency level is in range of 11-17% for QDS type raw material, 9-11% for QPSC kind of part and 21% for

PVSC. Finally, when MJ is examined, it is stated clearly that the most efficient level is achieved in this type around 36% (Pastuszak and Wegierek, 2022)

2.2.4. Fourth Generation PV Cells

Fourth generation PV cells are referred as hybrid inorganic cells. They unit the low cost and flexible of polymer thin films, with the durability of organic nanostructures such as, graphene, carbon nanotubes. Some researches express as this kind of material can become the future of photovoltaic systems (Wu et al., 2020). The last type of generation solar cell explained in Table 2.4.

Table 2.4. Benefits and Deficiencies of Fourth Generation Solar Cells

Type of Solar Cell	Benefits	Deficiencies
Carbon Nanotube	Superior inside features Low cost Environmental friendly Easy to find in nature	Being impurity Non uniformity in structure Hydrophobicity Tendency to bundle
Graphene	High carrier mobility Low resistivity Long lifetime Ensure stability	Complex for commissioning Adhesion of graphene thin film Poor hydrophilicity

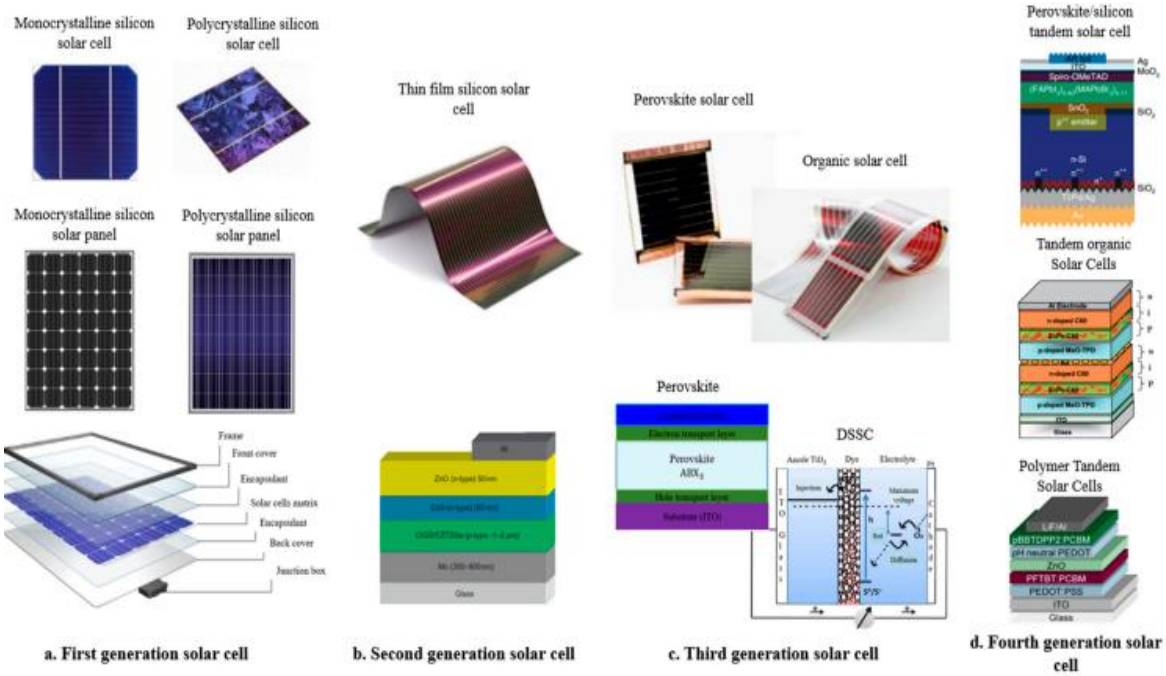


Figure 2.8. Four Different Generation Types and Inside Structures (Sarr et al., 2023)

2.2.5. Equivalent Circuit and Mathematical Expression

Creating electrical circuit models of each system is crucial for their reliability. Both design improvements and I-V curves can be easily extracted thanks to the circuit model. For a PV architecture, accurate modeling is vital. The best way to observed the attitude of the PV system is to adopt an equivalent circuit. Over the decades, important progress is applied in order to take more information of mathematical modeling. Many different types of model recommended in literature but two most well-known are called as Double Diode Model (DDM) and Single Diode Model (SDM). As it is understood from name, equivalent circuit models include diodes usually (Humada et al., 2016). Gaining of an accurate parameter from PV models is great significance for PV cell performance, design progressing, optimization of fabrication, quality observation. Firstly, when the DDM equivalent circuit is examined which is contained two diodes, the schematic structure of the circuit can be easily seen in figure 2.9. It involves five parameters which is called as light generated current source, two diodes for reverse saturation current, series resistance, shunt resistance. In this model, the source that provides the current produced by PV cell, diode 1, diode 2 and shunt resistance are connection parallel to each other. Series resistance is connected in series to the entire circuit.

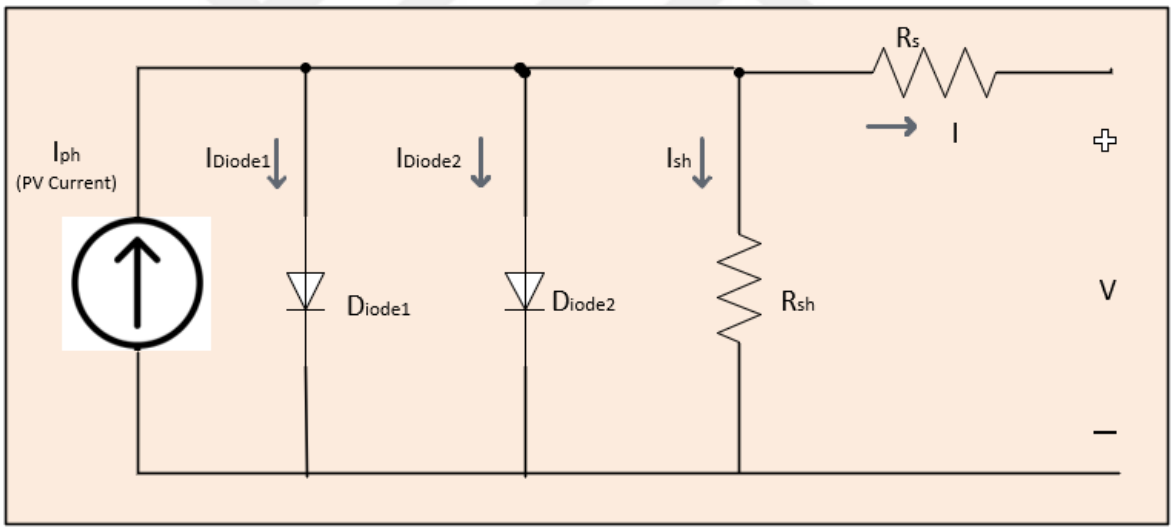


Figure 2.9. Double Diode Solar Cell Equivalent Circuit

Although double diode model provide advantage in terms of system performance, the model includes implicit nonlinear seen parameters. This situation increase complexity of DDM model. It led to more difficulties for cases such as long computational time, calculation of initial parameter, algorithm complexity (Nguyen-Duc et al., 2020). Therefore, SDM model can contain both accuracy and simplicity. Additionally, using one diode instead of two also offers a cost advantage for the system.

In this thesis, SDM equivalent circuit has been applied in the Photovoltaic Cell representation due to advantages. The model is given obviously in figure 2.10.

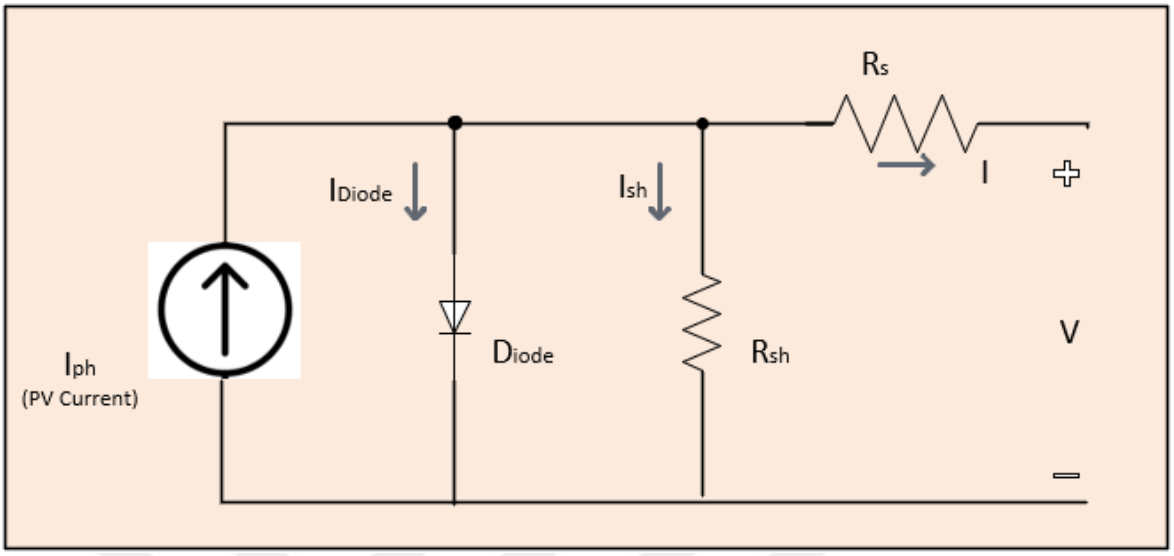


Figure 2.10. Single Diode Solar Cell Equivalent Circuit

The meanings of the basic parameters in circuit are given below (Ghosh and Yadav, 2021):

- I_{ph} is referred producing current from PV
- I_{diode} is meaning of diode saturation current
- R_s is called as series resistance of PV module
- R_{sh} is indicated as shunt resistance of PV module
- I is stated as output current
- V_t is thermal voltage
- A is the diode quality factor
- I_s is called as reverse saturation current
- T_{stc} is called as temperature at Standard Test Condition (STC) in Kelvin
- I_{array} is referred as module current constructed N_s series cell
- I_{array} is stated as array current constructed N_p parallel cell

General equation of I-V characteristic for SDM based PV cell is stated as follow:

$$I = I_{ph} - I_{Diode} - I_{sh} \tag{2.2.5.1}$$

$$I_{Diode} = I_s * \left[exp\left(\frac{qV + qIR_s}{AkT}\right) - 1\right] - \left(\frac{V + IR_s}{R_{sh}}\right) \tag{2.2.5.2}$$

$$V_t = \frac{AkT_{stc}}{q} \tag{2.2.5.3}$$

$$I = I_{ph} - I_s * \left[exp\left(\frac{qV + qIR_s}{AkT}\right) - 1\right] - \left(\frac{V + IR_s}{R_{sh}}\right) \tag{2.2.5.4}$$

PV equivalent cell equations were examined. When the diode current in equation 2.3.2 is written in 2.3.1, equation 2.3.4 is obtained easily. Moreover, the module current that includes Ns series cell can be expressed by Eq. 2.3.5 and array current that includes Np parallel cells and Ns series cell can be expressed by equation 2.3.6

$$I_{module} = I_{ph} - I_s * \left[exp\left(\frac{qV + qIR_s}{N_s AkT}\right) - 1\right] - \left(\frac{V + IN_s R_s}{N_s R_{sh}}\right) \tag{2.2.5.5}$$

$$I_{array} = N_p I_{ph} - N_p I_s * \left[exp\left(\frac{qV + qIR_s}{N_s AkT}\right) - 1\right] - \left(\frac{N_p V + IN_s R_s}{N_s R_{sh}}\right) \tag{2.2.5.6}$$

In addition to these equations, there are also some parameters and their equations for photovoltaic cells and they contribute to efficiency. Fill Factor (FF) is well known performance parameter which is calculated by dividing the maximum power by the open circuit voltage and short circuit current. It is stated by equation 2.3.7

$$FF = \frac{P_{MP}}{V_{oc} x I_{sc}} \tag{2.2.5.7}$$

Using the equation of 2.3.7, efficiency can be gathered with help of eq. 2.3.8

$$Efficiency_{(n)} = \frac{FF\ x\ V_{oc} x\ I_{sc}}{P_{input}} \tag{2.2.5.8}$$

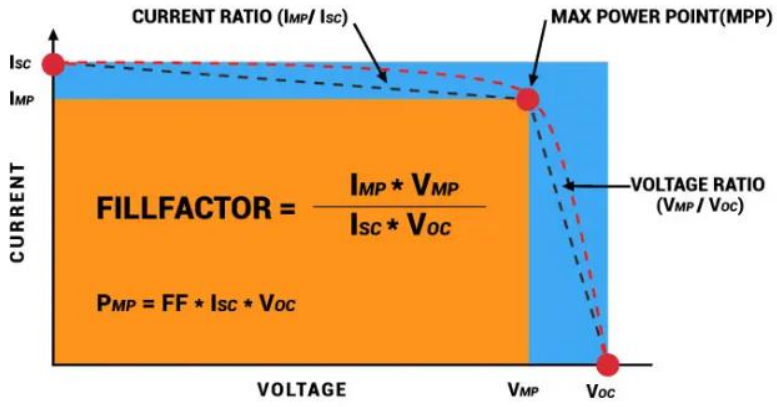


Figure 2.11. Fill Factor in I-V Characteristic Curve (Mollick, 2022)

2.3. Grid Connection Standards

International regulations regarding harmonic levels, power quality, power drops and electrical system architecture in grid connected PV systems have been specified. The different rules created by various institutes regarding this subject. However, the rules defined by two internationally recognized institutes are widely used (Çelik, 2015). They are determined by the Institute of Electrical and Electronics Engineers (IEEE) and the International Electrotechnical Commission (IEC). Standards are called as IEC 61727-2004, IEEE 1547-2018, IEEE 929-2000, IEEE 519-1992, EN50160, IEC 61000-4-7. Based on these documents are provided safety, reliability and well performance for various situation of electrical network systems and their connection with grid. Before making a grid connection, the effects of these standards should be thoroughly understood and the given conditions should be applied one by one to prevent any problems. The regulations of Republic of Turkey related with grid connection are also same as European norms. In Turkey, these standards are specified by Electricity Market Regulatory Authority (EMRA).

According to latest report of EMRA in July of 2023 the important parts related with frequency are listed below (EMRA, 2023):

- Rated frequency in Turkey is given 50 Hertz (Hz).
- Production facilities with using wind turbine or photovoltaic systems have to capable of generate their full rated power as long as grid frequency is between 47.5 and 50.3 Hz.
- If the grid frequency exceeds 50.3Hz, the relevant facilities must provide %4 speed reduction.
- If the grid frequency is 51.5 Hz the system should be completely disabled.
- In addition to these operating conditions, the additional wind turbine or solar panel group should not be activated when the grid frequency is above 50.2 Hz.

Wind and solar power plants must keep the processing time as specified in table 2.4 in order to work properly in changing frequency bands.

Table 2.5. Operating Time in Frequency Range (EMRA, 2023)

Frequency Range	**Minimum Operating Time**
$50.5Hz \leq f < 51.5Hz$	1 hour
$49Hz \leq f < 50.5Hz$	Continuously Operating
$48.5Hz \leq f < 49Hz$	1 hour
$48Hz \leq f < 48.5Hz$	20 minutes
$47.5Hz \leq f < 48Hz$	10 minutes

In distribution systems, there are certain limit values for harmonics as well as frequency. Harmonic limits are vital criteria to prevent any distortion and to increase system performance. According to IEC 61000-4-7, harmonic distortion cannot reached 5% for both the current and voltage. Moreover, it is expressed comprehensively in table 2.5 below

Table 2.6. Current Harmonic Distortion Limits (Teke, 2011)

Individual harmonic order (Odd harmonics)						
I_{SC}/I_L	**h< 1**	**11≤ h < 17**	**17≤ h < 23**	**23 ≤ h < 35**	**35 ≤ h**	**TDD**
Below 20	4.0	2	1.5	0.6	0.3	5.0
Between 20 - 50	7.0	3.5	2.5	1.0	0.5	8.0
Between 50-100	10.0	4.5	4.0	1.5	0.7	12.0
Between 100-1000	12.0	5.5	5.0	2.0	1.0	15.0
Above 1000	15.0	7.0	6.0	2.5	1.4	20.0
Even harmonics are restricted to 25% of the odd harmonics limits above						
Current distortions that results in a DC offset, e.g., half-wave converters, are not allowed						
All power generation equipment is limited to these values of current distortions, regardless of actual I_{SC}/I_L						
I_{SC} is meaning of short circuit current at point of common coupling I_L is called as load current at point of common coupling						

2.4. Switched Mode DC-DC Converter

The power which is generated from PV panel is strictly depend on atmospheric conditions. When the weather situations change, the power level can also alter. Photovoltaic facilities operate at low power efficiency for this reason. Researchers dealing with this issue have widely used DC-DC Converter applications both to use algorithms that will keep the power at maximum and to convert the power drawn from the PV at a certain efficiency rate. Since 1920s, the DC-DC converter device was developed to place with solar PV units (Raghavendra et al., 2019). Some papers which was published in the literature, it is also called Switched Mode DC-DC Converter. Some papers which was published in the literature, it is also called Switched Mode DC-DC Converter (Padhee et al., 2016a). Switch mode converters are basically structures which are triggered by a duty cycle as a result of comparing two signal. These signals are called as carrier and reference. In addition, it can be seen from the literature review that power electronic converters are often used in solar applications.

In the paper investigated in literature review (Lui and Li, 2006), a DC-DC converter was used to transfer producing power to multiple energy storage elements. In addition, the soft switching technique was applied with the method which was developed in this study.

Another paper investigated in literature review (Naayagi et al., 2012), in order to reach high power levels in aerospace applications, DC-DC converters have been used. The Dual Active Bridge type of bidirectional DC-DC converter was designed on the basis of proposed model.

In the paper investigated in literature review (Shahin et al., 2010), a DC-DC converter was used to provide high voltage ratio into fuel cell applications. Two interleaved step up converter is chosen and the results are compared.

In the paper investigated in literature review (Mishra and Singh, 2018), DC-DC converter is located in the system that provides energy to the pump motor used in agriculture sector. The continuous conduction mode (CCM) operation is used in converter to reduces the tension on its components. It is stated that the mode helps to improve system performance.

In the paper investigated in literature review (Khan et al., 2015) the performance analysis and comparison of two different kind of bidirectional dc-dc converters for plug in and hybrid electrical vehicles has been conducted. Converter designs are often used as one of the trending topics in the academic areas for vehicle to grid (V2G) and grid to vehicle (G2V) applications.

2.4.1. Classification of DC-DC Converter

The DC-DC converter family, which has an important place among power electronic devices, is a highly effective structure for DC voltage regulating and increasing efficiency in renewable energy systems. There are various types of devices found in the literature. The selection of appropriate converter for PV facility is a critical factor that makes a significant contribution to the overall system performance. According to the nature of device, ease of control, accuracy in response and speed of response are also quite important for performance. All these parameters should be taken into account and thoroughly examined and the useful type of converter should be selected (Mumtaz et al., 2021). Nowadays, various type of converter devices are preferred to arrange the input voltage based on desired requirements. DC-DC converters can be classified into two separate categories are called as isolated and non-isolated types. Isolated converters comprise transformer in order to ensure galvanic isolation between the input side and output side (A. Gopi and R. Saravanakumar, 2014). The output of the system can have positive or negative polarity depending on internal structure. It can run for a wide range of inputs and produce a stable output. Both categories include their own advantages and disadvantages. Isolated converters suffer from significant issues such as leakage inductance, core saturation, high voltage spikes, additional cost due to huge size compared to other type. On the other hand, non-isolated topology does not include any galvanic isolation among input and output side. Instantaneous changes occurring on the input side directly affect the output (Navamani et al., 2018). The commonly types of converters used in the literature are shown in figure 2.12.

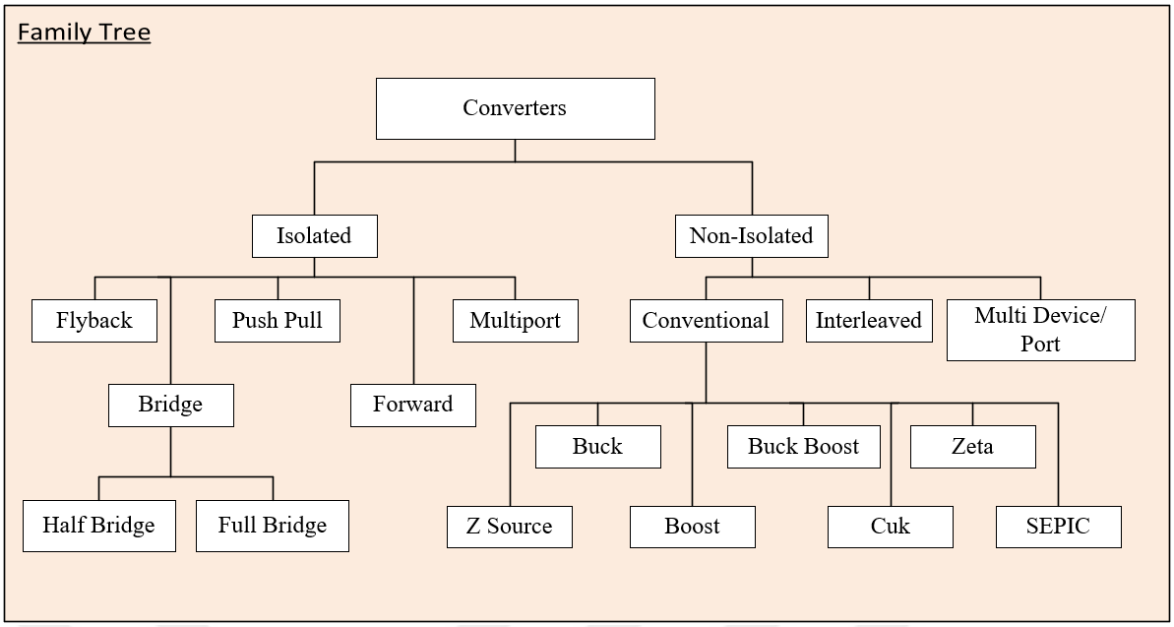


Figure 2.12. Different Topologies of DC-DC Converter

These various topologies have some advantages and disadvantages. Since the converter types to be used in this thesis are member of non-isolated group, the pros and cons of transformerless topologies are given in table 2.6.

Table 2.7. Benchmark of Non-Isolated DC-DC Converter Topologies (Mumtaz et al., 2021)

Topology	**Benefits**	**Deficiencies**
SEPIC	Low complexity Ease to control Non-inverting output	Hard to arrange duty cycle Low voltage gain
Buck Boost	Feasible for PV low power applications Ease to control	High ripples in output Discontinuity for output current Voltage imbalance
Cuk	Ease to control Utilized capacitor for energy storage	Low efficiency Reversed output polarity
Zeta	Non-inverting output Feasible for high power applications	Medium complexity Unidirectional power flowing Voltage imbalance
Z Source	Non-inverting output Ease to control	Unidirectional power flow Discontinuity for input current

2.4.2. Boost Converter

Power electronics applications have brought a revolution in the advancement of technology in many areas such as energy transmission and conversion, energy storage, electrical and hybrid vehicles, renewable energy. While energy conversion is being provided, DC-DC Converters have a significant impact. Besides all types of converter, the widely utilized kind is the Boost converter. It is called as step up converter due to ensures a higher output voltage compared to the input voltage. In many PV applications, the magnitude of voltage on the load side needs to be higher than the generated voltage from PV. Boost converters are used for this purpose (Gopi and Sreejith., 2018). A traditional boost type converter has comprised of an inductor, a diode, a transistor and an output capacitor being parallel to the load. The switching devices can be an Insulated Gate Bipolar Transistor (IGBT) or Metal Oxide Field Effect Transistor (MOSFET) (Adnan et al., 2017). Conventional DC-DC Boost Converter circuit design is indicated in figure 2.13

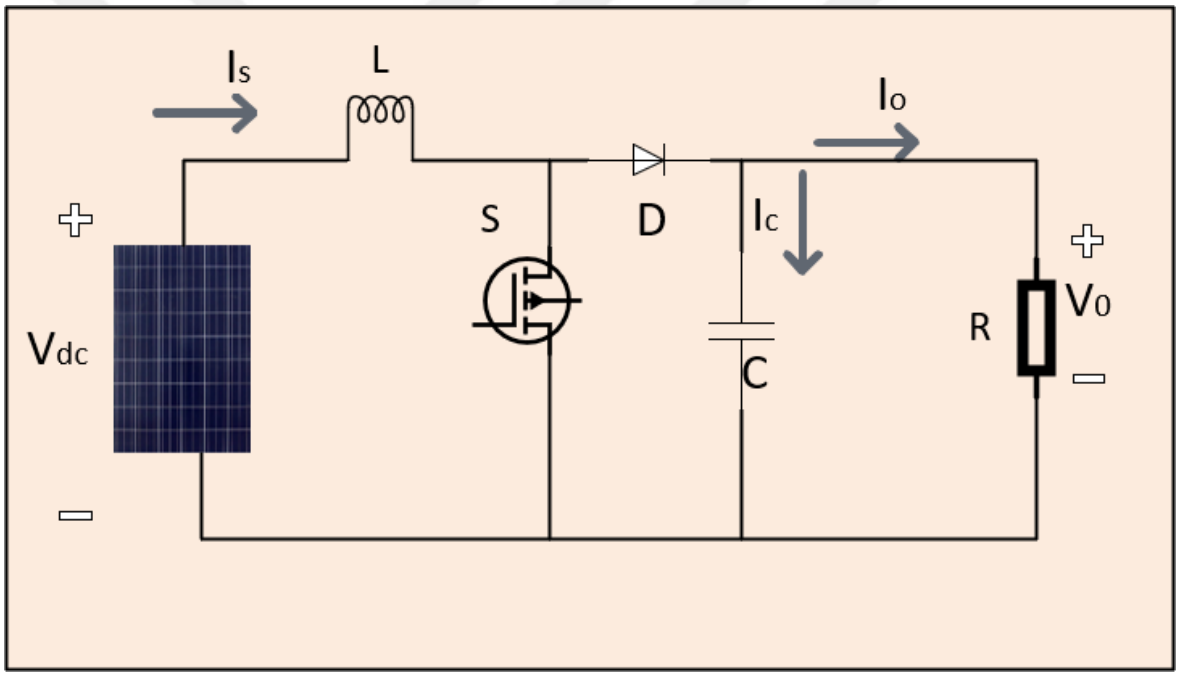


Figure 2.13. Circuit Analogy of Boost Converter

The symbols shown in figure 2.13 can be listed as follow:

- V_{dc} is referred as extracted voltage from photovoltaic.
- V_o is meaning of desired output voltage or load voltage.
- S is called as transistor can be MOSFET or IGBT.
- D is named diode, it is a device for transmission of current.
- I_C is expressed the current passing through the capacitor.
- C is stated as capacitor, one of the main component for boost circuit.
- I_S is referred as input current generated from photovoltaic.

- L is called as inductor, another main component for boost circuit.
- I_O is meaning of output current. It passes through the load.
- R can be indicated as load of the circuit.
- Switching frequency is symbolized as f_s.
- ΔI_L estimated inductor ripple current, in the design procedure, this parameter is taken 10% of output current.
- ΔV_o desired output voltage ripple, in the design procedure, this parameter is taken 1% percentage of output voltage.
- $Duty\ Cycle$ the ratio of time a circuit is on compared to one period. It arranges PWM control signal for desired V_o

Boost converter parameter calculations are made with the following formulas:

$$L = \left(\frac{V_{in}(V_o - V_{in})}{\Delta I_L x f_s x V_o}\right) \quad (2.4.2.1)$$

$$\Delta I_L = \left(\frac{(0.1) x I_o x V_o}{V_{in}}\right) \quad (2.4.2.2)$$

$$Duty\ Cycle = \left(1 - \frac{V_{in}}{V_o}\right) \quad (2.4.2.3)$$

$$\Delta V_o = (0.01 x V_o) \quad (2.4.2.4)$$

$$C = \frac{I_o x Duty\ Cycle}{f_s x V_{oc} x \Delta V_o} \quad (2.4.2.5)$$

$$R = \frac{V_o}{I_o} \quad (2.4.2.6)$$

Boost converter can be set to operate in two different modes. If switch is closed condition (on state) and diode is open condition (off state), switch permits the flow of current through it. All of current will pass through the closed way involving inductor L, switch S and dc source. If switch is open condition (off state) and diode is closed condition (on state), diode permits the pass of current through itself due to switch blocks the current flowing.

2.4.3. Bidirectional Buck Boost Converter

Another type of converter which used in this thesis is the Bidirectional Buck Boost Converter. It can be applied in many applications diversely. Due to this reason, the studies of bidirectional power converters has become a crucial field in power electronics research. As reversed to traditional unidirectional converters, power flows in both directions inside bidirectional converter. Current poured forward or reverse direction according to demand. These kind of converters are flexible and commonly utilized in electric vehicles. It can be also use for uninterruptible power supplies (UPS), fuel cells, wind turbines, photovoltaic systems, plug-in hybrid electric vehicle (PHEV), battery electric vehicle (BEV) smart grids(ONAR et al., 2012; Zhang and Chau, 2017). Bidirectional arrangements reduce the size of circuit and develop the efficiency and performance of the system. Thanks to bidirectional procedure, there is no need for two converters to flow the current forward and reverse. Entire process can be handled in single circuit. Thus, bidirectional buck boost converters ensure cost reduction and high reliability for charging station or batteries (Gorji et al., 2019).In this thesis, non-isolated bidirectional buck boost topology has been used and connected the battery. The figure of whole circuit is indicated below.

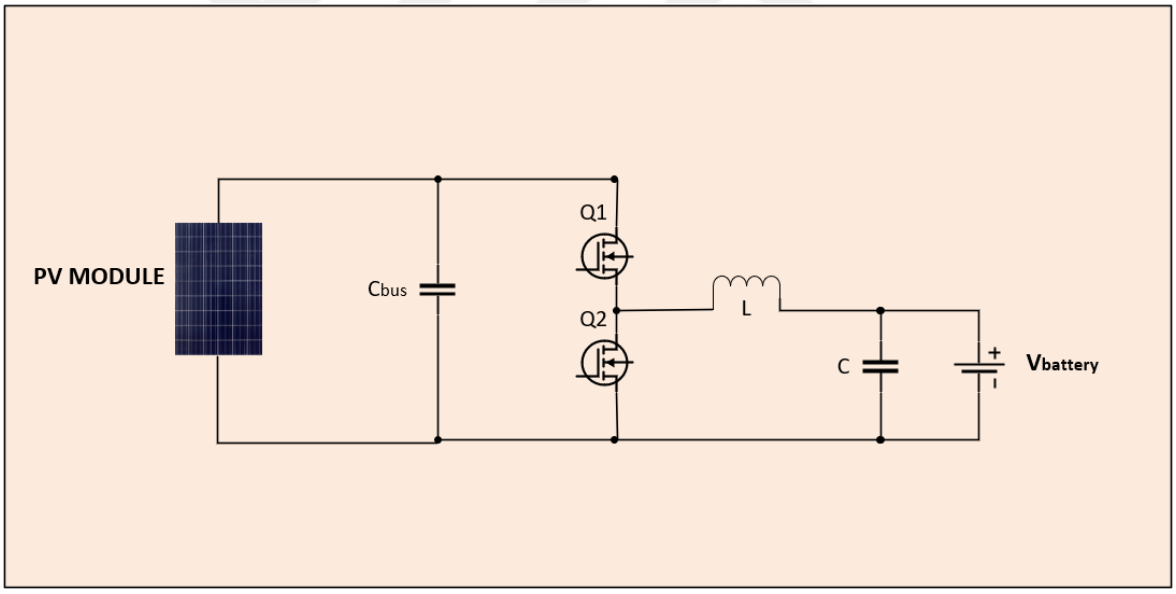


Figure 2.14 Circuit Analogy of Non-Isolated Bidirectional Buck Boost Converter

Non-isolated DC-DC converters can be separated into two main groups are called as isolated and non-isolated. The non-isolated analogies have sent the power without magnetic isolation. They provide advantage from simpler configuration. Inside structure of converter make them appropriate when size and weight are important issues in specific designs.

The circuit shown in figure 2.14 consist of two transistors, one inductor and two capacitors. It can be operated in two modes which is stated before. In first mode is called as forward, the electricity flows from battery to the high voltage line. Therefore, it acts like a boost converter. In addition, there are 2 diodes connected inside the transistors. Assume that the diode in Q1 is D1 and the diode in Q2 is D2. The forward mode architecture (boost mode) is remarked in figure 2.15.

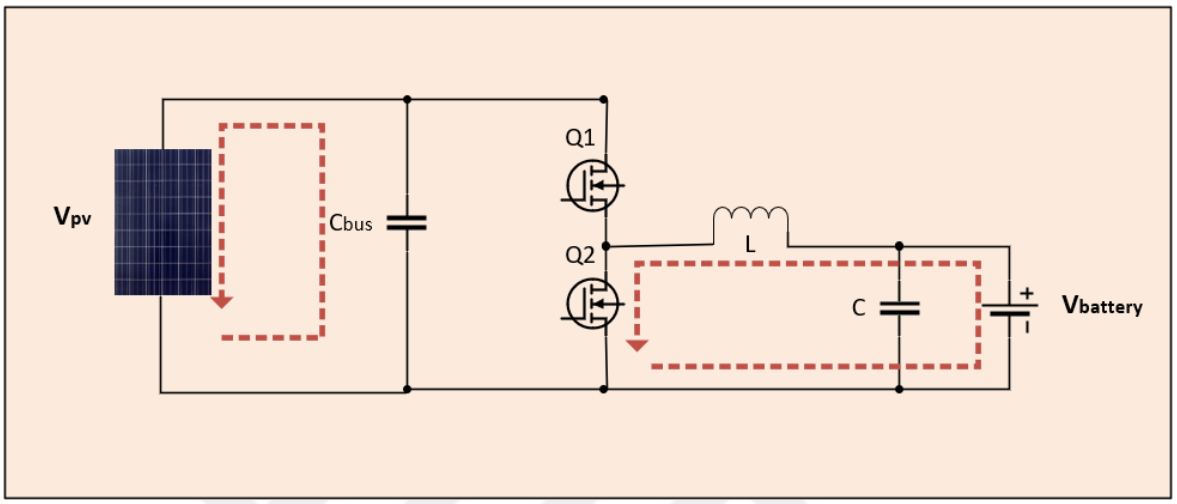


Figure 2.15. Current Flowing When S2 is On

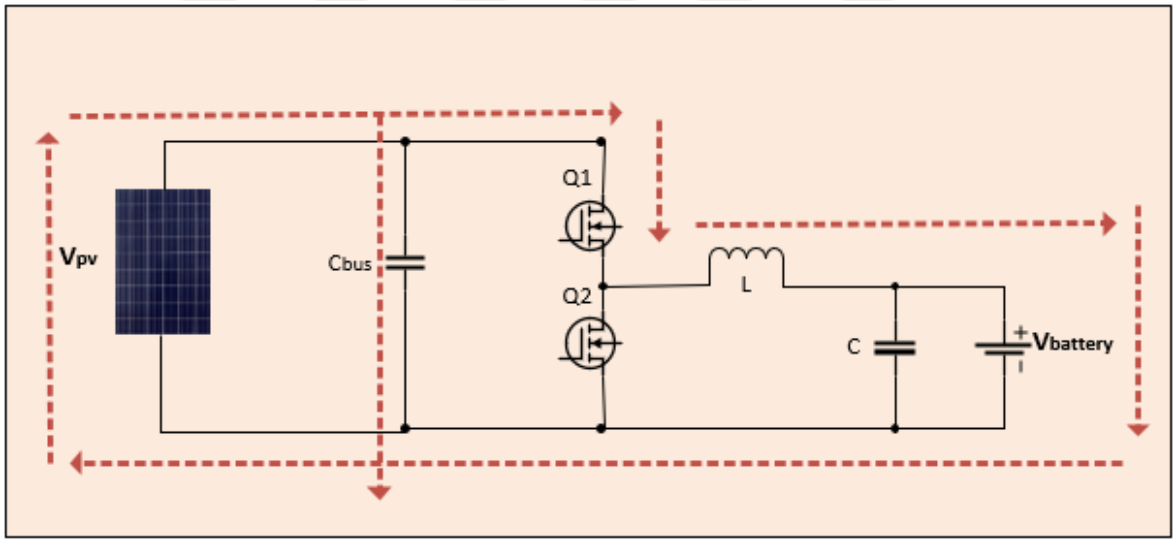


Figure 2.16. Current Flowing When D1 is Forward Biased

Figure 2.15 indicates how current flowing is when S2 is on and S1 is OFF. Inductor collect energy, charges and the current will enhance being linear. Figure 2.16 shows when D1 is ON, S1&S2 are in OFF position and D2 is reverse biased. The energy which was collected in the inductor, starts discharging. In boost mode status, the energy coming from battery and inductor will be sent to photovoltaic side. Due to this reason, there will be step up in voltage level (Viswanatha, 2022)

The second mode indicated as reverse mode, electricity flows from photovoltaic to battery. Thus it performs like buck converter. In most of regenerative braking systems for electric vehicles, utilizing reverse mode provide great advantage in order to increase system performance.

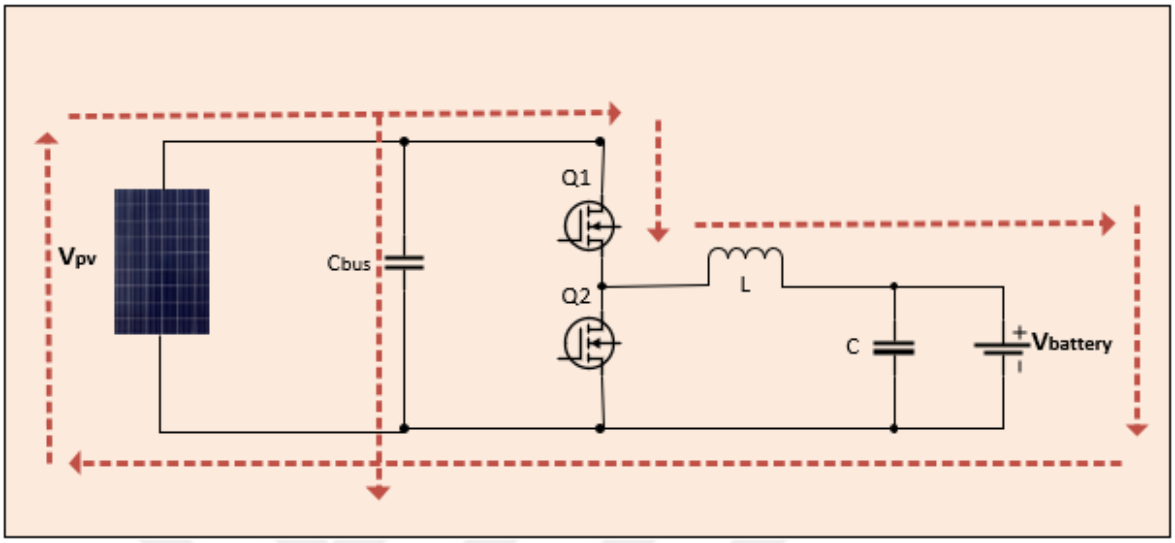


Figure 2.17. Current Flowing When S1 is ON

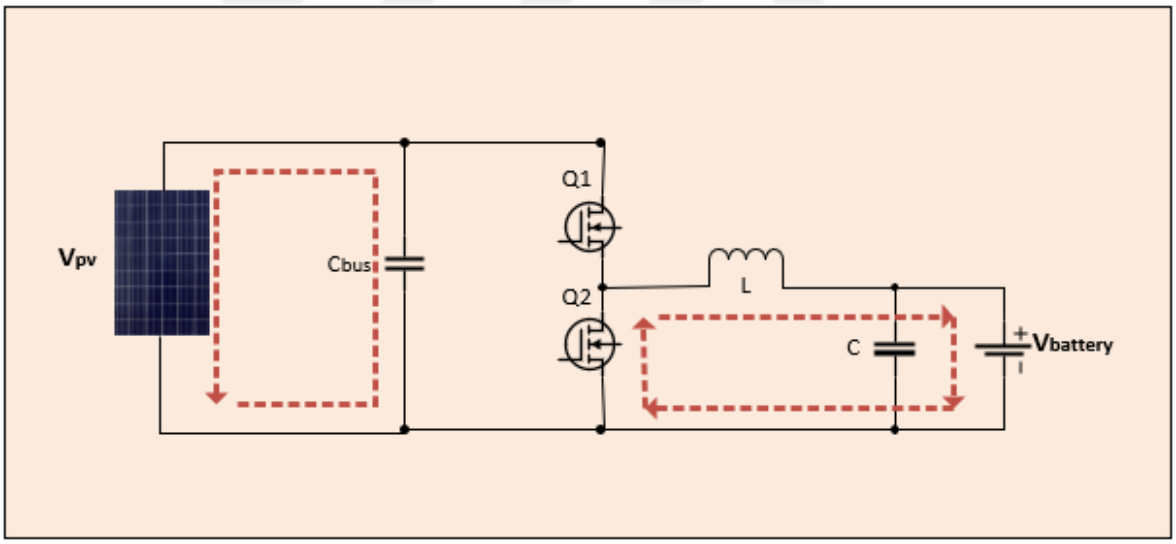


Figure 2.18. Current Flowing When D2 is Forward Biased

The figure 2.17. states how current is passing when S1 is ON, S2 is OFF and both diodes are in reverse biased status. Figure 2.18 states when diode D2 is ON, D1 is reverse biased status and both transistors are OFF position. During this operation, it provides to charge the battery.

2.5. Maximum Power Point Tracking Methodologies

In last decades, researchers observed ways to extract power from RES, mainly from PV systems. They are utilized either stand alone or grid connected type. Firstly, mechanical systems were progressed that follow the inside current and voltage of PV panels in order to take the maximum solar irradiation. Mechanical tracking is indicated as physical tracking. In this method, the location of the PV panel is also changed mechanically according to the change of the sun's angle of incidence. Thus, it is aimed that the angle of the rays coming to the PV always at the same level (Kumar et al., 2017). Other kind of tracker is stated electrical MPPT that constructed varying different algorithms. It depend on moving the operating voltage or current to get the maximum power (Karami et al., 2017). In this side, follows the I-V curve by using such algorithms, parameters (voltage, current, temperature and irradiance) are detected and fed in to the algorithm. The chosen technique calculates the reference values for different parameters. Gathered values are compared with the previous values. Two results are subtracted from each other. After gained the difference value, the duty ratio for the converters is set with the help of a Proportional Integral (PI) Controller or hysteresis controller(Karami et al., 2017). In addition, MPPT algorithms are a convenient solution to provide continuous operation of the PV systems and overcome nonlinear structure under all situations (Alrubaie et al., 2022). The trackers usually need a DC-DC Converter to harvest the maximize of PV power. This requirement is valid to a two stage grid connected system, on the other hand, an inverter is needed for a single stage grid connected system. Up till today, different kind of tracking algorithms and implementations have taken part in the literature. They differ from each other according to the efficiency, complexity, cost, applicability and so on. MPPT can be applied not only for PV panels, but also for some other renewable energy resources such as wind energy, fuel cell. It computes duty cycle until the design reaches maximum power point. The gained duty cycle is sent the input of power electronic circuit being control signal. Efficiency levels for the applied tracker methods must comply with the European Standard EN 5030. MPPT methods can be diversified by internal features such as complexity, control techniques, circuitry, algorithm accuracy, speed and total cost. Thus, structures are classified into four categories.

First group needs PV modelling and it depends production parameters for the photovoltaic panels. In order to construct control signals, parameters are deployed in some mathematical formulas. During the operation of tracking, control signals will remain constant. These methods ensure cost advantage because they have fewer sensors compared to others. This group is called as off-line.

The other group is referred by on-line Methods. They need instant voltage and current in order to generate PWM control signals. The principle of operation is to achieve the output power by stimulating the voltage and current in small amount. This can also be named perturbation. Since the perturbation state changes according to the output power status. Due to this reason, the control signal will not remain stable as in off-line Methods. The system aims to produce an efficient control signal to capture the best output power.

Intelligent MPPT Methods is referred as third category techniques. It includes soft computing algorithms and enhances accuracy of systems in face of non-linear problems (Salam et al., 2013). To utilize intelligent MPPT methods ensure more robust and reliable systems. When the performance parameters observe, nonlinear PV characteristics can be followed easily with help of intelligent algorithms. As mentioned before, the most basic problem of solar systems is power levels decrease under changing weather conditions. Thanks to powerful computer-aided algorithms, this problem is also eliminated.

The fourth group of MPPT method combines two different algorithms at the same time. By some researchers, this group is also called the hybrid method. It involves one off-line method and other method. Off-line methods will track MPP and give fast response according to the changing weather conditions. The other method has taken from on-line group generally. It brings system accuracy and low steady state error.

All these studies, which are included in four different categories, are indicated in figure 2.19. below

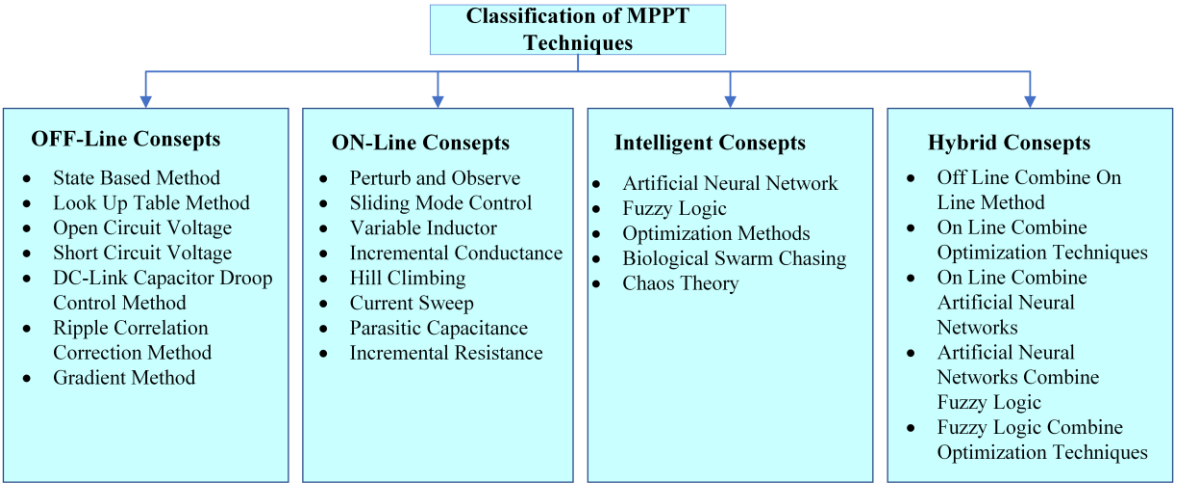


Figure 2.19. Classification Diagram of MPPT Methodologies

Some of the MPPT procedures mentioned in figure 2.19. were used in this thesis. The algorithms are indicated below

- Perturb and Observe
- Incremental Conductance
- Artificial Intelligence

2.5.1. Perturb and Observe Method

P&O algorithm is the most well-known and conventional tracking method which is used to extract power from photovoltaic modules. The simplicity and being low cost of the method becomes it one of the most preferred technique. On the other hands, conventional P&O algorithm has several drawbacks such as power loss and lack of efficiency (Alik et al., 2015). Main purpose of this topology is to adjust the duty ratio by comparing the present value of the power and the previous value. It achieves this by applying perturbation to the voltage. The topology ensures that the specific parameter to stay around the maximum power point by repeatedly perturbing the operating point. If there is a momentary power drop due to changing weather conditions, the P&O algorithm perturbs the system and pull the power level upper position. Two common design approaches can be applied into P&O algorithm. First is specified as direct duty ratio perturbation, the duty ratio of the MPPT converter is applied directly being control parameter. Other type is referred as reference voltage perturbation. For reference voltage perturbation, the PV module output voltage is used reference control parameter with carrier signal. In order to arrange duty ratio of MPPT power for converter, PI controller can be used generally (Elgendy et al., 2012).

In this thesis, the P&O topology was applied with direct duty ratio perturbation. The flowchart of the design can be expressed easily in figure 2.20 below

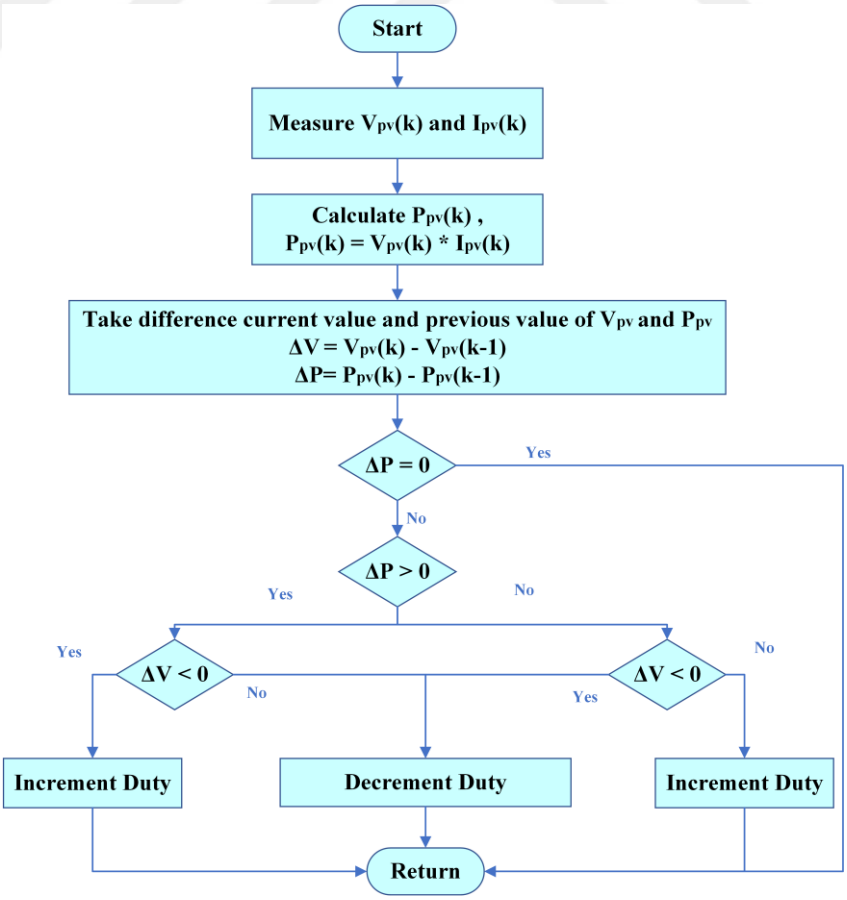


Figure 2.20. Flowchart of Conventional P&O Algorithm

From the parameters that included in figure 2.20, $P_{pv}(k)$ shows the instantaneous power generated by photovoltaic panel. $V_{pv}(k)$ shows producing instantaneous voltage. $I_{pv}(k)$ represents momentary current extracting from PV. ΔP symbolizes the difference between current generated power with the previous power. ΔV means the difference between the generated instant voltage with the previous voltage. Some of studies in which P&O is used, are indicated in table 2.7.

Table 2.8. Literature Review of Perturb and Observe Algorithm

PV and Capacity	**Summary of the articles**
PV: 100.7kW Grid Voltage:25kV	In this paper, modified P&O algorithm is recommended for MPPT of double stage grid connected system. PV module consist of 5 series connected modules per string and 66 parallel string of array. In addition to the PV system, a transformer was used to send the generated power to grid (Abdelwahab and Hamada, 2020).
PV: 14.4kW PMSG: 8.5kW	A hybrid standalone facility where solar and wind energy production work together is modeled. A battery has also been used to ensure power continuity in the design of plant. In the study, P&O, Sliding Mode Control (SMC), Fuzzy Logic Control (FLC) structures were used to keep the power generated from both solar and wind sources at MPP. (Zebraoui and Bouzi,2020)
PV: 40W PV Voltage: 21V	In this PV facility design, the P&O method was implemented on the basis of direct duty perturbation and given as PWM into boost converter. The main difference of this paper from the others is that it was studied as a single phase and was carried out at low power values (Hajare et al., 2020).
PV: 300W V_{mp}: 54.7V I_{mp}: 5.58A Batt: 18AH, 12V Type: Lead Acid	A PV based charger designed with using lead acid battery in this paper. For charging the battery a synchronous buck converter is used. Being low cost and efficient, lead acid battery is recommended for rechargeable batteries. The SPR-305-WHT PV module of the Sunpower brand was used to feed the circuit. Charge controller of this circuit is designed with P&O MPPT method (Padhee et al., 2016b).
PV: 32.4kW V_{mp}: 26.3 V I_{mp} : 7.61 A	A grid-connected single stage three phase PV system is designed with Improved P&O method. It has been proposed because it eliminates the deficiencies other P&O methods and increases stability. The system is planned for a 30kW (kilowatt) facility, it includes 27 series tied strings and 6 parallel tied arrays (Singh et al., 2016)

2.5.2. Incremental Conductance Method

The method was developed in 1993 to eliminate the slow response and steady state errors of the P&O algorithm. It has advantageous under fast changing weather conditions due to giving well response. However, the INC is more complex and harder to implement than other one. It aims to track MPP using slope of the P-V curve. This procedure uses instantaneous conductance which is represented by $\frac{I}{V}$ and incremental conductance which is symbolized by $\frac{dI}{dV}$ for MPPT (Shang et al., 2020). The formulization parameter is shown in equation 2.5.2.1.

$$\frac{dP}{dV} = \frac{d(V.I)}{dV} = I\,\frac{dV}{dV} + V\,\frac{dI}{dV} = I + V\,\frac{dI}{dV} \tag{2.5.2.1}$$

The $\frac{dP}{dV}$ is specified as maximum power point identifier factor. The result of this factor is taken into account in order to quickly perform the tracing process. The following equations express the mpp orientation according to the result of the factor.

$$\frac{dP}{dV} = 0\ at\ MPP \tag{2.5.2.2}$$

$$\frac{dP}{dV} > 0\ left\ of\ MPP \tag{2.5.2.3}$$

$$\frac{dP}{dV} < 0\ right\ of\ MPP \tag{2.5.2.4}$$

The visual version of all these equations can be easily indicated as in figure 2.21 below. If the identifier factor is less than zero, the system will try to move it to the left. If it is greater than zero, the system will try to move it to the right.

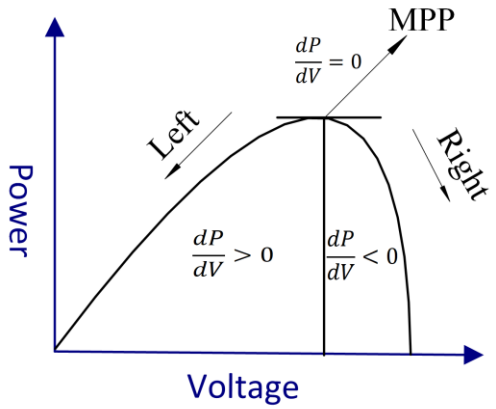


Figure 2.21. P-V Curve of INC Methodology

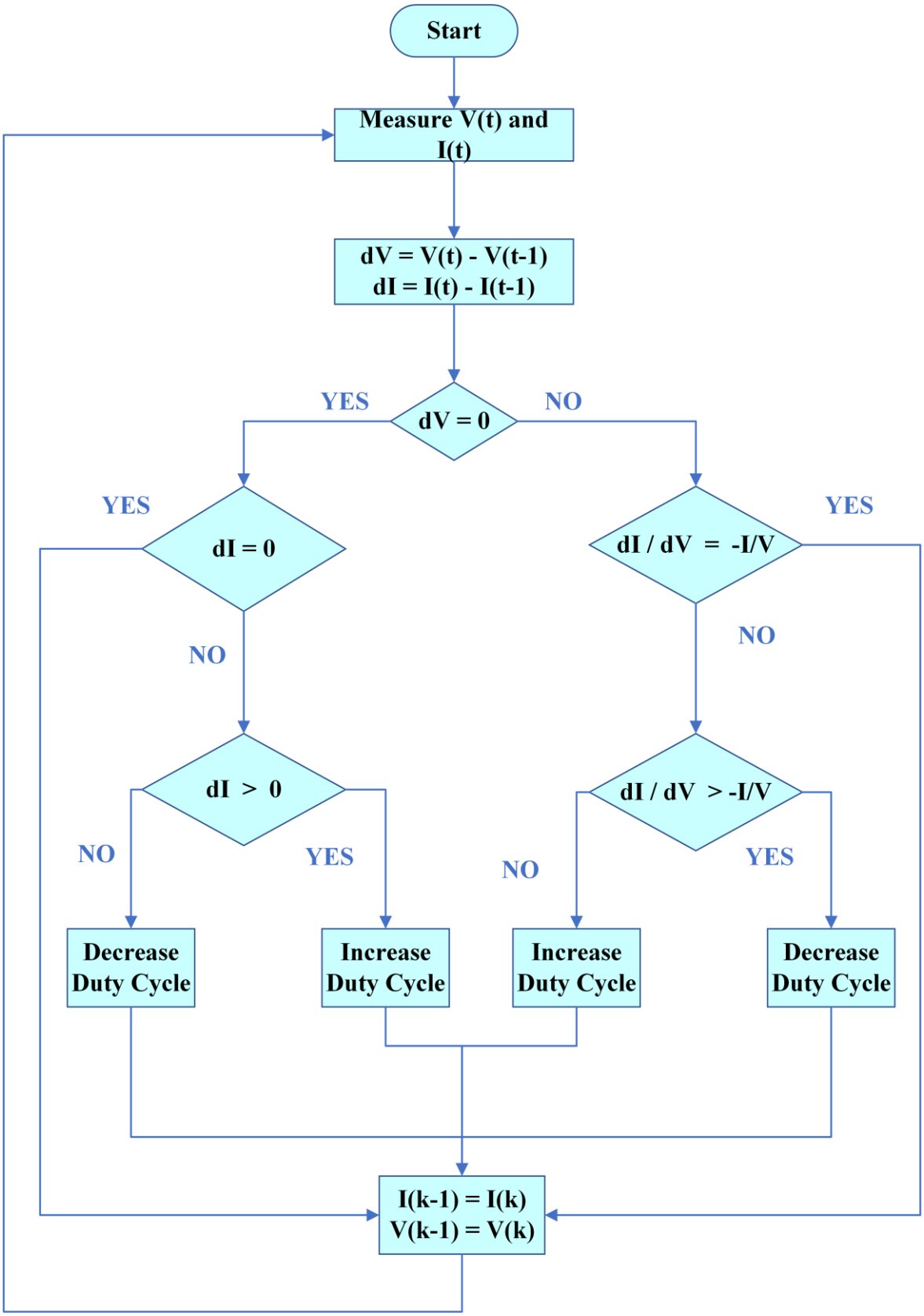


Figure 2.22. Flowchart of Incremental Conductance Algorithm

Some examples of INC procedure which is widely worked in the literature, are given in the table 2.8 below.

Table 2.9. Literature Review of Incremental Conductance MPPT

PV and Capacity	Summary of the articles
PV: 22W Batt: 7AH, 12V	The paper focuses on the INC topology step size in PV systems. Firstly, the MPPT algorithm was run with fixed step size after that variable step size was operated. Result of this study, two outcomes were compared each other. In addition a battery was also used to ensure power continuity (Gupta et al., 2021).
PV: 85W	In this study, Fuzzy Logic Estimator (FLE) was used to increase the system performance of INC algorithm and focused on duty cycle. The simulation work was carried out in MATLAB/SIMULINK platform and the implementation stage was realized on the dSPACE ACE11104 (Radjai et al., 2014).
PV: 850W V_{dcbus}: 220V $V_{battery}$:48V	A grid connected, low power PV system was designed. A battery was used in the plant to ensure power continuity and energy efficiency. In addition, PWM was obtained by INC algorithm in the proposed method. A transformer has been added to the inverter output to convert. A transformer was added to the inverter output to align the low power system with grid. (Dhillonet al., 2022)
PV: 3.5kW Batt: 6.5 AH, 100V Type: NiMh	A solar power generation area has been designed for a residential home plug in hybrid electric vehicle. In this application, the incremental conductance topology has been used to keep the power at maximum. Moreover, two battery cells connected to cascade were used to support the system (Gürkaynak et al., 2009).
PV: 95kW V_{cell} :321V	The paper expressed a combine tracking control method Incremental Conductance and Integral Regulator. In this way, it is stated that the efficiency of the system increases. Furthermore, a different converter proposed to eliminate voltage deviation and grid disturbance (Stephen et al., 2022).

2.5.3. Artificial Neural Network Method

The efficiency of power drawn from PV is an important performance parameter in solar power generation systems. In order to ensure, MPPT is a mandatory stage of whole design. The response of traditional algorithms such as P&O and INC to changing weather conditions is quite low. The output power efficiency is poor. For these reasons, studies have replaced traditional methods with intelligent algorithms. Designing a tracker using an ANN is one of the intelligent ways. ANN based controllers has several capabilities like nonlinear mapping, robust operation, high level efficiency, high speed response (Elobaid et al., 2015). ANN are constructed artificial neurons which are derived from biological neurons. There are three separate layers in the structure. These layers are seen in figure 2.23 below

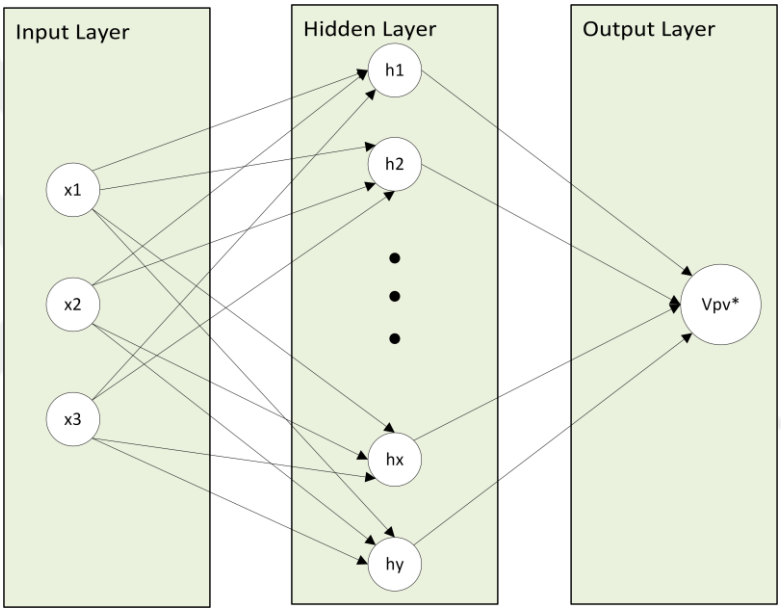


Figure 2.23. Structure of ANN

Input layers are specified as initial datas neural network architecture. Hidden layers are mid layer between input and output layers. All the calculations are performed in this layer. It is the part where information is processed. Output layer is the stage where the final value is reached. The given task results in this area. The ANN algorithm can be analyzed four fundamental steps (Jyothy and Sindhu, 2018):

- Data collection
- Selection of network structure
- Training the network
- Testing the network

The inputs of ANN controller are temperature and irradiance. Aim of neural network is to arrange duty ratio for DC-DC converter. For every change in temperature or irradiation level, the system is quickly sets duty ratio again. In this thesis, Levenberg-Marquardt algorithm was used to train the network. Train process can be indicated as configuring the weights of layers to gain the target values. Moreover, unlike other methods, instead of applying direct duty, direct V_{ref} and PI controller have been applied. The following figure 2.24 is the general circuit diagram with load connection.

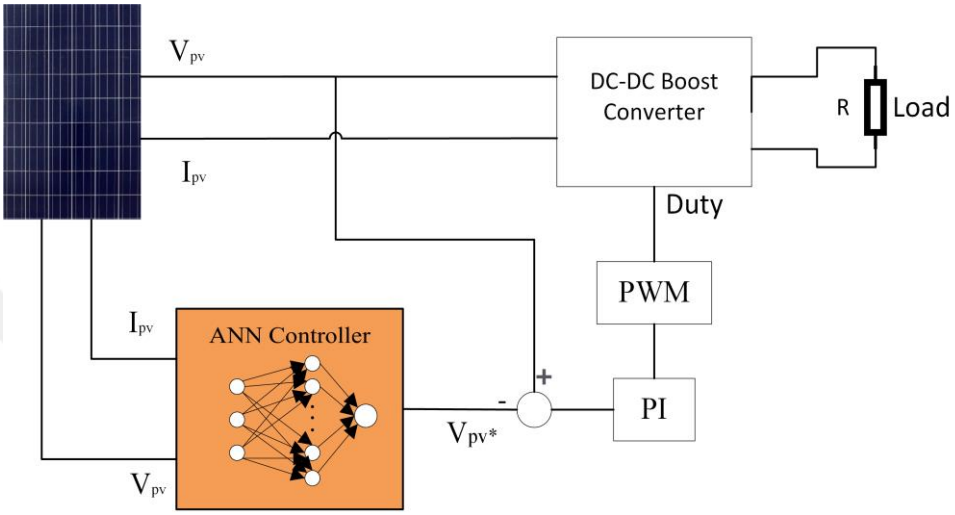


Figure 2.24. Load Connected PV System with ANN MPPT Controller

Table 2.10.Literature Review of ANN MPPT

PV and Capacity	**Summary of the articles**
PV: 10.8kW Batt: 4 x12V Type: Lead Acid	In this paper, tried to apply an efficient ANN algorithm for battery charging process off grid PV systems. Moreover the algorithm different from others because of adaptive ANN. Average efficiency was gained 99.33% (Triki et al., 2022)
PV: 12.7kW	This recommended model was trained with 1000 dataset of solar irradiance, temperature and voltages. 15% of data applied for validation and 15% data is used for testing process. Remain part of total data is utilized for training. Levenberg-Marquardt algorithm was applied for training (Roy et al., 2021).
PV: 10.8kW V_{oc}: 32.9V	In this study, traditional P&O topology and intelligent ANN method are compared each other. According to the outcomes of the two methods, the advantages and disadvantages was focused on (Chorfi et al., 2018).

2.6. DC/AC Inverter

Since there is not enough electricity produced from fossil fuels in the world, it is necessary to transfer the electricity produced from RES to the grid. The installations of grid connected PV systems are becoming popular due to rapid progress in power electronics technology. One of the devices that has an important share in this developing technology is called inverter. It is useful in converting DC power to AC power for various applications. It can be applicate in RES. Inverters are key component which combined grid and PV circuit design. In single stage system inverter will apply both MPPT and grid synchronization. Additionally, in double stage system, inverter will only perform grid integration (Khan et al., 2020).

DC to AC inverter supports in controlling the power factor by injecting sinusoidal current inside the grid. Thanks to inverter, DC energy extracted from the PV is converted into AC side and efficiently transferred. It can be used for both single phase and three phase applications. To acquire the best performance from panel, choosing an appropriate grid connected inverter is a critical topic (Kolantla et al., 2020). The different types of PV inverter topologies can be classified according to the source.

It can be examined in three main headings:

- Voltage Source Inverters
- Current Source Inverters
- Z Source Inverters

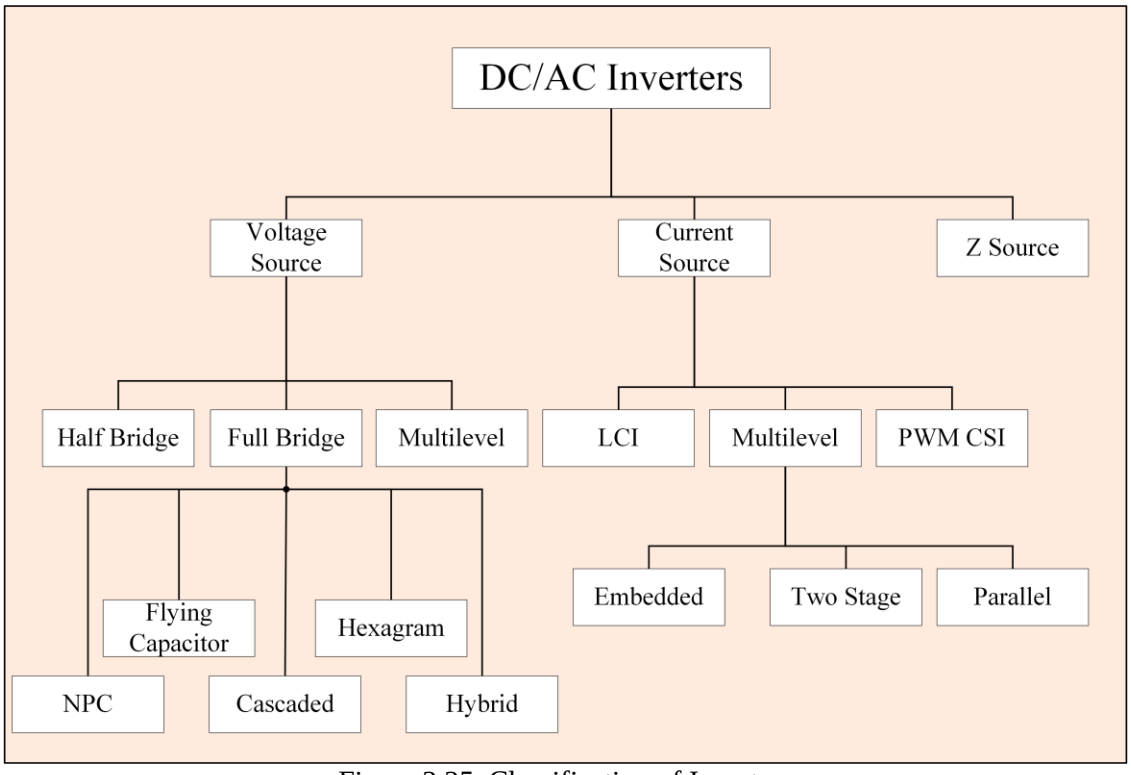


Figure 2.25. Classification of Inverters

One of the inverter types included in figure 2.25 is Current Source Inverter (CSI). In CSI, the input side of device is connected to a DC current source and then, the polarity of input current stays the same. An AC current waveform can be generated with a variable width and constant amplitude.

Another commonly used kind of inverter is Voltage Source Inverter (VSI). In this topology, a DC voltage source is connected the input side, therefore the polarity of input voltage stays same but the sign of input DC current designates the direction of average power flow through the inverter. At the output part of circuit, an AC voltage waveform can be generated with a variable width and constant amplitude (Zeb et al., 2018). The main aim of this procedure is to design three phase VSI that controls the voltage, frequency and amplitude waveforms. It has some advantages compared with CSI. The total power loss is minimum due to low conduction loss. A constant input voltage is provided. Against the input DC side of VSI, a parallel capacitor is connected. DC capacitor is low cost and efficient for energy storage applications (Xiao et al., 2013). For these reasons, the VSI is chosen frequently in PV applications. Single phase VSIs are suitable for low power implementation. Three phase VSIs are convenient for medium and high power applications.

In this thesis, a 3 phase full bridge VSI design with IGBTs was applied to connect DC power, which was extracted from PV, with grid. To attain the three phase AC current in three phase VSI contains six gating signals and six corresponding IGBTs. The IGBTs are tied to each other in three series lines through two parallel connections. There is a phase difference of 120° between each symmetrical switch. Additionally, two switches connected to the same parallel line cannot be in ON position at the same time. The three phase full bridge VSI design is indicated in figure 2.26 below.

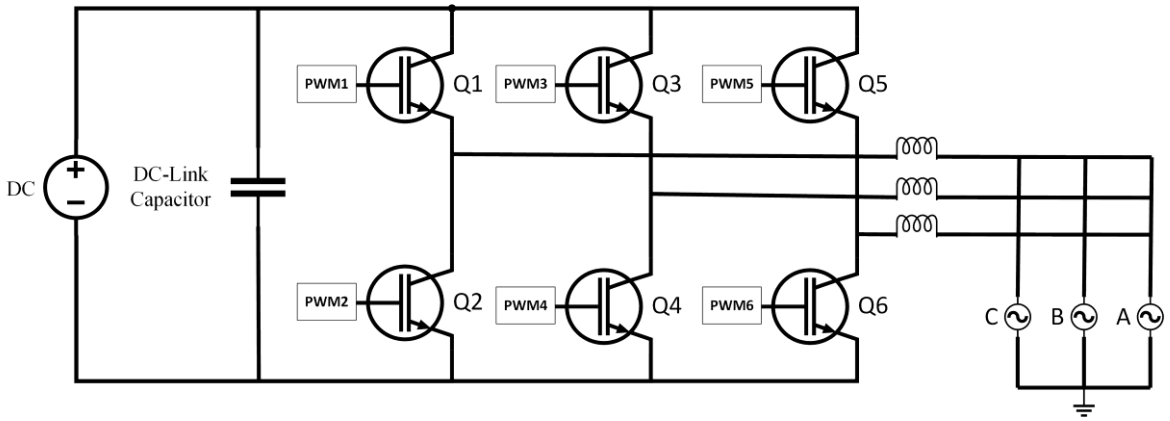


Figure 2.26. Three Phase Full Bridge Voltage Source Inverter

In the figure 2.26, what is expressed by A, B, C is the grid connection of each phase. The electronic components notified by Q are IGBT modules. The PWM signals specified in the trigger part of the modules are used to activate IGBTs

Some examples of full bridge inverter which is widely used in the literature for PV system, are given in the table 2.10.

Table 2.11. Literature Review of Inverter for PV System

PV and Capacity	Summary of the articles
PV: 200 W V_{mp}: 48 V I_{mp}: 7.61 A	The paper shows to control a three phase five level neutral point clamped inverter (NPC) for grid connected PV system. In order to reach MPP, fuzzy logic controller was used in design stage. The fuzzy MPPT is combined with inverter due to single stage system (Ravi et al., 2011).
PV1: 550 W PV2: 500 W PV3: 450 W	A new scheme was designed for grid connected PV interface by combination of quasi- Z source inverter using cascaded H bridge is recommended in this study. Three PV are designed separately and combined in series. A total of 1.5kW photovoltaic plant is simulated on the MATLAB/SIMULINK platform (Sun et al., 2012).
PV: 12.6kW	In this paper states a three phase grid connected PV system with unity power factor for any solar radiation level. The classical six transistor inverter structure is used. The direct quadrature zero(dq0) transformation are proposed to control PWM inverter (Schonardie et al., 2012)
PV: 4kW	A dual stage three phase inverter was designed. In this topology, dual stage inverter is responsible for MPPT and grid current control. A rectifier circuit has been added between the first inverter and second one (Casaro and Martins, 2009).
PV: 1kW $f_{carrier}$: 20kHz	In this paper was expressed PV conversion circuit of single phase full bridge inverter. STM8S207R8 core processor was used as the controller. To eliminate harmonic effects, LC filter was used in the circuit (Jun and Han, 2016).
PV: 10kW	In this study, three phase inverter types for grid connected PV systems are focused on. Both transformer and transformerless simulations were run. Analytical results thanks to transformer parameters, it can provide up to 50kW, 100kW and 200kW power ratings (Özkan and Hava, 2014).

2.7. LCL Filter

In the design of grid connected inverters, filter is recommended for producing pure sine wave. It should be placed between the inverter and electric grid. The most effective filter for damping of the current harmonics taking place from the switching frequency is the LCL filter (Yu et al., 2014). It can be used at low switching frequencies. It has lower voltage drop and higher absorption factor compared with conventional L and LC filters (Dursun and Döşoğlu, 2018). To acquire high quality grid currents LCL filter must be applied in the circuit. The LCL circuit model for a basic three phase grid connected inverter circuit is shown in the figure 2.27.

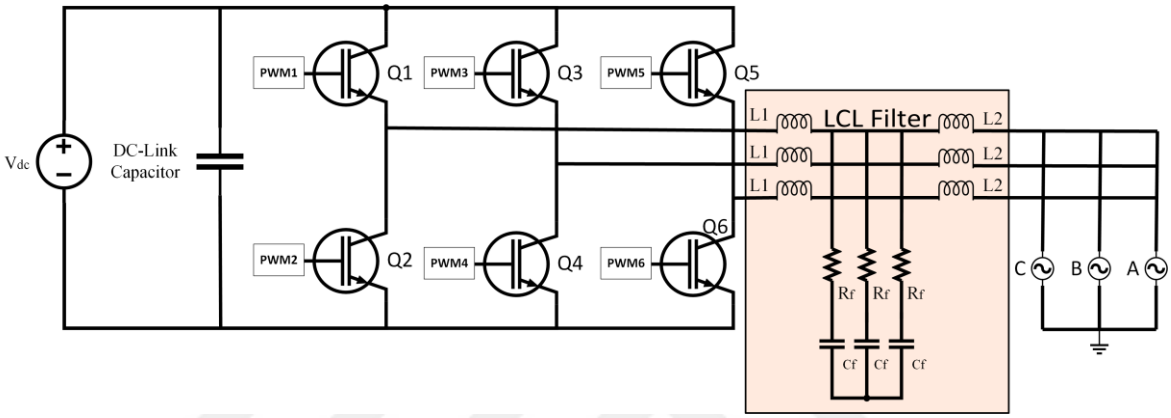


Figure 2.27. Three Phase Grid Connected Inverter with LCL Filter

The parameters included in the LCL filter in figure 2.27 are designed by calculating according to the results of particular mathematical formulas. These formulas are as follows:

$$Z_b = \frac{(E_n)^2}{P} \tag{2.7.1}$$

$$C_b = \frac{1}{w_g Z_b} \tag{2.7.2}$$

$$I_{max} = \frac{P\sqrt{2}}{3V_f} \tag{2.7.3}$$

- E_n is referred as one phase effective voltage.
- P is meaning of active power.
- C_b is called as base capacitance.
- w_g is named grid angular velocity.
- Z_b is expressed the base impedance.
- V_f is indicated as filter voltage.

$$\Delta I_{Lmax} = 0.1 I_{max} \tag{2.7.4}$$

$$L_1 = \frac{V_{dc}}{6 * f_{sw} * \Delta I_{Lmax}} \tag{2.7.5}$$

Assume the rated current is permitted to fluctuate by 10% for the design parameters, the equation 2.7.4 can be applied in order to acquire result of ΔI_{Lmax}.

- ΔI_{Lmax} referred as ripple factor
- f_{sw} indicate as a switching frequency

$$C_f = 0.05 * C_b \ , \ k_a = 0.2 \ (20\%) \tag{2.7.6}$$

$$L_2 = \frac{\sqrt{\frac{1}{(k_a{}^2)}} + 1}{C_f * (w_{sw})^2} \tag{2.7.7}$$

$$w_{res} = \sqrt{\frac{L_1 + L_2}{L_1 * L_2 * C_f}} \tag{2.7.8}$$

$$f_{res} = \frac{w_{res}}{2\pi} \tag{2.7.9}$$

$$C_{bus} = \frac{4 * P}{V_{dc}{}^2} * t \tag{2.7.10}$$

$$R_f = \frac{1}{3 * C_f * w_{res}} \tag{2.7.11}$$

- L_1 is referred as inverter side inductance.
- C_f is indicated as filter capacitance.
- L_2 is meaning of grid side inductance.
- w_{res} is stated as resonance angular velocity.
- f_{res} is specified as resonance frequency.
- R_f is named filter resistance. It eliminates ripples and resonances.
- C_{bus} is expressed the DC bus capacitor

2.8. Phase Locked Loop

In the grid connected systems, the phase angle information of utility voltage is a crucial part for controlling inverters. (Kaura and Blasko, 1997). Phase information is used into the stage of power control. PLL system acquires this information in order to synchronize the utility and the three phase inverter. The main duty of PLL is extracted phase angle with the help of some specific operations (Golestan et al., 2017). The method is applied not only in inverters, but also static var compensators, cycloconverters, active harmonic filters and energy storage systems integrated into the grid. The system performance directly depends on quality of phase locked loop circuit design. Besides taking of phase information, PLL should provide low distortion output and suppress frequency variations. It includes negative feedbacks. Thus, circuit structure becomes closed loop.

Traditional PLL design stage, there are three main blocks has a specific role. It consists of a phase detector, a VCO and a loop filter (Nandurkar and Rajeev, 2012). The schematic diagram can be shown in figure 2.28.

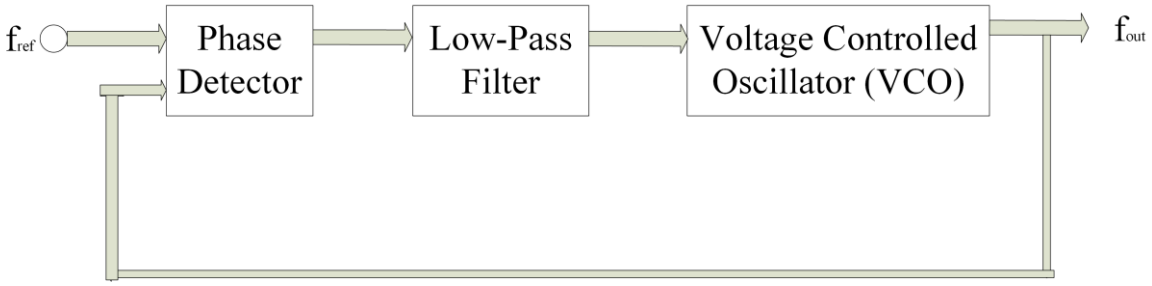


Figure 2.28. Block Diagram of PLL Circuit

2.9. Summary

In this chapter, a comprehensive overview of main topics is given with a wide literature review. These main topics comprise from PV technologies, grid standards, converter topologies, bidirectional buck boost converter for battery support, LCL filter for harmonic elimination, inverter topologies, deeply studies o MPPT techniques especially three main methods, PLL design for grid synchronization. Additionally, to all these issues, the formulas used to calculate the system parameters are also mentioned in this section.

3. DESIGN STAGE FOR OVERALL SYSTEM

In this part of thesis, it is targeted to minimize harmonic distortion by progressing two LCL circuit compared with two modes. The first mode is called as daytime mode. During daytime, energy is ensured from PV array. After that, current passes through first LCL filter to reach electrical grid. The parameters of this filter are calculated according to the power generated by the PV. In daytime mode, the battery holds itself in the charging position. During the night mode, there is not electrical power generation in the PV because of irradiance is equal to zero. Thus, the energy going to the grid is supplied from the battery instead of PV. The charged battery system transfers its energy to the inverter via the DC bus. When the current goes to the grid in night mode, the first LCL filter becomes cut off position and the second LCL filter becomes active position. Current passes through second LCL circuit. The parameters of this circuit are calculated according to the power values of the battery. The desired design of the entire system can be seen in figure 3.1.

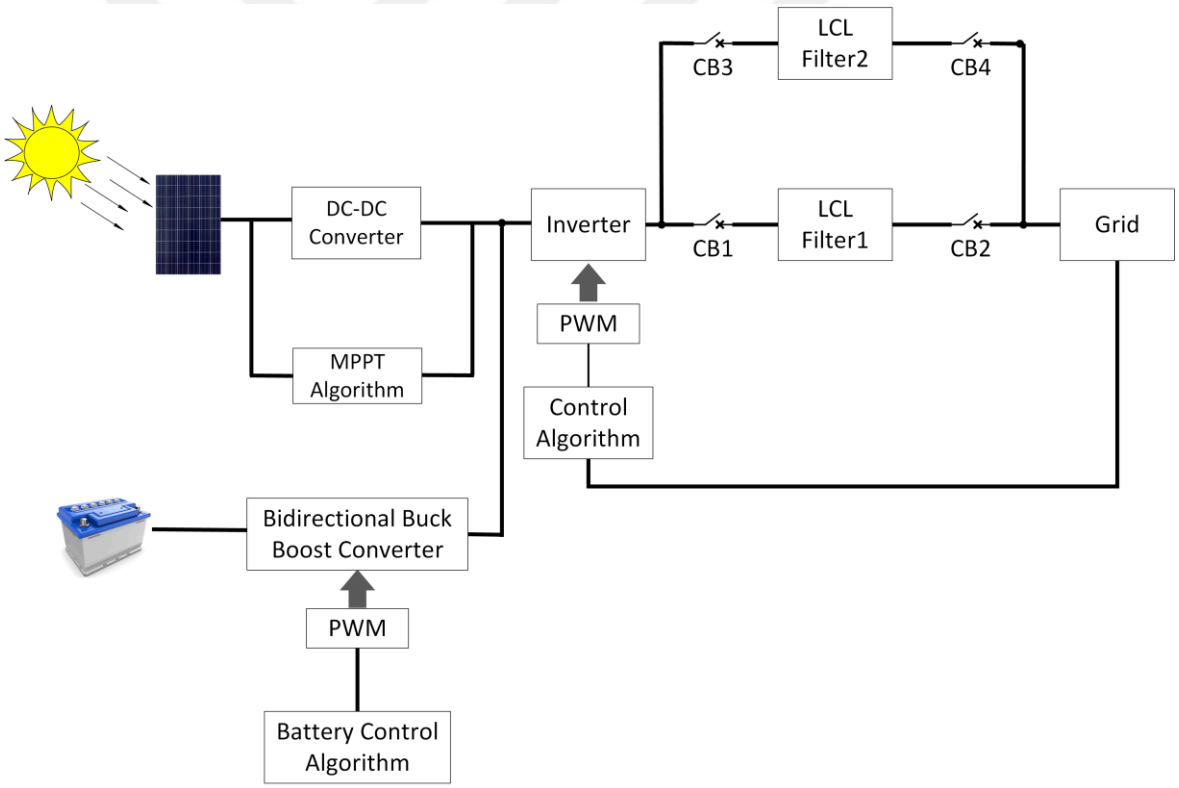


Figure 3.1. Proposed PV&BESS to Grid System

Besides reducing the harmonics, the efficiency is vital parameter for comparing datas P&O, INC, ANN MPPT algorithms are designed to keep maximum power point and improve their efficiency. When building these algorithms 1000 W/m^2 and 800 W/m^2 were selected as two separate irradiance levels.

The sub-circuits required for the installation of the circuit can be examined in eight main headings. These are PV design, boost converter, MPPTs include three different types, battery design,

bidirectional buck boos converter, battery control algorithm, inverter and control algorithm, design of a two LCL circuit respectively.

3.1. PV Array Parameters

The PV array structure consist of cells connected in series and parallel. Panel type and the number of cells differ according to the desired power level to be produced. In this thesis, 1Soltech 1STH-FRL-4H-260-M60 product was used as panel cell. Parameter values of a single cell of this panel are available in the table below.

Table 3.1. Technical Features of 1Soltech-1Sth-Frl-4H-260-M60 Cell

Technical Properties of PV Cell	
Maximum Power at STC (P_{max})	259.4W
Maximum Power at PTC (P_{max})	231.4W
Open Circuit Voltage (V_{oc})	38.6V
Voltage at Mpp (V_{mp})	31.6V
Short Circuit Current (I_{sc})	8.93A
Current at Mpp (I_{mp})	8.21A
Cell Length (mm)	1645mm
Cell Width (mm)	1014mm
Cell area (m^2)	1.67m^2
Power Density at STC (W/ m^2)	155.3W
Efficiency	15.6%
Temperature Coefficient of V_{oc} (% / °C)	-0.356
Temperature Coefficient of I_{sc} (% / °C)	0.07
Shunt Resistance R_{sh} (ohms)	108.71Ω
Series Resistance R_s (ohms)	0.27Ω
Nominal Operating Cell Temperature	48.3°C

PTC refers to PV USA Test Conditions. Most of manufacturers express maximum power values of the panels in both STC and PTC format. Panel efficiency is stated as the maximum power falling on the panel area at $1000\ (W/m^2)$ irradiance, as in equation 3.1.1

$$\eta = \frac{P_{max}}{1000(W/m^2) * \ area(m^2)} = \frac{259.4}{1000 * 1.645 * 1.014} * 100 \approx 15.6\ \% \qquad (3.1.1)$$

The output graph of single 1Soltech cell can be stated in figure 3.2. Current versus voltage and power versus voltage graph was specified outcomes of MATLAB/SIMULINK

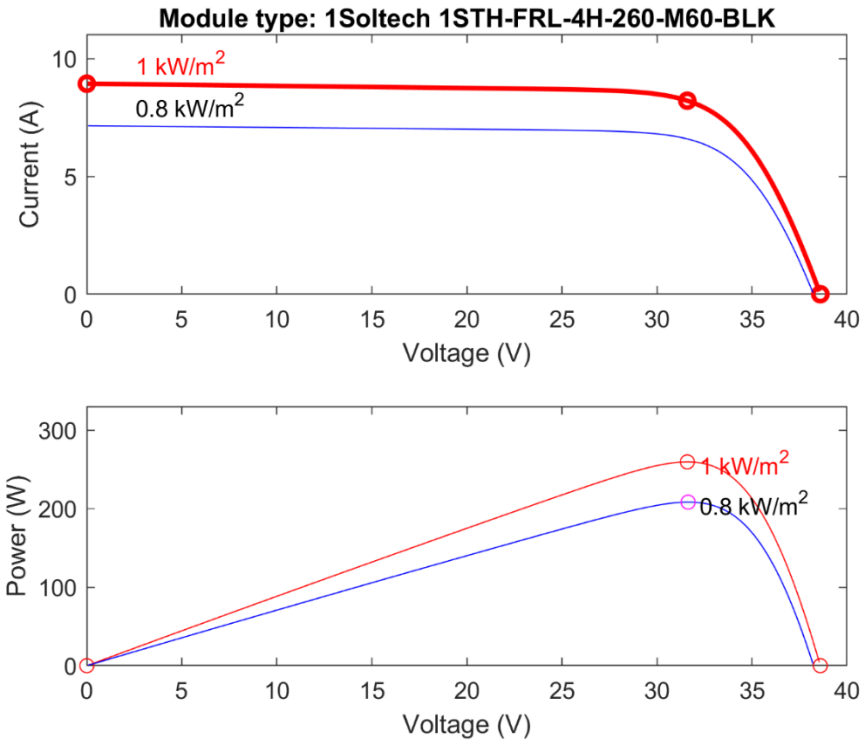


Figure 3.2. Chosen PV Cell and I-V, P-V Curves

In the design, it was targeted to produce 12.45kW power. To reach the specified power, the PV cells are connected to each other in 4 series and 12 parallel. The number of serial connections in the module is expressed as N_s. The number of parallel connections is indicated as N_p

Table 3.2. Technical Features of 1Soltech-1Sth-Frl-4H-260-M60 Array

Technical Properties of PV Module	
Maximum Power at STC (P_{max})	12.45kW
Maximum Power at PTC (P_{max})	11.10kW
Number of Series Cell	4
Number of Parallel Cell	12
Voltage at Mpp (V_{mp})	379.2V
Current at Mpp (I_{mp})	32.84A

Maximum current point of the array is obtained by multiplying the N_s value with the maximum current of the cell. On the other hand, maximum voltage point of the array is obtained by multiplying Np value with maximum voltage point of cell.

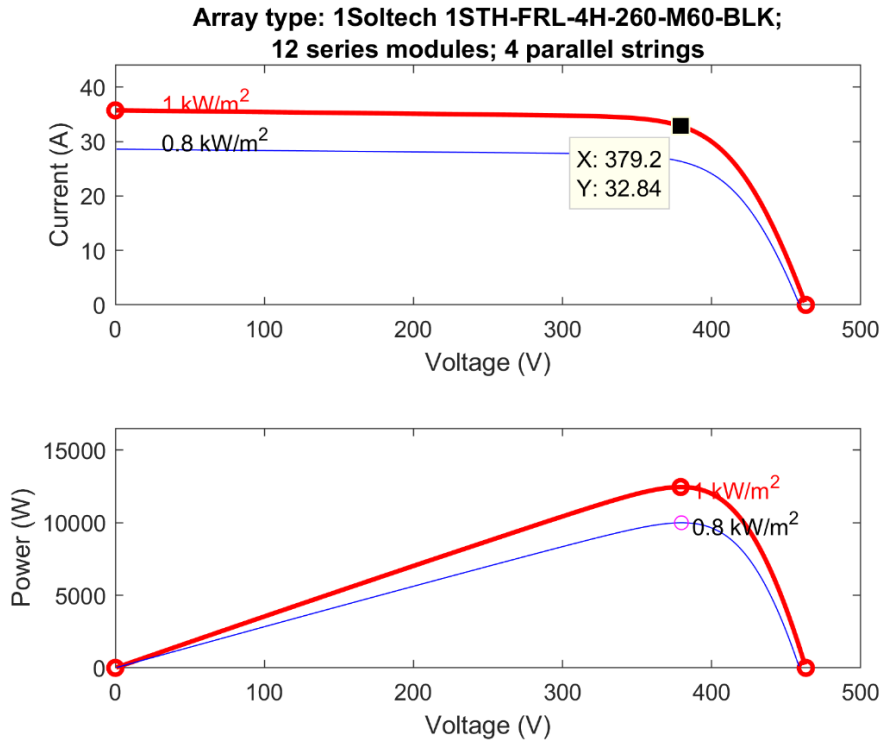


Figure 3.3. PV Array Output Graphs I-V and P-V

3.2. Boost Converter and Parameter Calculation

The DC voltage generated from panel is about 380 V. The system DC bus voltage is chosen 700 V. It is necessary to use a boost converter to enhance the produced voltage to the bus voltage. In addition, current and voltage fluctuations in circuits occur for many reasons. These are called ripples. In order to improve system performance, ripples probability should be added in the parameter calculation. The voltage ripple percentage is taken 1% and current ripple percentage is taken 10%. In this thesis, traditional boost converter was designed. It is included conventional boost circuit, which was simulated in SIMULINK/MATLAB program, is shown in figure 3.4.

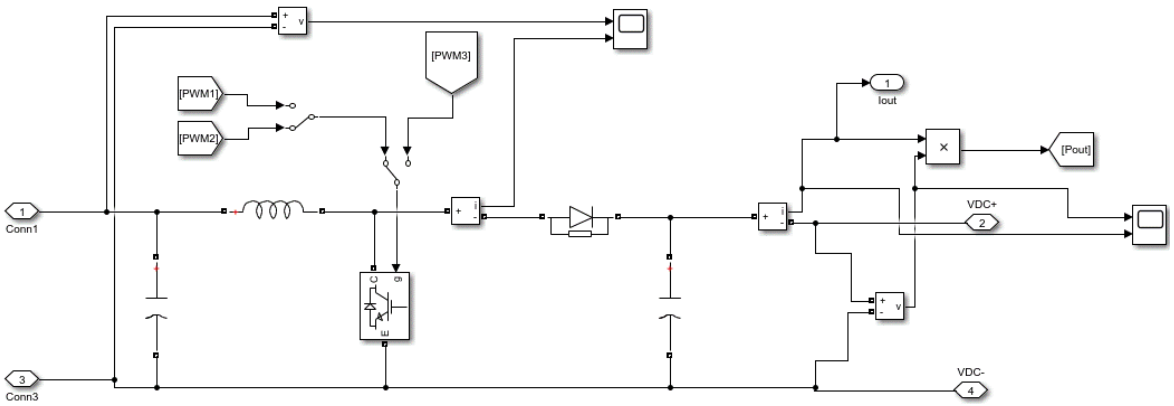


Figure 3.4. Simulation Circuit of Boost Converter

The capacitor located on the left side of the figure 2.32 is used to filter the ripples formed in the generated current and voltage from PV. The other capacitor, inductor and IGBT are the fundamental elements of the boost converter. PWM1, PWM2, PWM3 are seen as the trigger signals of IGBT. These modulation signals are produced by P&O, INC, ANN MPPT algorithms respectively. The duty cycles generated by these algorithms are compared with the reference signals. Thus PWM signals are obtained and matched IGBT as a trigger signal.

Table 3.3.Boost Converters Design Parameters

Fundamental Parameters of Boost Converter	
Input Voltage (V_{in})	380V
Output Voltage (V_{out})	700V
Duty Ratio (D)	0.4571
Switching Frequency (f_{sw})	20000Hz
Output Current (I_{out})	17.78A
Voltage Ripple (DV)	7
Current Ripple (DI)	1.78
Capacitor (C_{out})	58.076μF
Desired Output Voltage (di)	58.27A
Inductor (L)	2.6519mH
Load (R)	39.36Ω

$$Duty\ Cycle = \left(1 - \frac{380}{700}\right) = 0.4571 \quad (3.2.1)$$

$$Output\ Current = \left(\frac{12450}{700}\right) = 17.78A \quad (3.2.2)$$

$$Voltage\ Ripple = 0.01 * 700 = 7V \quad (3.2.3)$$

$$Current\ Ripple = 0.1 * 17.78 = 1.78A \quad (3.2.4)$$

$$Desired\ Input\ Current = 3.27A \quad (3.2.5)$$

$$Inductor = \left(\frac{380(700-380)}{3.275x20000x700}\right) = 2.65mL \quad (3.2.6)$$

$$Capacitor = \left(\frac{17.78*0,4571)}{20000x7}\right) = 58.076\,\mu F \quad (3.2.7)$$

$$Load = \left(\frac{700}{17.78}\right) = 39.36\,\Omega \quad (3.2.8)$$

3.3. Configuration of MPPT Algorithms

In this thesis, the PWM signal of boost converter is produced as a result of MPPT algorithms. This ensures that the dc power is kept at maximum point. The efficiency and steady state speed of each algorithm are different from each other. This situation provides researchers with the opportunity to compare the results of different designs. In this study, the PWM1 signal was generated using the P&O MPPT method. The PWM2 signal was obtained using INC MPPT method. The PWM3 signal was produced using ANN MPPT method.

3.3.1. Design of a P&O MPPT

The purpose of this algorithm is to compare the differences between the present values of power - voltage and the previous values. After the comparison, it adjusts the duty cycle. The algorithm can be handled in two different ways. The first one is called reference voltage perturbation. In this system, an additional PI controller is needed to configure the V_{ref}. This situation enhances the cost. Another way is direct duty perturbation. In this option, the system aims to set the duty cycle directly and no need to add any additional controllers. In this way, a cost advantage is also provided. Direct duty perturbation was used in the P&O algorithm applied in this thesis. The voltage and current generated from the PV are given as inputs to the algorithm. Duty cycle is obtained as a result of the necessary perturbations. Due to the structure of PWM, it needs a reference signal and a carrier signal. The reference signal in the system is received as the duty cycle. The carrier signal is a triangular wave oscillating with a frequency of 20kHz, with an amplitude of 0.5 and peak values of 0-1. This wave was obtained using repeating sequence block on the SIMULINK/MATLAB platform.

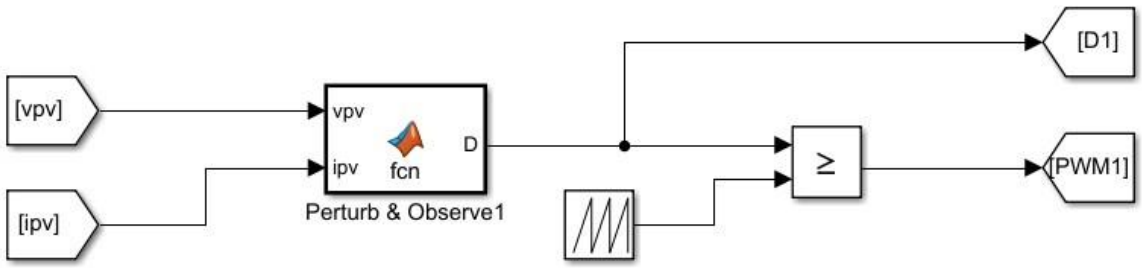


Figure 3.5. Implementation of P&O MPPT

P&O algorithm is encoded as a function block in the simulation. The designed system is available in figure 3.5. The duty cycle produced by P&O is called D1 and the produced PWM signal is referred as PWM1

3.3.2. Design of an INC MPPT

In this thesis, the INC algorithm was used to eliminate the steady state errors and slow response times experienced in the P&O method and to compare the traditional methods. In an electronic circuit, conductance is calculated by dividing the current by the voltage. Conductance is obtained also same way in the INC algorithm. The duty cycle adjustment is made by comparing the current conductance value and the previous conductance value.

This algorithm can be applied in two ways like P&O. To perform cost reduction, direct duty perturbation was used in this study. Additional PI controller is eliminated from design topology with help of direct duty perturbation methodology. The instant voltage and current generated from the PV are given as inputs to the algorithm. In addition to these inputs, previous value of voltage and current is put the algorithm and give an input parameter to conduct analogy. After the comparison, duty cycle can calculate easily. Duty cycle is obtained as a result of the necessary perturbations. Due to the structure of PWM, it needs a reference signal and a carrier signal. The reference signal in the system is received as the duty cycle. The carrier signal is a triangular wave oscillating with a frequency of 20kHz, with an amplitude of 0.5 and peak values of 0-1. This wave was obtained using repeating sequence block on the SIMULINK/MATLAB platform. INC algorithm is encoded as a function block in the simulation. The designed system is available in figure 3.6.

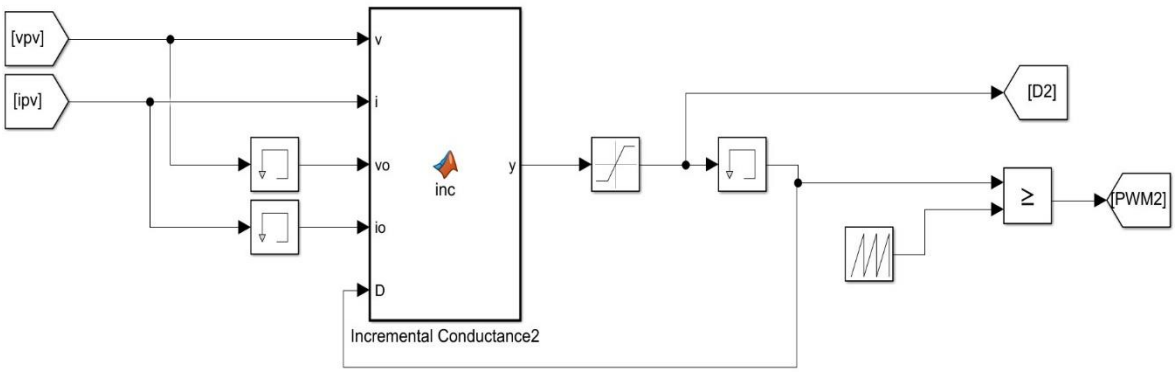


Figure 3.6. Implementation of INC MPPT

INC algorithm is encoded as a function block in the simulation. The duty cycle produced by INC is called D2 and the produced PWM signal is referred as PWM2

3.3.3. Design of an ANN MPPT

The targeted MPPT controller is constructed with artificial neural network methodology which is specified as intelligent procedure. The aim of designing of ANN based MPPT controller is to ensure fast response to variable weather conditions and overcome the deficiencies of conventional MPPT techniques in terms of tracking accuracy, overall system efficiency, unstability. However, ANN controller method has some drawbacks such as complexity, strictly depend on PV panel

characteristic. The power gathered from the modules is directly influenced by the variable weather conditions.

MATLAB Neural Network Training Tool is utilized for creating network architecture. In this methodology, the vital process is input collection for creation of a robust network. Thus, the obtained inputs are separated 70% for training part and 15% for testing part.

PV voltage includes nonlinear output of two main parameters is called temperature and irradiance. In this controller, Levenberg-Marquart training function is used to obtain non-linear problem solution. Number of hidden layers are taken as ten. The main structure of the network is in figure 3.7 below.

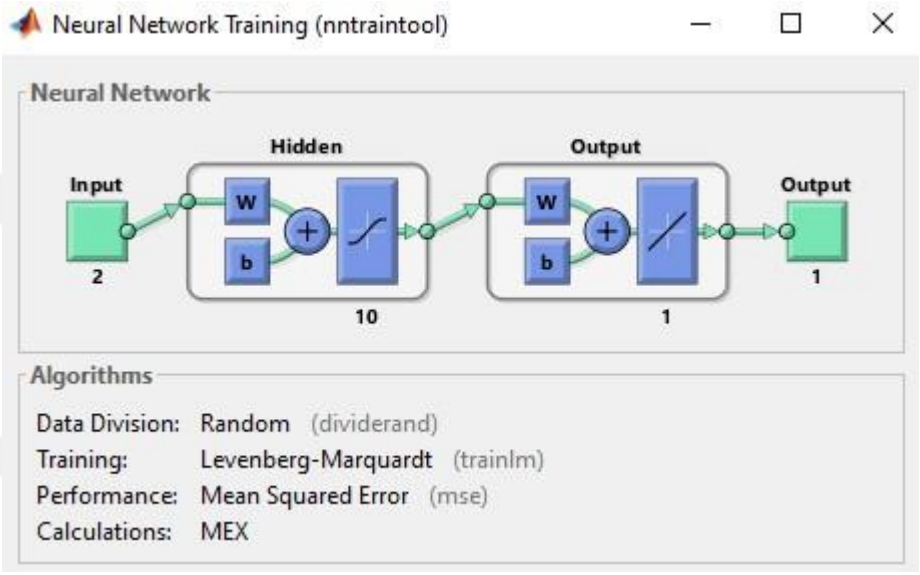


Figure 3.7. Neural Network Training Tool

In this method, besides the others, the direct duty perturbation has not been applied. The output signal produced by the algorithm is taken as reference voltage. The instantaneous voltage generated by the PV and the reference voltage are taken difference and given to the PI controller as an input. After that, the duty cycle is occurred output of the PI controller. This signal is indicated as D3 in figure 3.8. Moreover, it is compared with a carrier signal to generate a PWM signal from D3. Thus, the trigger signal called PWM3 which is located in figure 3.8 is generated.

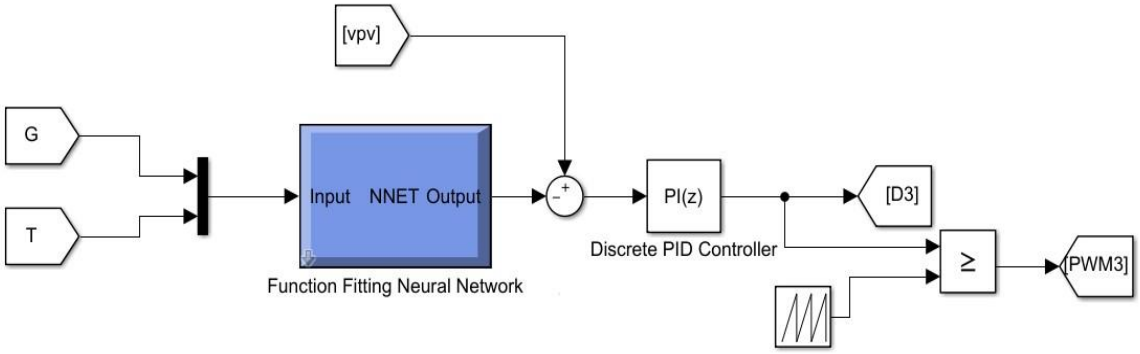


Figure 3.8. Implementation of ANN MPPT

3.3.4. Recommended Technique Hybrid MPPT: Combination of P&O, INC and ANN

This method is progressed to eliminate the shortcomings of traditional tracking algorithms and intelligent algorithms. The aim of this issue is to determine the types of algorithms that give highest efficiency for irradiance levels and to ensure the transition between each other. The measurement results are processed and when the irradiance down low levels, algorithm adjusts to ANN automatically. Thanks to the structure tracking algorithm, the highest efficiency is achieved while the irradiation level is low. It affected to improve the system performance significantly. Moreover, when the lowest algorithm efficiencies at some radiation levels were examined, there was an increase of up to 2% thanks to the hybrid method.

The PWM signals obtained from the three tracking methods are entered into the Hybrid MPPT function as input signal. Along with these inputs, the irradiance function is also included as an input to the system for comparison purposes. As a result of the operations that performed in the function block, a PWM signal is obtained according to the irradiance level and given to the converter as a trigger. In this way, the highest efficiency algorithm is adjusted in each irradiance. This mentioned system is shown in figure 3.9 below.

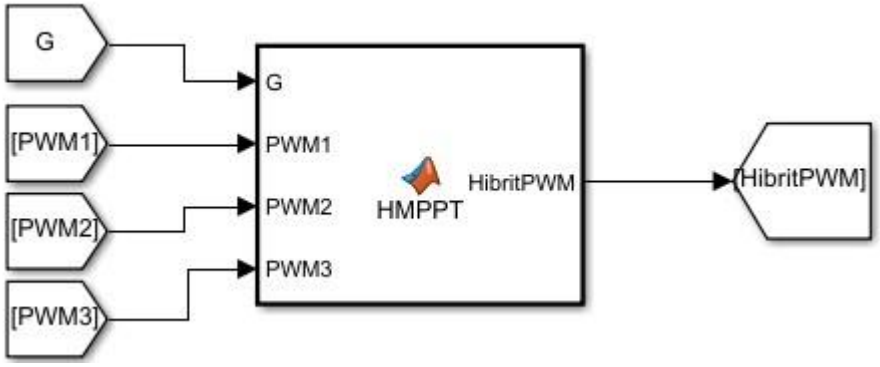


Figure 3.9. Function Block of Hybrid MPPT

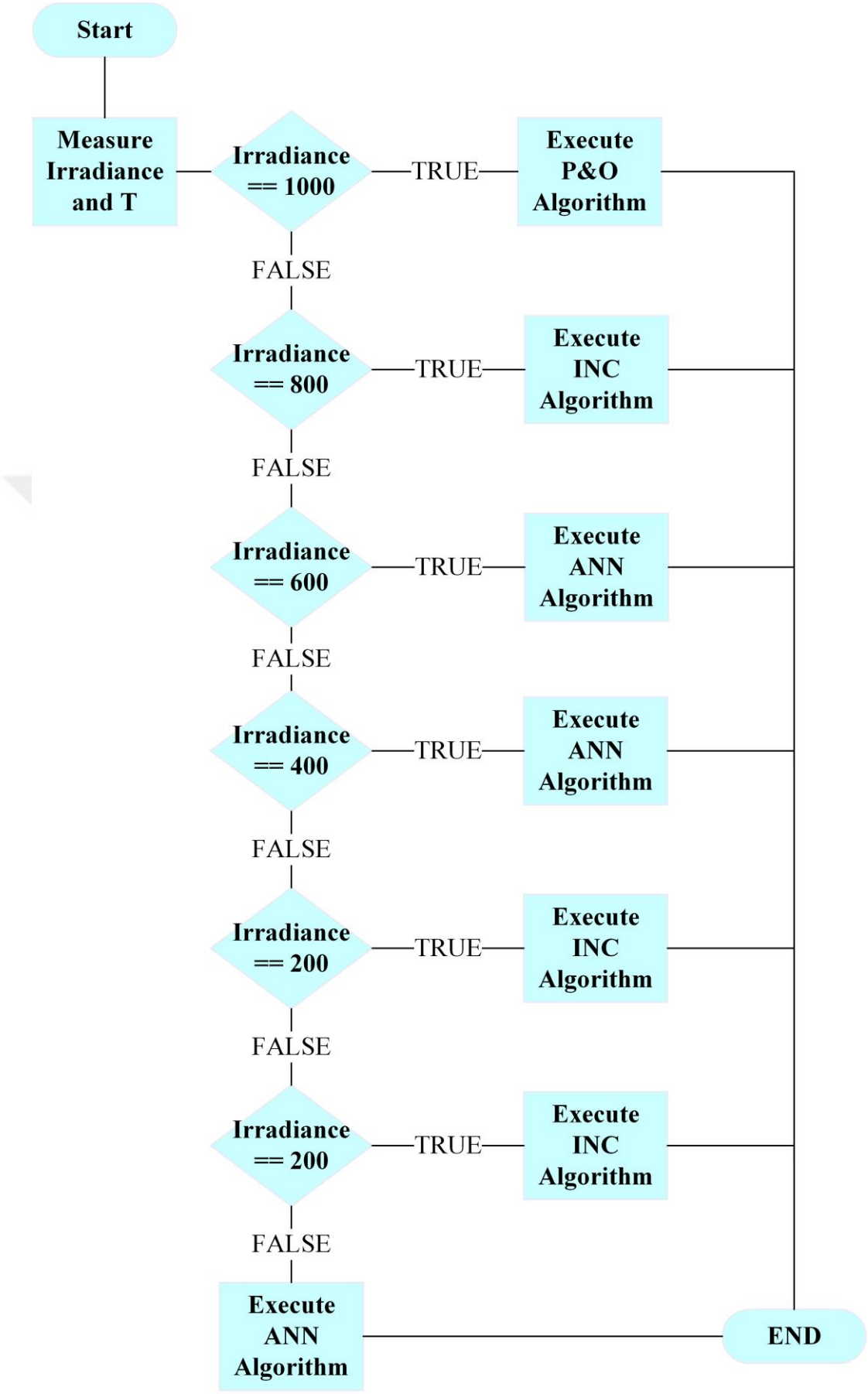


Figure 3.10. Flowchart of Hybrid MPPT

3.4. Battery Energy Storage System

BESS applications in solar energy are a widely used method. These type of applications presents more ecological energy solution for every area. In the past, although utilize this hybrid system locate in rural areas, today this designs are used in homes, companies, schools, free space. It is a vital system used to ensure power continuity in solar energy production facilities. Especially at night, there is not current or voltage generation because there is not reflecting any light to the solar panel. In this case, the battery is activated and provides that the power flow continues and the system does not run out of energy.

BESS system is formed by combining some different stages. These stages are to build a DC-DC bidirectional buck boost converter, design of a battery with internal parameters, design of the PI controller for the charge and discharge procedure of the battery respectively.

First of all, the battery is chosen lithium-ion battery block of MATLAB/Simulink with 420 rated voltages and 24Ah (ampere-hour) rated capacity (Bozkurt, 2022). The capacity of battery power is taken as 10kw. The State of Charge (SOC) are determined as 50% for starting stage. Battery parameter adjustments in Simulink is represented in table 3.4.

Table 3.4. Chosen Battery Parameters for Designing Criteria

Fundamental Parameters of Battery	
Type of Battery	Lithium-Ion
Nominal Voltage	420V
Rated Capacity	24Ah
Cut off Voltage	315V
Full Charged Voltage	488.87V
Capacity (Ah) at Nominal Voltage	21.7V
Nominal Discharge Current	10.43A

The designed battery is tied to DC bus with the help of a bidirectional buck boost converter. This power electronic device is used to decrease or increase voltage levels during the discharging and charging stages. A bidirectional buck boost converter has two sides which are called as high side and low side. The DC bus voltage is taken 700V as the high voltage side of bidirectional buck boost converter. Battery voltage is chosen 455V as the low side of the converter. This procedure provides bidirectional current flow.

In this thesis, daytime period is assumed to be 1 sec. and night time period is assumed to be 1sec. These periods were taken into account in the battery design. Since the PV panel generates power during the daytime, the battery performs charging process. At night, the battery is adjusted the

discharge mode automatically because the battery cannot generate power. The battery circuit diagram is shown in figure 3.11.

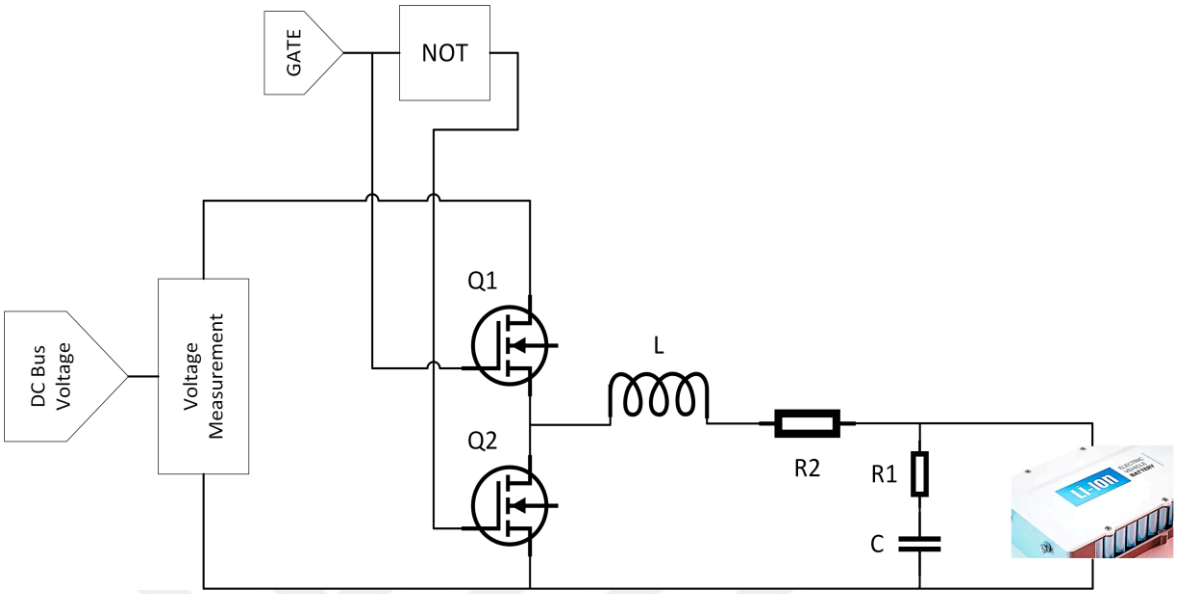


Figure 3.11. Block Diagram of BESS

The bidirectional buck boost converter circuit consist of six main components as mentioned before. These are two transistors, one inductor, one resistor series connected with inductor, one capacitor, one resistor series connected with capacitor. Parameter values were selected for four main components at the design stage. The selected parameters are also indicated in table 3.5 below.

Table 3.5. Chosen Bidirectional Buck Boost Converter Parameters

Bidirectional Buck Boost Converter Parameters	
Capacitor (C)	1mF
First Resistor (R_1)	1Ω
Inductor (L)	6mH
Second Resistor (R_2)	0.05Ω
DC Bus Voltage (V_H)	700V
Battery Voltage (V_L)	455V
Switching Frequency	10kHz
Input Current Ripple	10%
Output Current Ripple	1%

The most crucial point after the parameter design is generation of PWM pulse for triggering the transistors. The charging and discharging processes take place thanks to these trigger signals. Properly generated PWM signals contribute to the correct operation of the process.

In the charging state procedure, the difference between the battery voltage and the reference voltage is taken. This obtained value is given to the controller as an input signal. After that, the output of controller is used to acquire charging current. At the end of all these operations, the current required to charge the battery is obtained. As a result, both the battery voltage is controlled according to reference value, and the reference charging current is acquired. This operation is represented in figure 3.12.

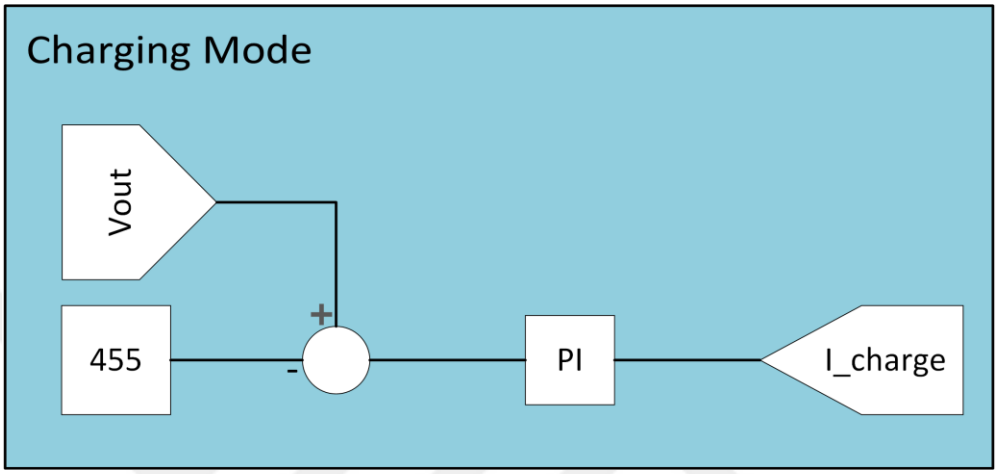


Figure 3.12. Charging Process of the BESS

The reference voltage is chosen as 455 V and maximum charging current is taken as 10.43A same with the rated discharge current of battery. Only the P and I parameters were used in the PI controller and the D value is taken as zero. The charging operation was assumed as 1 second (between 0 to 1) in the simulation part. The system works for 1 second in daytime mode and switches to night mode. Then the battery automatically switches from charging mode to discharging mode.

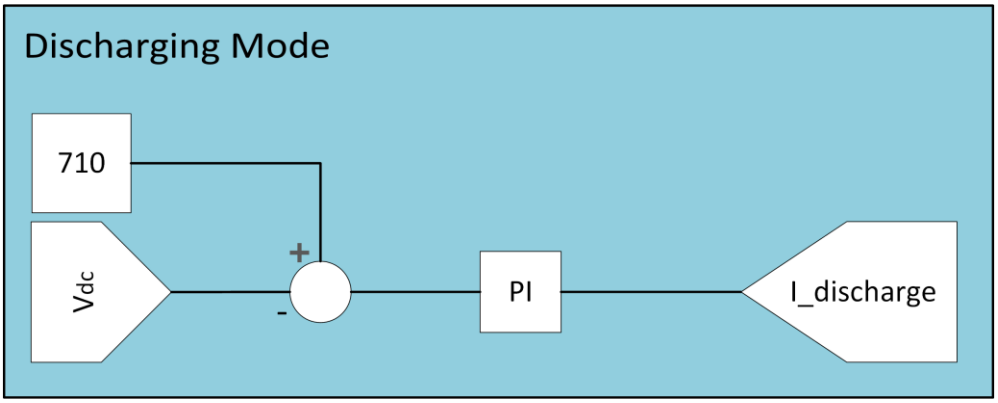


Figure 3.13. Discharging Process of the BESS

In another process called discharging mode, the difference is taken between the DC bus voltage and reference voltage. The result of difference is given as input for PI controller. Like charging mode, only P and I parameters were used in the controller and the D value is taken as zero.

After the output of controller is acquired, the discharge current is equal it. This process is indicated in figure 3.13. The discharging operation was assumed as 1 second (between 1 to 2) in the simulation part. The system works for 1 second in night time mode and switches to daytime mode. Then the battery automatically switches from discharging mode to charging mode.

The state changing switch structure, which is located in figure 3.14 below, decides whether the battery is on charge mode or on discharge mode. Thanks to this switch, the battery alters state automatically. The output of switch is referred as the reference current.

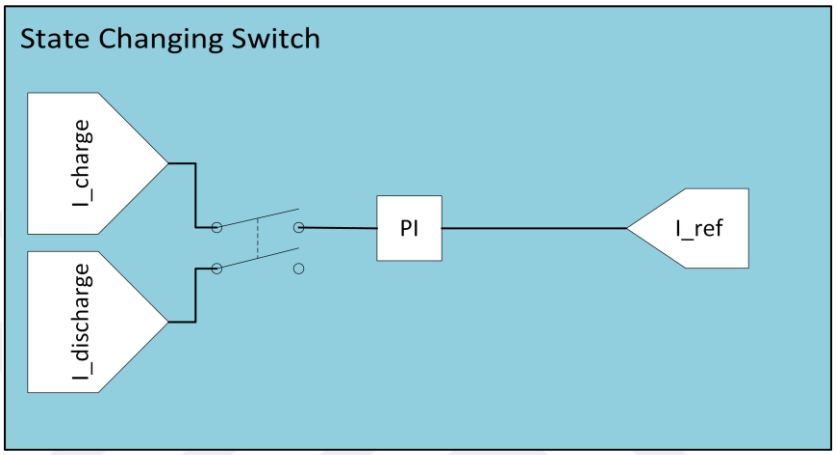


Figure 3.14. Setting the Status Switch for Charge or Discharge Operation

After the reference current is constructed, the gate signal of transistor is produced using this current. When performing this operation, the battery current is subtracted from the reference current and the difference is given to the PI controller as an input. As a normal PWM logic, the output of the controller is compared with a carrier signal and a PWM signal is manufactured. While the generated gate signal is connected directly to the transistor in the upper position, the complement is taken and connected to the lower side transistor at the same time.

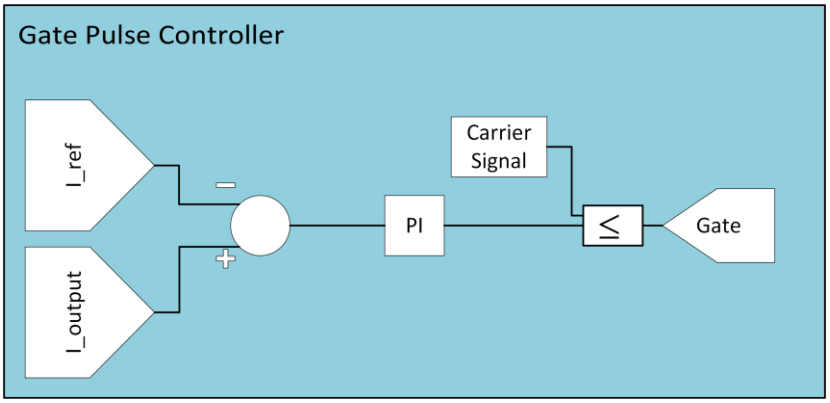


Figure 3.15. Gate Pulse Controller Diagram

3.5. Energy Management System

For hybrid power systems, it is very important to control the battery energy according to a specific algorithm. The algorithm designed to manage this energy is called as energy management system. As it is no exact version of this system, it can be changed according to the study performed or depending on demand.

In this thesis, the designed energy management system measures the PV current firstly. If the PV is generating current, the daytime mode is activated and the battery goes into a charging state. If the PV is not producing current, night mode is activated and the battery enters the discharge state and transfers the stored energy to the circuit. The flowchart of this algorithm is indicated in figure 3.16.

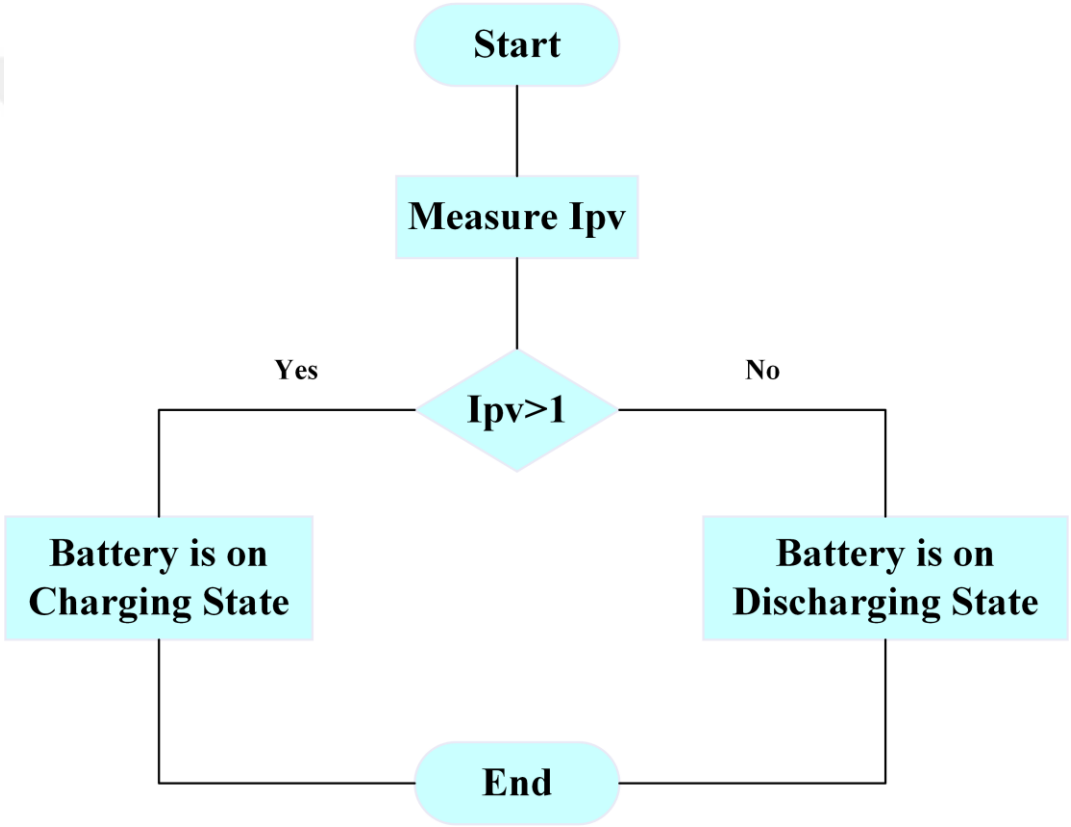


Figure 3.16. Energy Management System Scenario

3.6. Grid Connected Inverter and Control

In this thesis, a conventional six transistor inverter structure was used to convert the dc voltage and current which is supplied from the dc bus to AC. Thanks to advanced control applications, the six separate PWM signals are generated from the incoming signal and given to each switch mode transistor as a trigger signal. There are two important control mechanism in this stage. Firstly, an inverter controller is designed to control the inverter and produce PWM. The second is the PLL controller, which plays an important role in grid-connected systems.

While PLL control is performed in this circuit, V_{abc} and I_{abc} are converted into direct(d)-quadrature(q) components. Since it is more difficult to process sinusoidal components, voltage and current are transferred to the d-q domain which is referred as rotating frame based on input angular position in terms of radian (rad) with the help of Park transformation (Macit, 2023). By use of Equation 3.6.1 and 3.6.2 is acquired V_d, V_q and I_d, I_q. These attained components are utilized in the inverter current controller to get reference dq0 vectors.

Voltage vector a-b-c to d-q conversion is shown as in Equation 3.6.1

$$\begin{bmatrix} V_d \\ V_q \\ V_0 \end{bmatrix} = \frac{2}{3}\begin{bmatrix} \cos(wt) & \cos\left(wt - \frac{2\pi}{3}\right) & \cos\left(wt + \frac{2\pi}{3}\right) \\ \sin(wt) & \sin\left(wt - \frac{2\pi}{3}\right) & \sin\left(wt + \frac{2\pi}{3}\right) \\ \frac{1}{2} & \frac{1}{2} & \frac{1}{2} \end{bmatrix}\begin{bmatrix} V_a \\ V_b \\ V_c \end{bmatrix} \tag{3.7.1}$$

The current vector a-b-c/d-q transformation is calculated in Equation 3.6.2.

$$\begin{bmatrix} I_d \\ I_q \\ I_0 \end{bmatrix} = \frac{2}{3}\begin{bmatrix} \cos(wt) & \cos\left(wt - \frac{2\pi}{3}\right) & \cos\left(wt + \frac{2\pi}{3}\right) \\ \sin(wt) & \sin\left(wt - \frac{2\pi}{3}\right) & \sin\left(wt + \frac{2\pi}{3}\right) \\ \frac{1}{2} & \frac{1}{2} & \frac{1}{2} \end{bmatrix}\begin{bmatrix} I_a \\ I_b \\ I_c \end{bmatrix} \tag{3.7.2}$$

These d-q voltages are controlled by two PI controller. Only PI is used in simulation for d-q domain. Parameter D is taken as zero. After passing of d-q domain, inverter controller operation is implemented. Result of inverter controller, two materials are constructed which are called as E_d and E_q. According to these components, most of the inverter control operation is completed. However, staying in the d-q domain is not enough to completely control the inverter. In order to generate six separate PWM signals, it is necessary to switch from the d-q domain to a-b-c domain again. To switch the a-b-c domain, the inverse park transformation is applied into V_d, V_q and I_d, I_q components with using equation 3.6.3 below.

The voltage vector d-q/a-b-c (inverse park) transformation calculated in Equation 3.6.3.

$$\begin{bmatrix} V_a \\ V_b \\ V_c \end{bmatrix} = \begin{bmatrix} \cos(wt) & -\sin(wt) & 1 \\ \cos\left(wt - \frac{2\pi}{3}\right) & -\sin\left(wt - \frac{2\pi}{3}\right) & 1 \\ \cos\left(wt + \frac{2\pi}{3}\right) & -\sin\left(wt + \frac{2\pi}{3}\right) & 1 \end{bmatrix}\begin{bmatrix} V_d \\ V_q \\ V_0 \end{bmatrix} \tag{3.7.3}$$

The rated value of DC link voltage is specified as 700V in table 3.3. It is taken as reference voltage and compared with measured DC link voltage. After the result of comparison give an input parameter of PI controller. Besides the DC link voltage, the current component is also obtained with the same logic.

In addition, phase information is also needed when applying the inverse park transformation which is represented d-q to a-b-c block in MATLAB/ SIMULINK. The phase information component can be easily taken from the PLL circuit performed in the simulation. The inverter controller and the PLL circuit are shown in figure 3.17 and 3.18. The PWM signals in figure 3.17 are given to each inverter transistors as a trigger signal

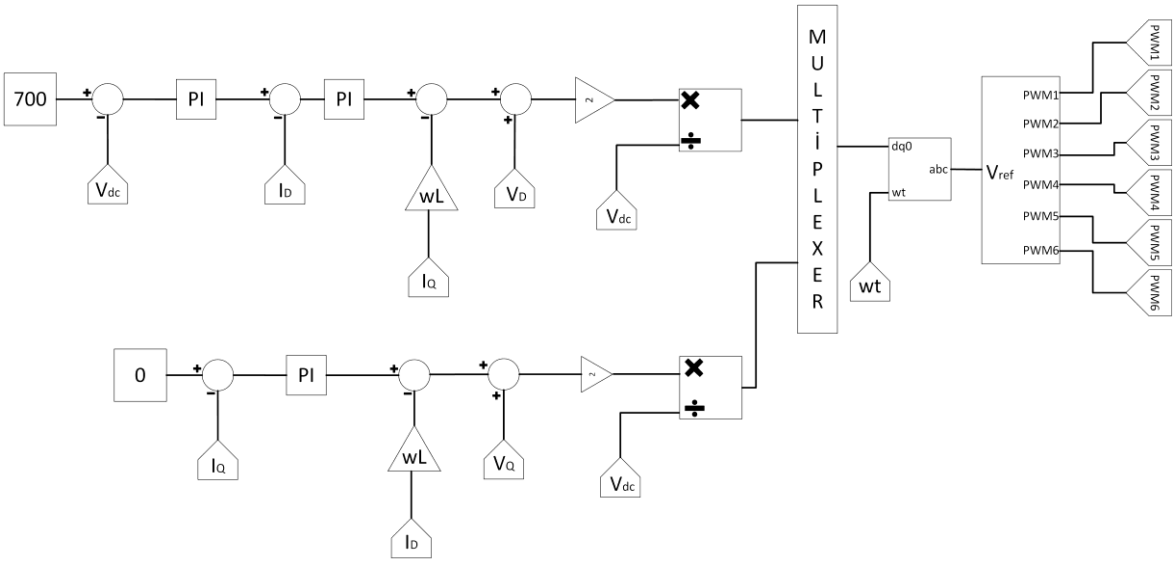


Figure 3.17. Power Control of the Three Phase Inverter

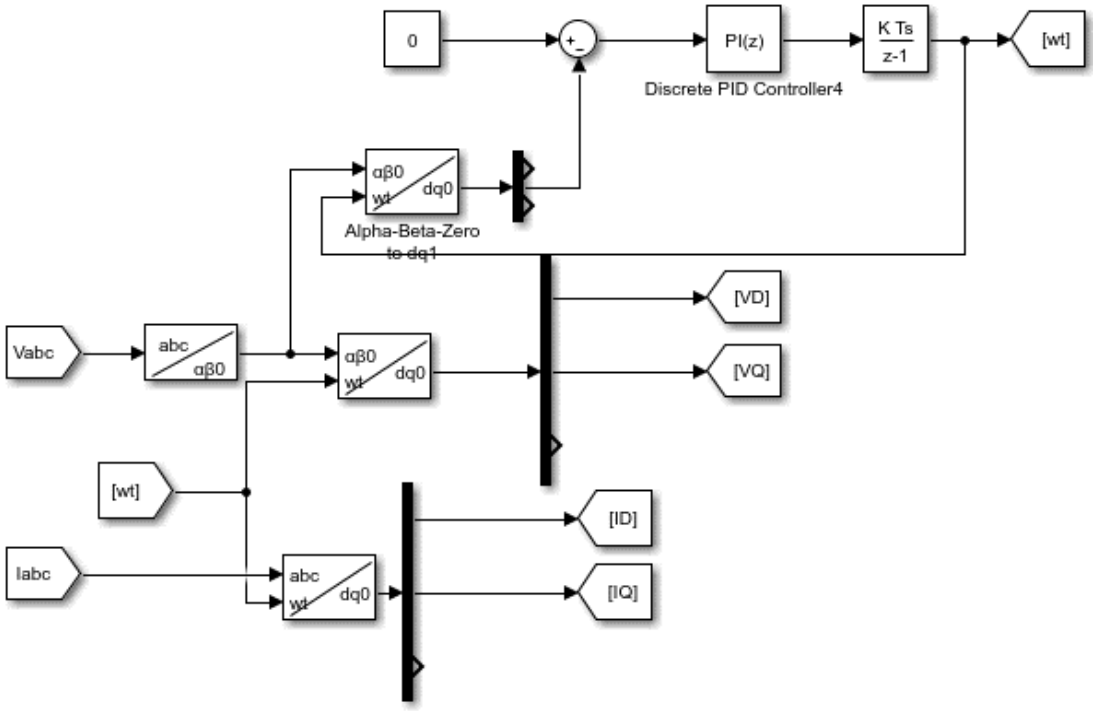


Figure 3.18. Designed PLL Circuit for Inverter Control and Grid Synchronization

3.7. Harmonic Mitigation with Two Mode LCL Filter

In circuits where DC current and DC voltage are converted to AC with the help of inverter, the inverter output voltage and current contain undesirable components at a high level. These undesirable components are called as harmonics. If a signal has harmonic distortion at a high level, it loss purity, efficiency and robustness. It departs from pure sine waveform. Therefore, reducing harmonic distortions is a vital stage for electronic circuits.

A LCL filter was used to mitigate harmonics. When designing this filter, six inductors, nine resistors, three capacitors were used. The three phase LCL filter representation is available in figure 3.19.

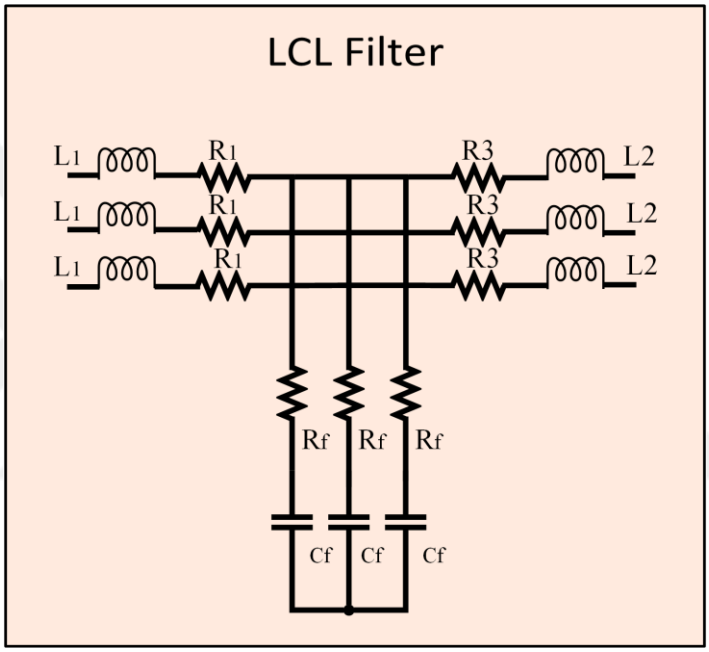


Figure 3.19. Representation of Three Phase LCL Filter

In this thesis, a different study was applied for LCL filter design. In the literature review is conducted, this type of LCL filter was not encountered. The study is to design two separate filter modes over a single LCL filter.

Since the battery and PV power are different, it was determined that the THD increased in a single LCL filter when switching from day mode to night mode. To prevent this situation, two robust filter modes have been designed according to two separate power levels. During the daytime, the first mode LCL filter works when the PV is in active region. The second mode LCL filter is in the off position. During the night time, when the PV is in passive region, the second mode LCL filter works. The first mode LCL filter is in the off position. In other words, the first mode LCL filter corresponds to the daytime mode, and the second mode LCL filter corresponds to the night time mode. In this way, THD is significantly reduced.

While PV produces energy, the parameter values of the LCL filter are as shown in table 3.6.

Table 3.6. Daytime Mode LCL Filter

First Mode LCL Filter	
L_1 (Left Side Inductor)	2.5mH
R_1 (Left Side Resistor)	1mΩ
Capacitor	22μF
R_f (Bottom Side Resistor)	2Ω
L_2 (Right Side Inductor)	100μH
R_2 (Right Side Resistor)	1mΩ

While PV does not produce energy, the parameter values of the LCL filter are as shown in table 3.7.

Table 3.7.Nighttime Mode LCL Filter

Second Mode LCL Filter	
L_1 (Left Side Inductor)	2.1535mH
R_1 (Left Side Resistor)	1mΩ
Capacitor	18.76μF
R_f (Bottom Side Resistor)	0.6286Ω
L_2 (Right Side Inductor)	68.85μH
R_2 (Right Side Resistor)	1mΩ

Thanks to two mode filter design, some product costs have been saved. Cost reductions are acquired 32% on the right side inductor, 15% on the capacitor, 14% on the left side inductor and 31% on te right side resistor.

3.8. Summary

In this chapter, a comprehensive description of the PV-BESS hybrid power system design is ensured. It comprises and design considerations for PV Array parameters, BESS parameters, design of P&O INC and ANN MPPT, recommended Hybrid MPPT procedure and design, boost converter parameter calculation for PV, bidirectional buck boost converter for BESS, two mode LCL filter design, grid connected inverter controller and PLL design. The inside structure of the whole system and suitable control strategies are described in deeply, energy management, and the proposed MPPT method, two mode LCL filter for bringing novelty to thesis is mentioned.

4. RESULTS AND DISCUSSIONS

In this part of the thesis, the simulation results of the circuit were taken according to specified irradiance levels. The tested irradiation levels are 1000, 800, 600 W/m^2 respectively. In addition, the output results of P&O, INC, ANN tracking algorithms were taken in each test and the hybrid method was applied after these stages. All methods, including the hybrid method, have been evaluated for performance among themselves. The simulation results obtained in this section are clearly discussed in the summary part. According to the acquired results, THD and efficiency percentages were observed. The most efficient way that can be used for the system has been studied and proposed.

4.1. Simulation Outcomes at 1000 W/m2 with P&O

Firstly, when starting the simulation on the MATLAB/SIMULINK platform, it is necessary to adjust the irradiance level from the sun and air temperature parameters. In this section, it has been assumed that 1000 W/m^2 irradiance comes from the sun and the air temperature is 25°C. After these parameters are entered and the simulation is run, the PV starts to generate energy. The produced current and voltage enter the boost converter directly. The incoming 380V to the boost converter is increased to 700V levels. It is called as DC bus voltage. At this stage, the P&O method is used to keep the generated power at maximum point. The DC bus voltage is supplied to the input of the inverter. Using a conventional six-transistor inverter, the DC current and DC voltage enter this device. The output waveform of the device changes to the AC shape. The distortion rates and efficiency levels of the waveforms formed at the output of the inverter depend on the performance of MPPT methods. The output waveforms of inverter with the P&O method are shown in figure 4.1 below.

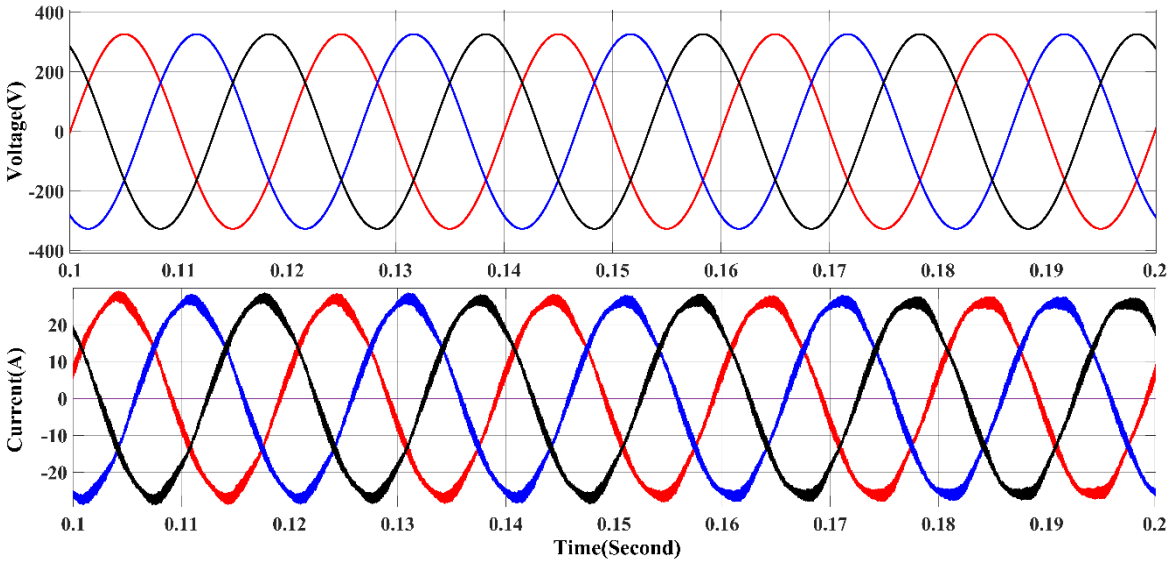


Figure 4.1. The Inverter Output Voltage and Current Waveform at 1000 W/m^2 with P&O

As can be seen in figure 4.1 the output waveform of the inverter current resembles a pure sine wave, but it has ripple on it.

In the next stage, the battery is operated for a total of 2 seconds, day mode and night mode. The SOC percentage of the battery, the output voltage value of battery, the current value are indicated in figure 4.2 below. According to battery control algorithm, the material is in the charge position between 0-1 seconds. Charging the device shows that the PV can generate power when the battery is in daytime mode. The SOC value increases in this time interval. Output voltage is up to 455 volts, which is the charging state reference value. After the charging situation, the battery set the discharging position between 1-2 seconds. During this time interval, the system is running in night mode and the PV panel is in cut off zone. SOC is decreasing because energy is supplied from battery. The battery voltage drops and sets the rated discharge current to 10.43A. In addition to these outcomes, the status of the DC link voltage is given in figure 4.2.

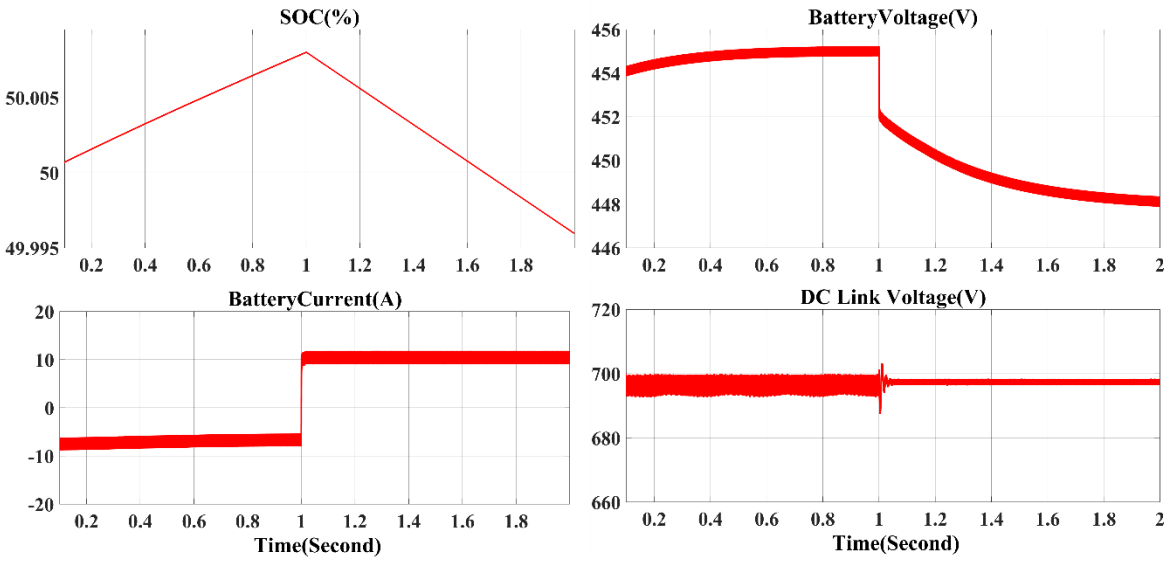


Figure 4.2. The Graphs of Battery Outcomes and DC Link Voltage with P&O at 1000 W/m^2

The DC bus voltage set to 700V. It oscillates depending on MPPT performance. As can be seen in figure 4.2, there are ripples on the DC bus voltage. This situation reduces the performance of the DC signal.

When the P&O method is deployed, the ripples in the dc link voltage cannot be eliminated completely. Therefore, while the THD of the system seems high, its efficiency seems low. This is one of the biggest problems of P&O, which is referred as a traditional method. Another problem is that it takes longer to respond to any changes. When state switching is completed, this method reacts later compare with the other methods.

The efficiency result, which is an important parameter for system performance, is available in figure 4.3. According to this figure, the efficiency of the P&O MPPT at 1000 irradiance is in the 95.87% band.

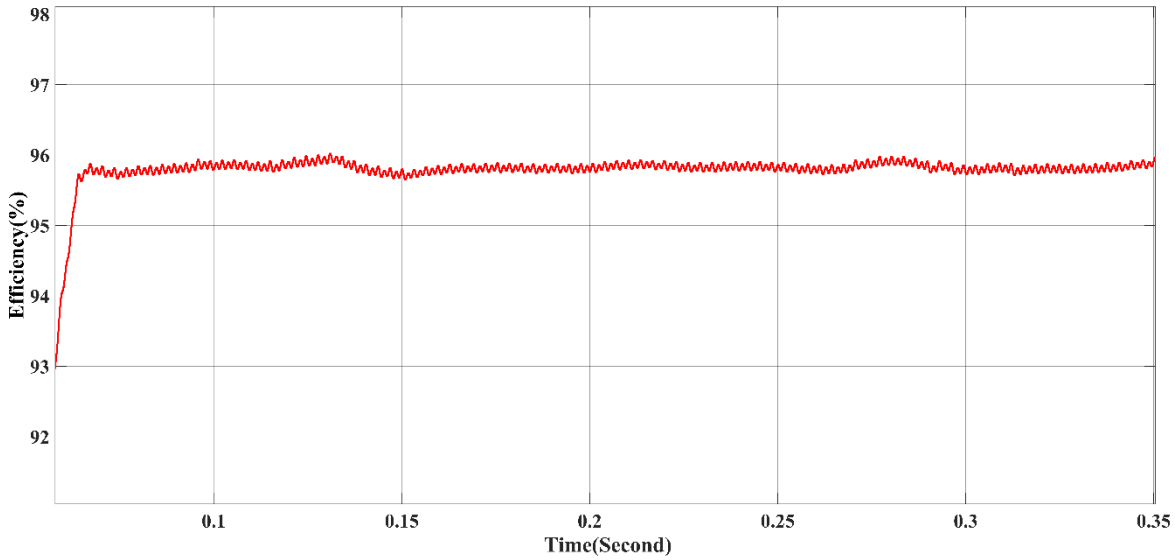


Figure 4.3. Efficiency of Power with P&O at 1000 W/m^2

The ripples formed in efficiency graph also depend on the robustness and performance of the MPPT method, as in THD. When the figure 4.3 is examined, P&O which is referred as conventional method shows more ripples on efficiency at 1000 W/m^2.

Another result of simulation is in figure 4.4. In this shape specifies the THD percentage constructed by daytime mode LCL filter.

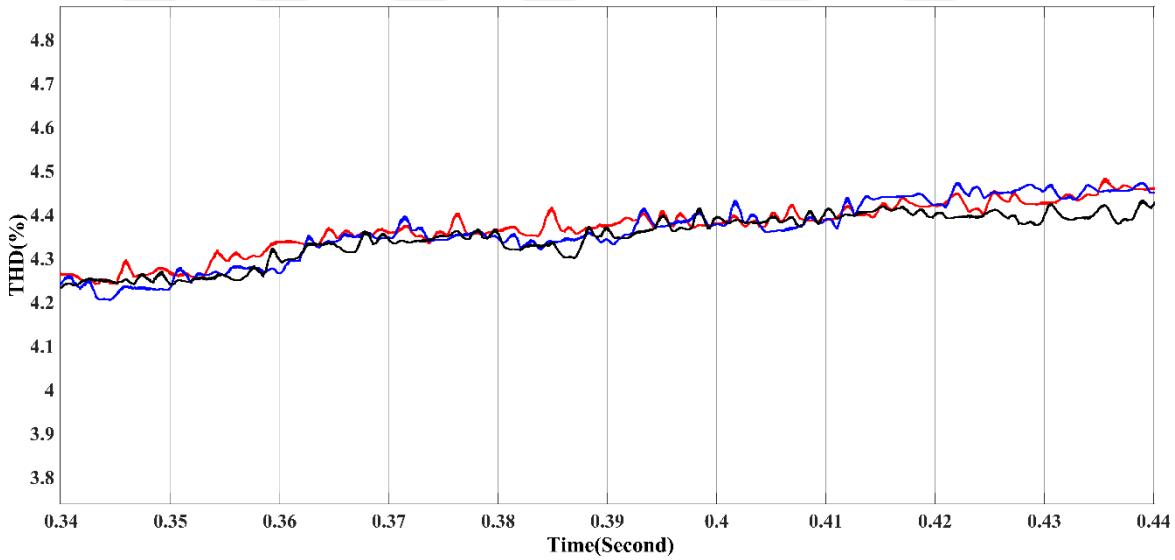


Figure 4.4. The THD of Daytime Mode LCL Filter with P&O at 1000 W/m^2

While the PV panel generates power, the output current THD level varies between 4.2% to 4.5%. This value is closer to 5% during the night period. A new LCL filter design has been made so that the THD does not rise while the system is powered from the battery. In this way, THD has been reduced to 3.2% and its oscillation has been decreased. This type of study has not been encountered

in the literature review. Therefore, thanks to the new LCL filter design, an academic contribution has been made.

The THD results of the simulation with two filters for both daytime and nighttime mode are available in figure 4.5 below.

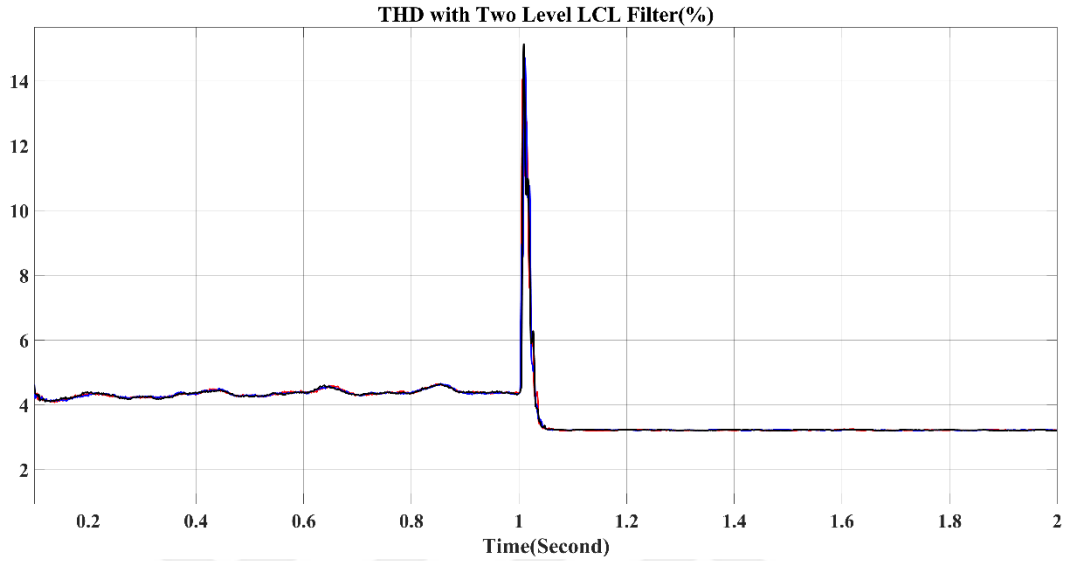


Figure 4.5. The THD of Two Mode LCL Filter with P&O at 1000 W/m^2

4.2. Simulation Outcomes at 1000 W/m^2 with INC

Another tracking method which is indicated as INC is used to run with a boost converter. The method is one of the traditional tracking algorithms. The current and voltage waveforms observed at the output of the inverter are specified in figure 4.6 below.

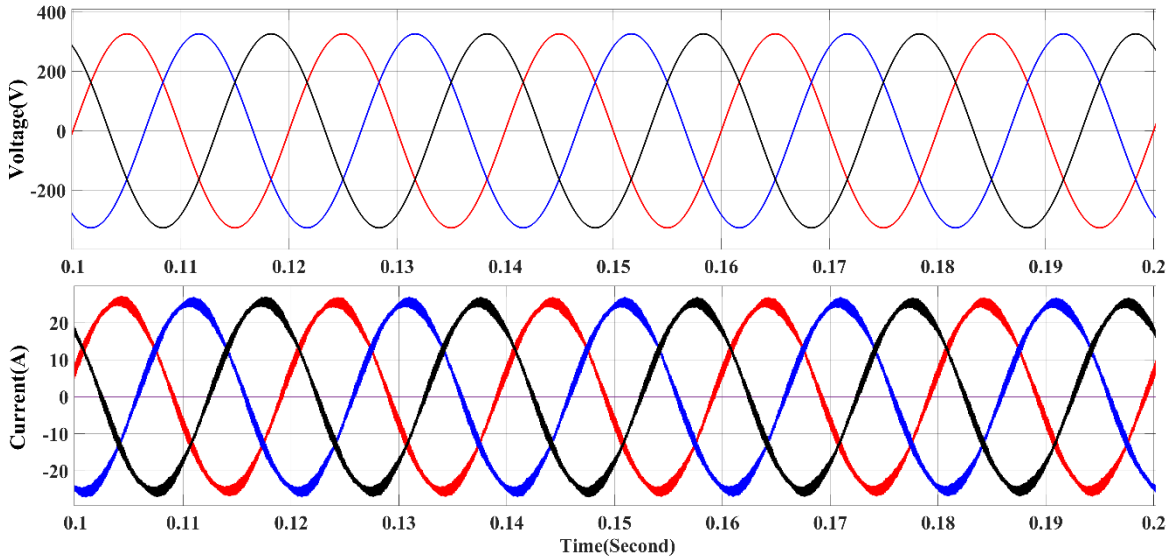


Figure 4.6. The Inverter Output Voltage and Current Waveform at 1000 W/m^2 with INC

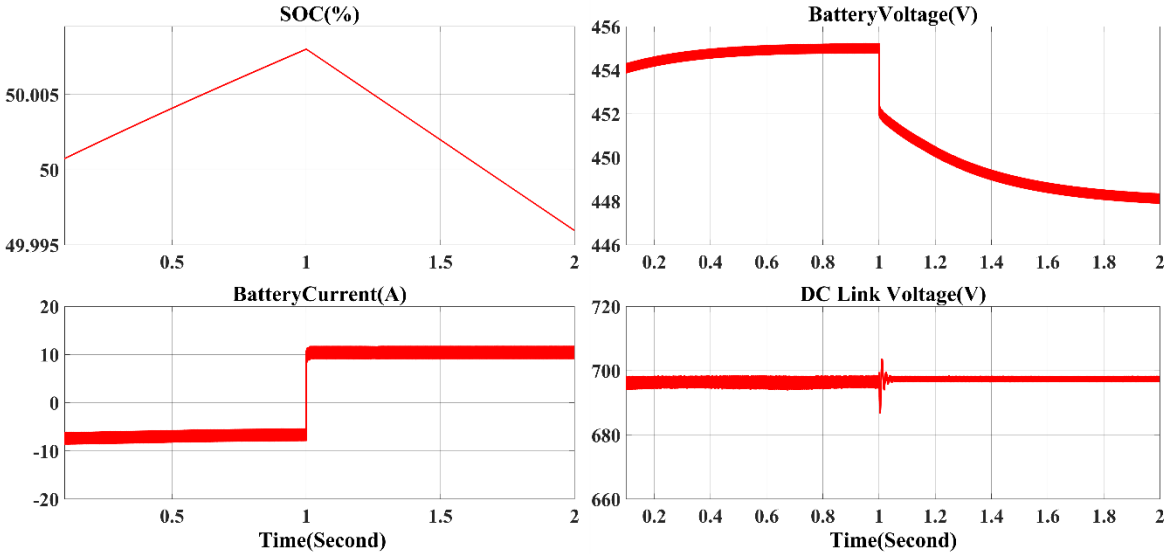


Figure 4.7. The Graphs of Battery Outcomes and DC Link Voltage with INC at 1000 W/m^2

When the INC method is applied for 1000 irradiance, part of the output power goes to the inverter and remain part feeds the battery. The SOC graph showing the charging and discharging states of the battery, the change graph of the battery voltage and current, the DC link voltage graph are shown in figure 4.7.

Especially when the DC link voltage of the INC method is compared with the P&O, it is observed that there are fewer ripples in this method. This shows that using the INC tracking algorithm, the pure DC signal form is approached. Unwanted ripple levels are higher than INC when creating DC bus voltage by P&O method.

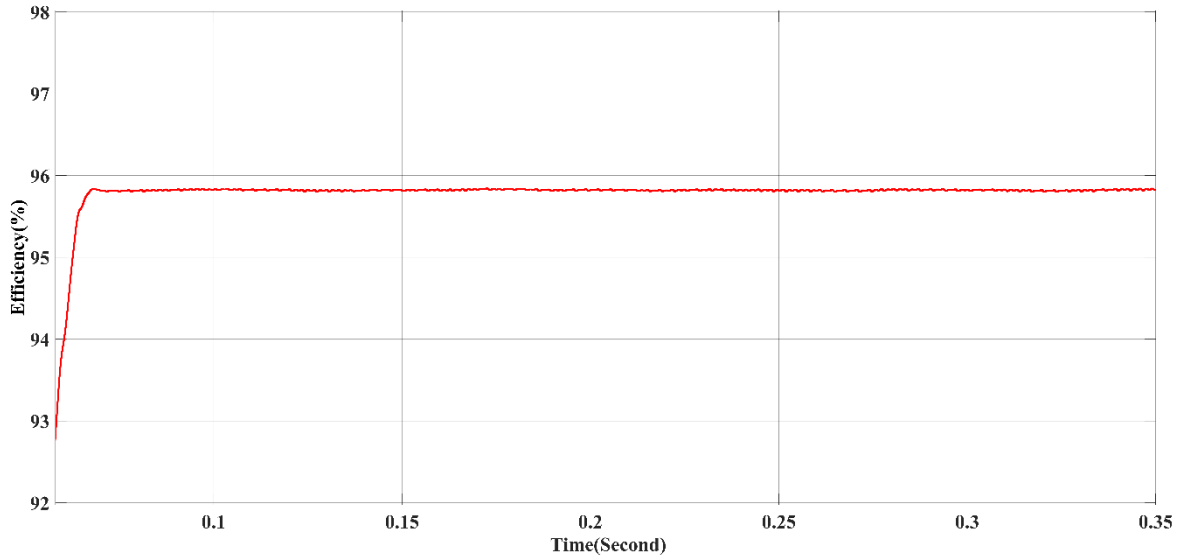


Figure 4.8. Efficiency of Power with INC at 1000 W/m^2

The efficiency graph of output power with using INC method is indicated in figure 4.8. When the efficiency levels of two traditional methods were examined at 1000 irradiance, it was realized that they were almost the same. The instantaneous fluctuation in power efficiency is decreased in this method.

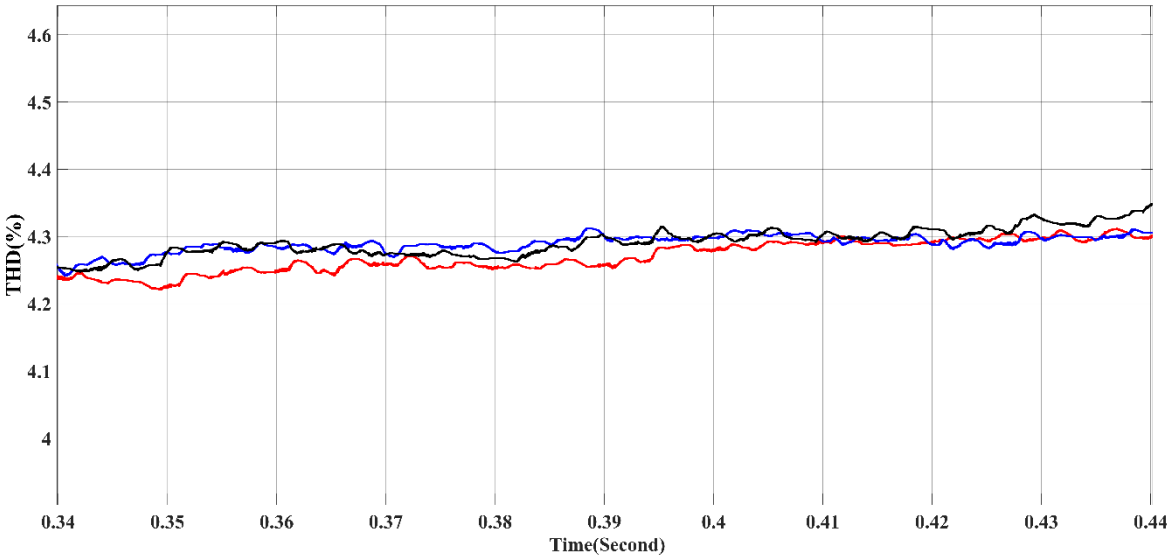


Figure 4.9. The THD of Daytime Mode LCL Filter with INC at 1000 W/m^2

In figure 4.9 and 4.10 show the THD graphs of the inverter output current. In figure 4.9, the THD was examined for a specified interval of seconds. When the system was only in daytime mode and it was found that this value decreased compared to P&O. While the THD level of the P&O method is between the range of 4.2%- 4.5% in daytime mode. In the INC method, this value is in the range of 4.2%- 4.3%. In night mode, the THD level drops to 3.2% because the second filter is activated.

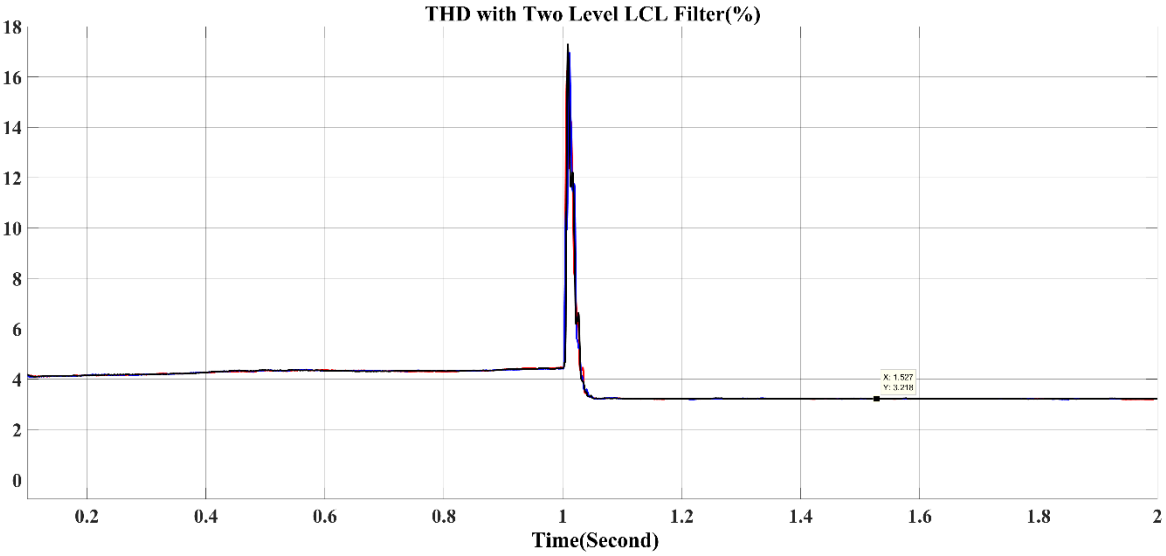


Figure 4.10. The THD of Two Mode LCL Filter with INC at 1000 W/m^2

4.3. Simulation Outcomes at 1000 W/m^2 with ANN

In this part, the intelligent ANN tracking method was used in 1000 irradiance, which is different from the traditional methods. When the inverter voltage and current output graphs are examined, it is seen that the similarity of this method to pure sinewave is greater than others. This indicates that the THD level is lower. The inverter output graphs obtained using the ANN tracking method are remarked in figure 4.11. While the graphs were moved from MATLAB/SIMULINK into this thesis, they were taken in the same time interval with other tracking methods.

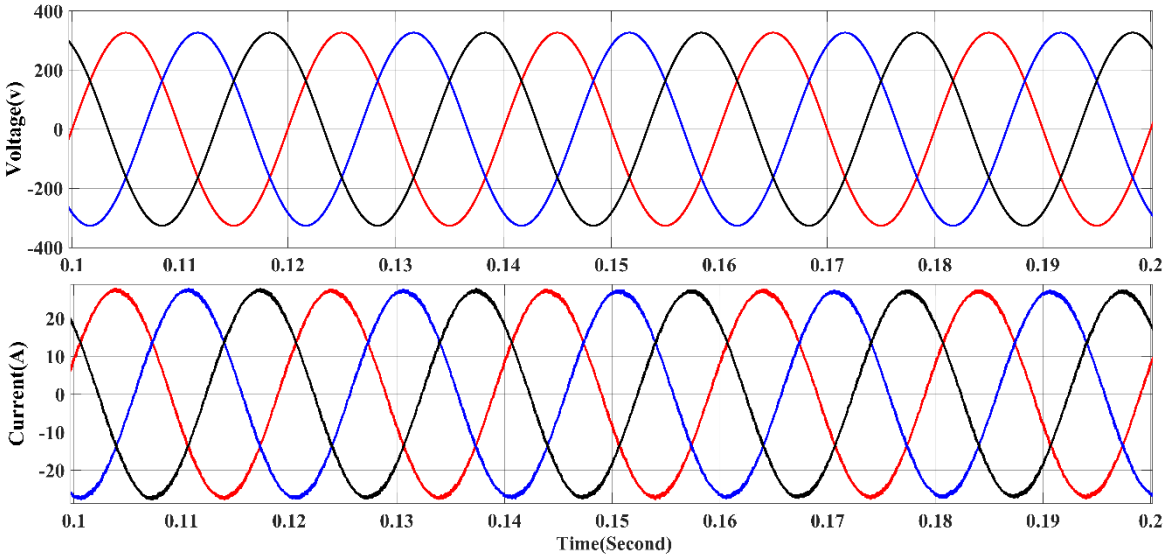


Figure 4.11. The Inverter Output Voltage and Current Waveform at 1000 W/m^2 with ANN

When the DC link voltage of the ANN method is analyzed in the figure 4.12, it is observed that there are fewer ripples in this method according to conventional algorithms. This situation shows that using the ANN algorithm, the pure DC signal form is approached.

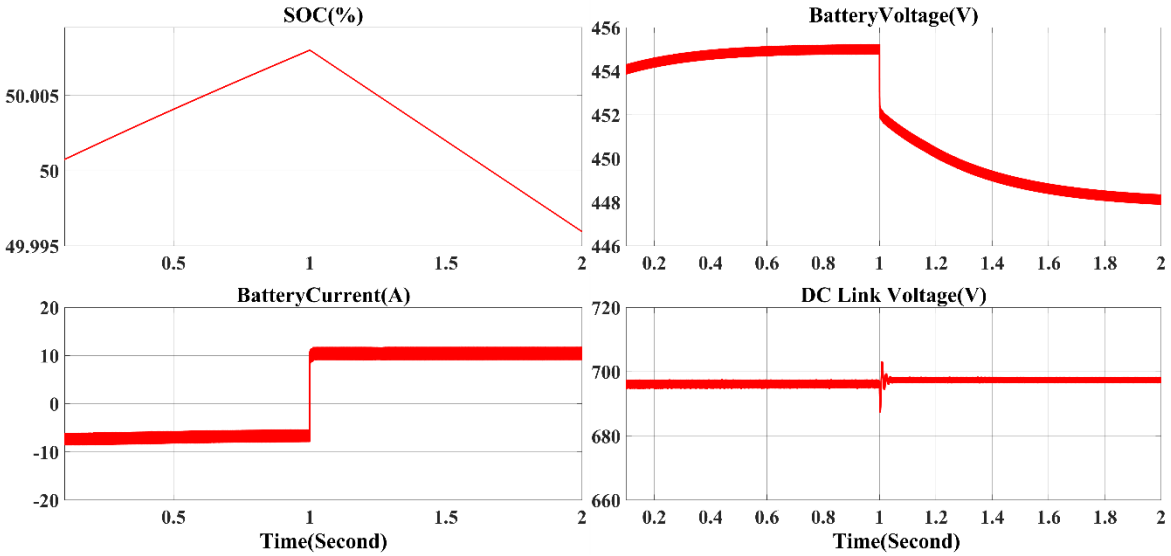


Figure 4.12. The Graphs of Battery Outcomes and DC Link Voltage with ANN at 1000 W/m^2

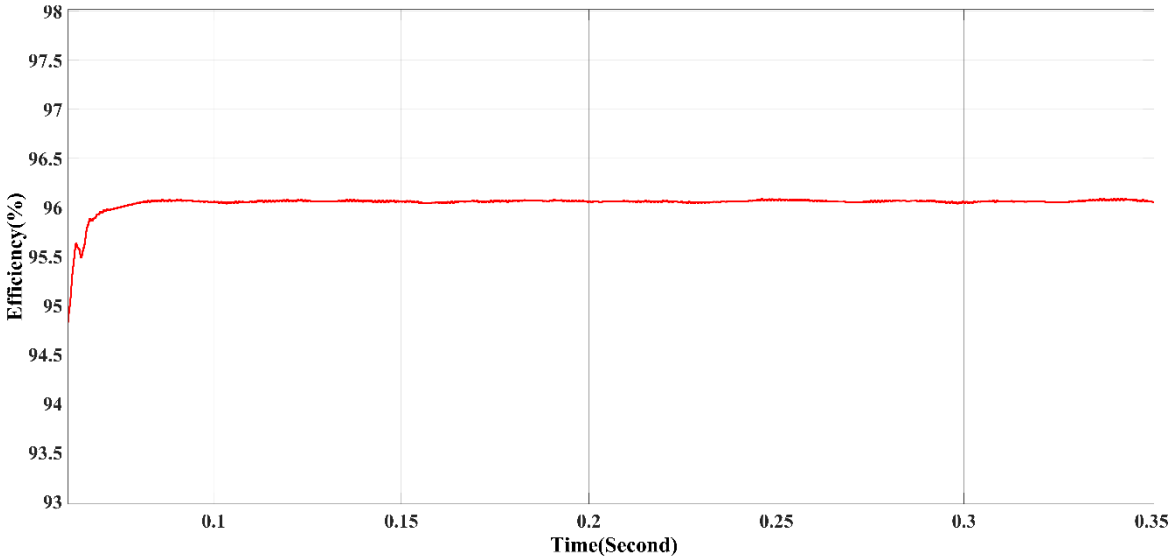


Figure 4.13. Efficiency of Power with ANN at 1000 W/m^2

The efficiency graph of output power with using ANN method is indicated in figure 4.13. When the efficiency levels of ANN were examined at 1000 irradiance and compared with other methods, it was realized that they were almost the same. The instantaneous fluctuation in power efficiency is decreased in this method.

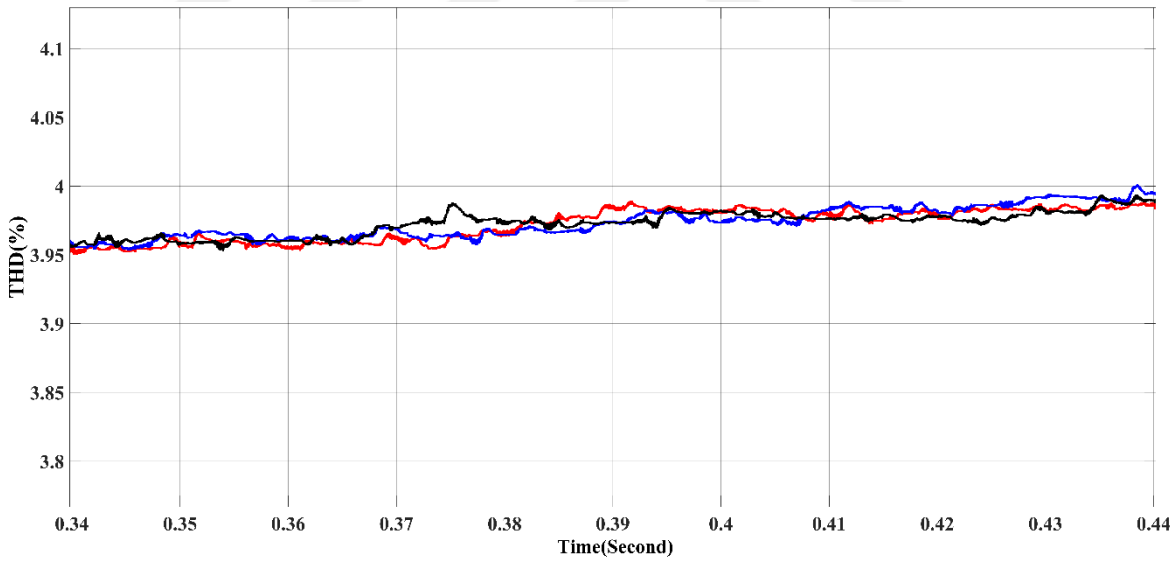


Figure 4.14. The THD of Daytime Mode LCL Filter with ANN at 1000 W/m^2

In figure 4.14 and 4.15 indicate the THD graphs of the inverter output current. In figure 4.14, the THD was examined for a specified interval of seconds when the system was only in daytime mode and it was found that this value decreased compared to conventional MPPT methods. While the THD level of the ANN method is between the range of 3.9%- 4% in daytime mode. In the INC method, this value is in the range of 4.2%- 4.3%, P&O method is in range of 4.2%- 4.5%. In night mode, the THD level drops to 3.2% because the second filter is activated. If the second LCL filter

structure had not been applied in this circuit, the THD value of the current would have increased up to 5%. This value is considered high for the design criteria.

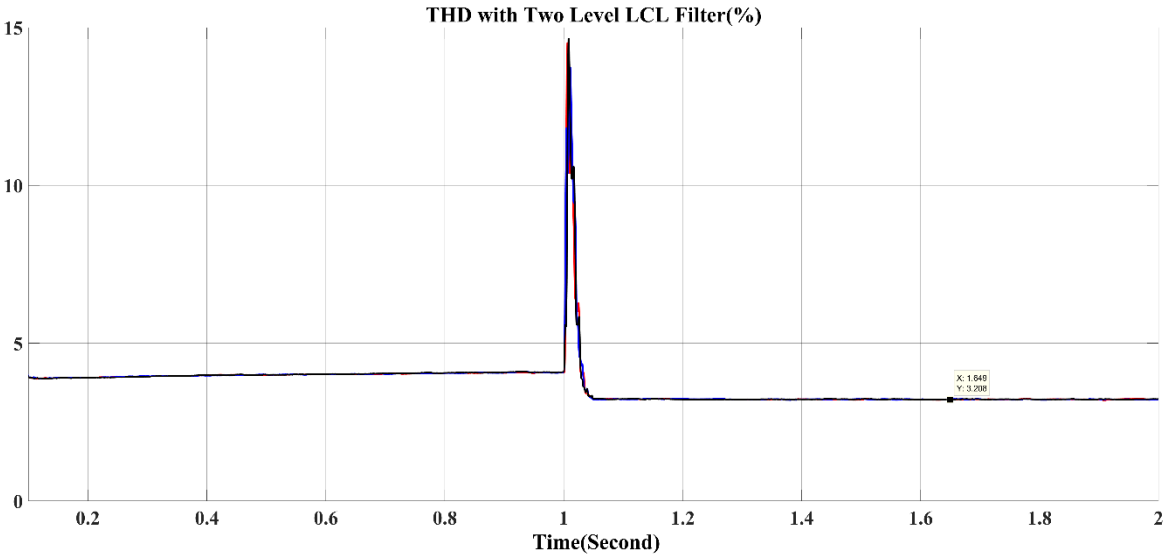


Figure 4.15. The THD of Two Mode LCL Filter with ANN at 1000 W/m^2

4.4. Simulation Outcomes at 800 W/m^2 with P&O

In this section, it is assumed that the irradiance level extracted from the sun is 800 and the design results are taken according to this value. The current and voltage generated by the solar panel are increased in the boost converter and kept at the maximum power level with the help of P&O MPPT. The output current and voltage graphs of the inverter are also available in figure 4.16.

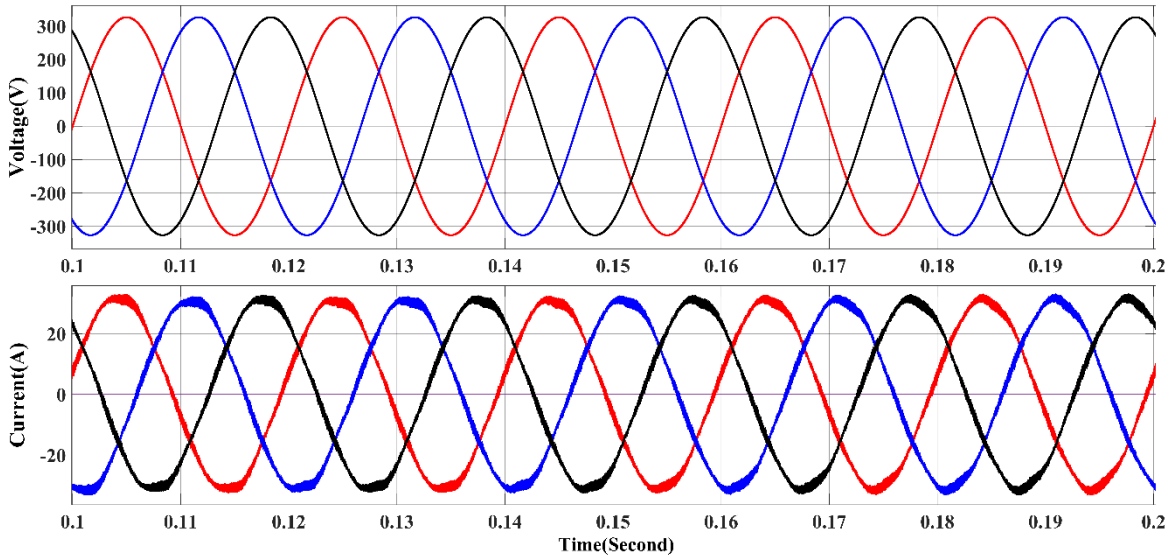


Figure 4.16. The Inverter Output Voltage and Current Waveform at 800 W/m^2 with P&O

After that, the battery parameters of the P&O method at 800 irradiance were examined. All battery parameter graphs are indicated in figure 4.17. The first of these parameters investigated is the SOC graph showing charging and discharging status the battery. The second one indicates the battery voltage. It has been observed that when the battery is in the charging state, it approaches 455V which is called as reference value. When the battery is in the discharging state, the voltage of battery flows around 448V.

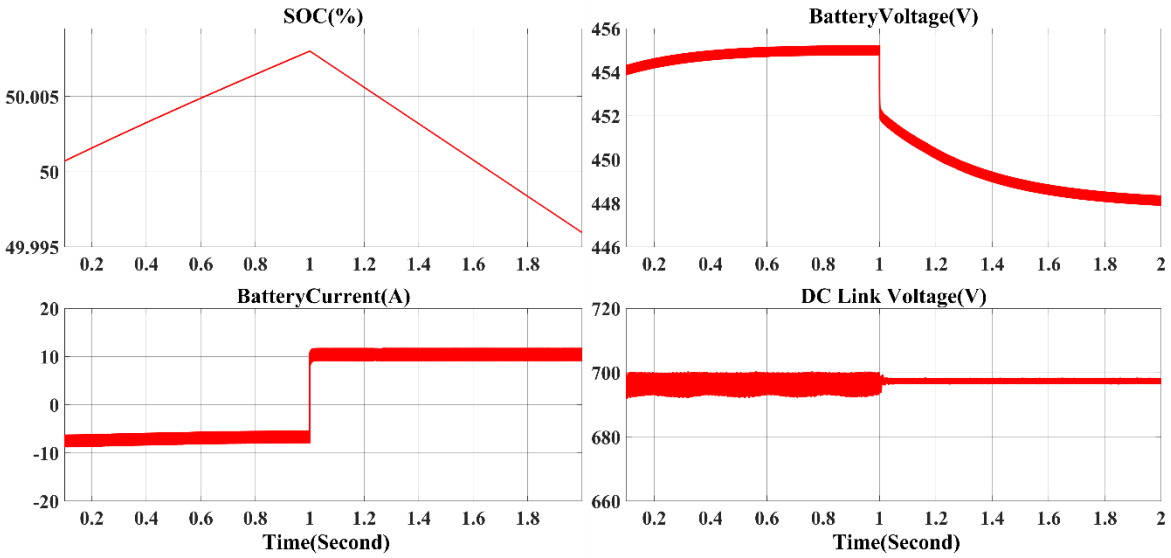


Figure 4.17. The Graphs of Battery Outcomes and DC Link Voltage with P&O at 800 W/m^2

After examining the battery and inverter, another important parameter in this simulation, the power efficiency level was observed. The result of this observed graph is shown in figure 4.18. According to the figure, it can be seen that the power efficiency level of P&O method used at 800 irradiance is 95.5%.

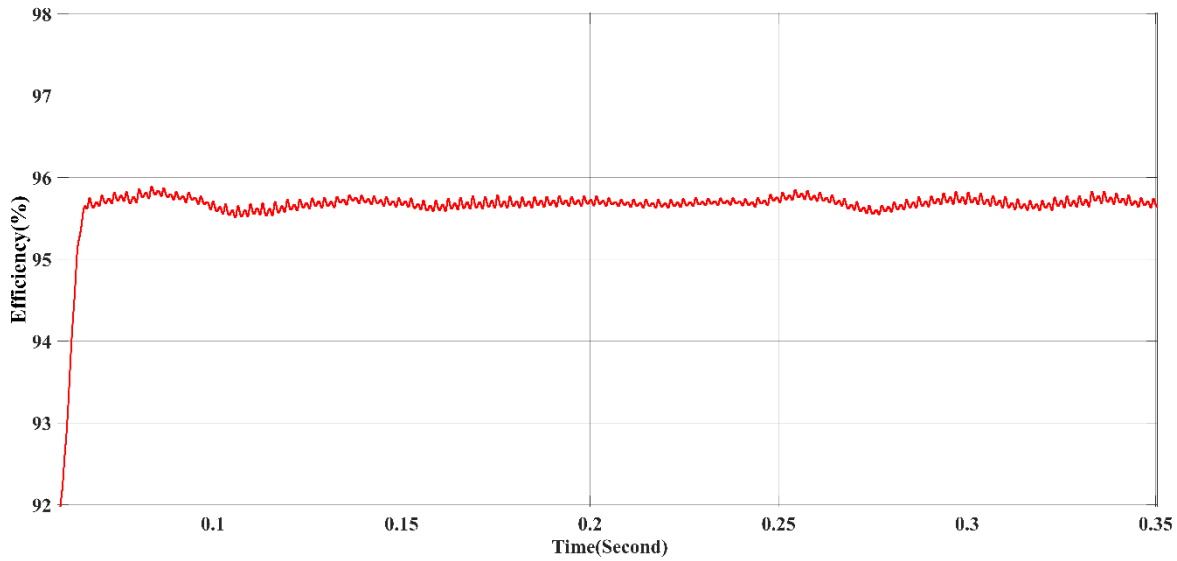


Figure 4.18. Efficiency of Power with P&O at 800 W/m^2

In the figure 4.19 is indicated the THD result obtained from the LCL filter applied for daytime mode. According to this result, the THD level fluctuates between 3.6% and 3.9%. In table 2.6, the limit level of total harmonic distortion is specified as 5%. Thus, the level of THD is under limit and valid. However, in order to reduce their distortion, a second filter has been applied in night time mode at 800 irradiance with P&O MPPT method.

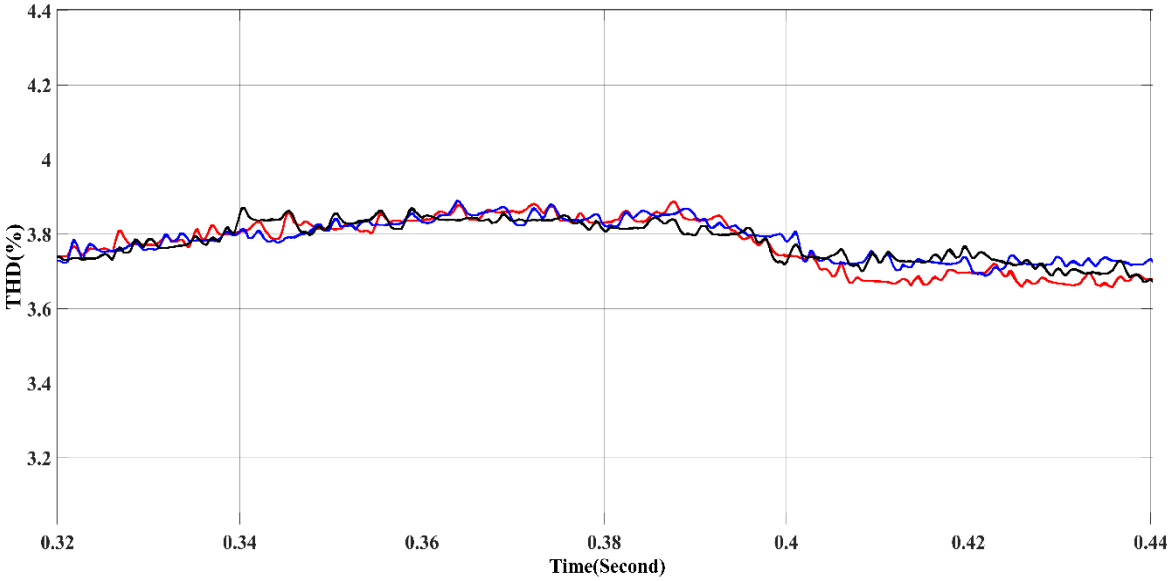


Figure 4.19. The THD of Daytime Mode LCL Filter with P&O at 800 W/m^2

The THD result graphs of two different LCL circuits operated for both daytime mode and nighttime mode are specified in figure 4.20 below. According to this figure, the LCL level in daytime mode has been decreased to 3.2% in nighttime mode.

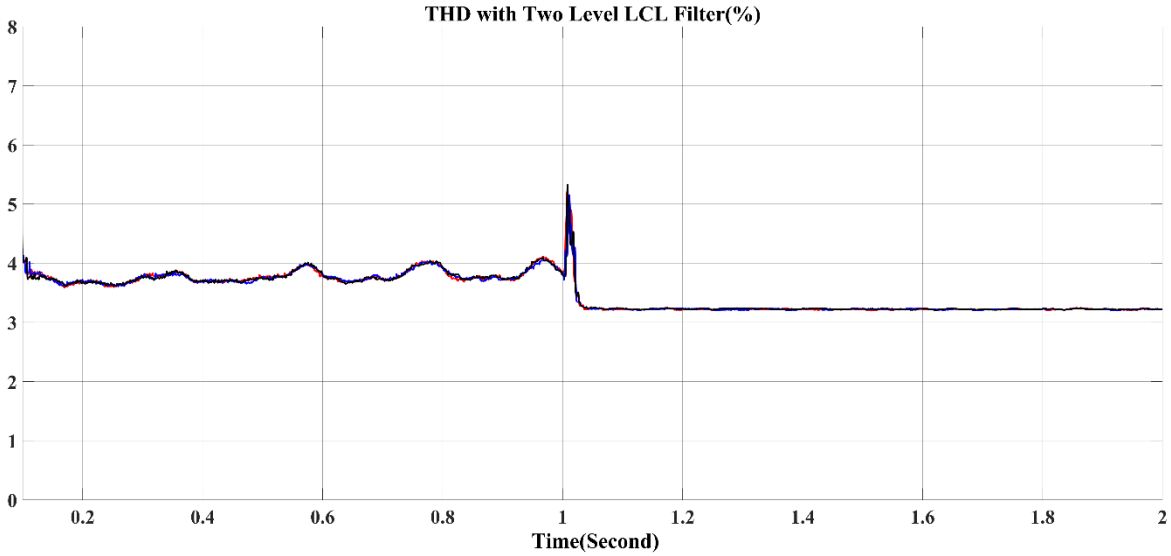


Figure 4.20. The THD of Two Mode LCL Filter with P&O at 800 W/m^2

4.5. Simulation Outcomes at 800 W/m^2 with INC

In section 4.5, the simulation results of the INC MPPT method were evaluated in 800 irradiance. The inverter output graphs for these values are shown in figure 4.21. Compared to figure 4.16 with 4.21, it seems that the waveform of the figure 4.21 is smoother. The INC method provided a smoother sinusoidal chart at 800 irradiance benchmarked with P&O

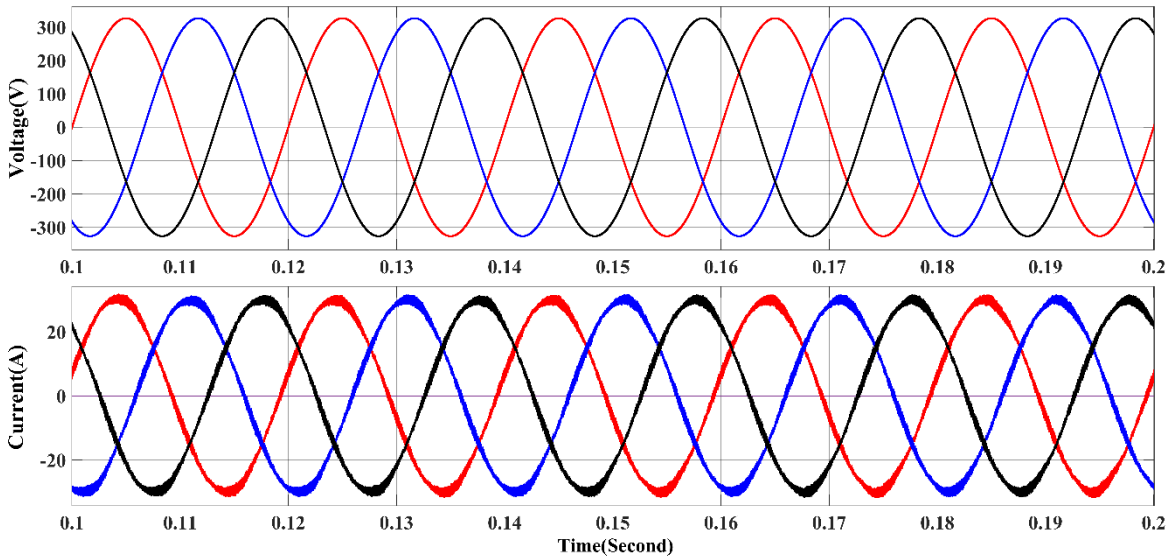


Figure 4.21. The Inverter Output Voltage and Current Waveform at 800 W/m^2 with INC

In figure 4.22, the battery simulation results are given below. In this simulation stage, it is clearly seen that the ripples on the DC link voltage have decreased according to the P&O method. This result shows that the INC method is more robust.

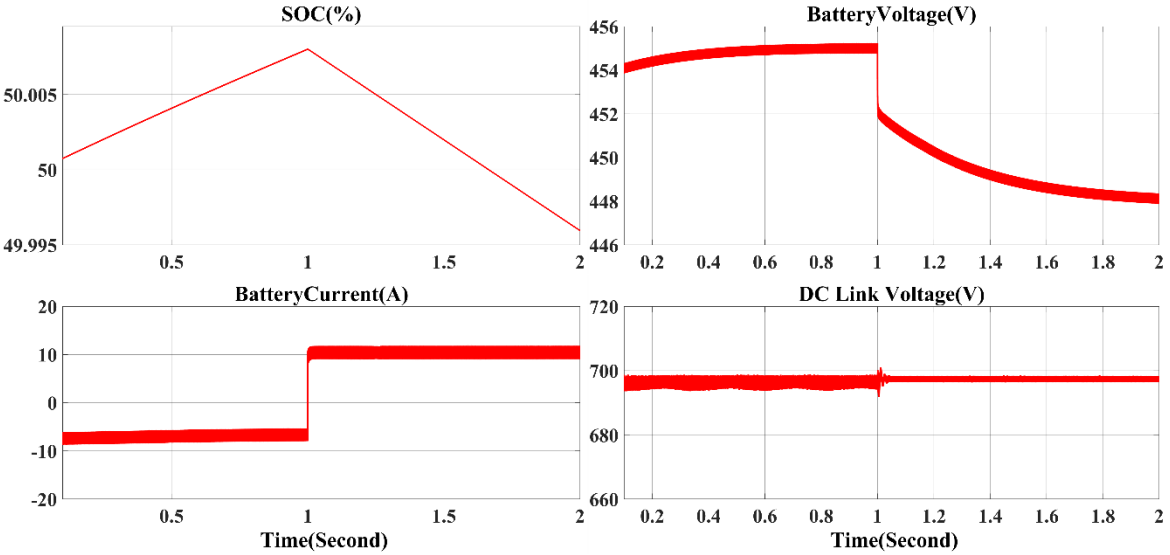


Figure 4.22. The Graphs of Battery Outcomes and DC Link Voltage with INC at 800 W/m^2

The power efficiency of the INC method at 800 irradiance is shown in figure 4.24 below. According to the output of the figure 4.23, the efficiency is around 95.7%. This outcome resembles at 1000 irradiance INC. The result seems higher than P&O at the same irradiance.

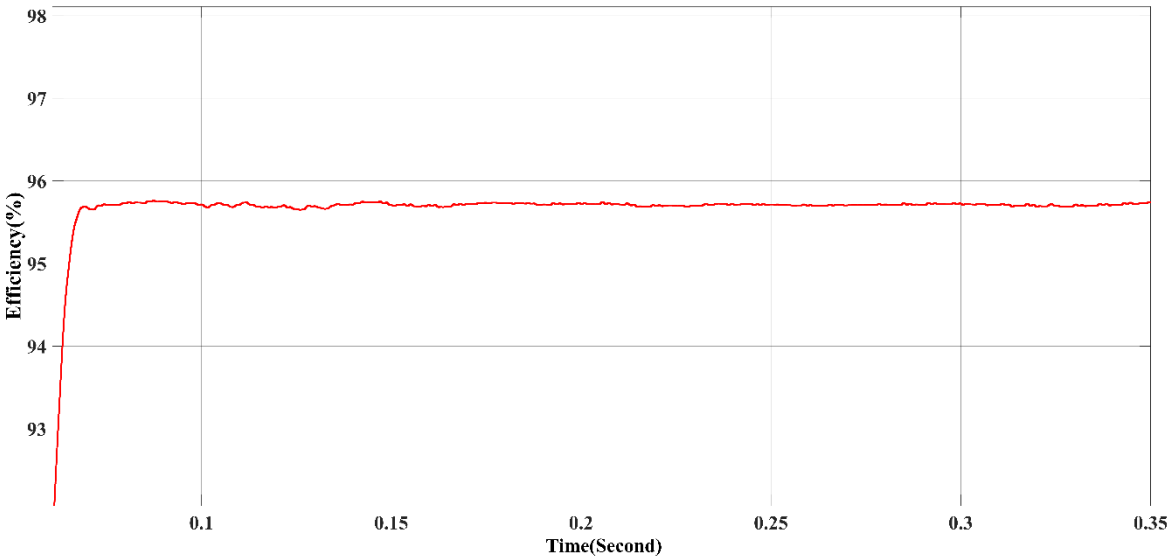


Figure 4.23. Efficiency of Power with INC at 800 W/m^2

In the figure 4.24 is stated the THD result gained from the LCL filter applied for daytime mode. According to this result, the THD level fluctuates between 3.55% and 3.65%. THD values obtained in daytime mode seem to be close each other. In nighttime mode the distortion level increases around 4.3% so the second filter activates and suppress THD.

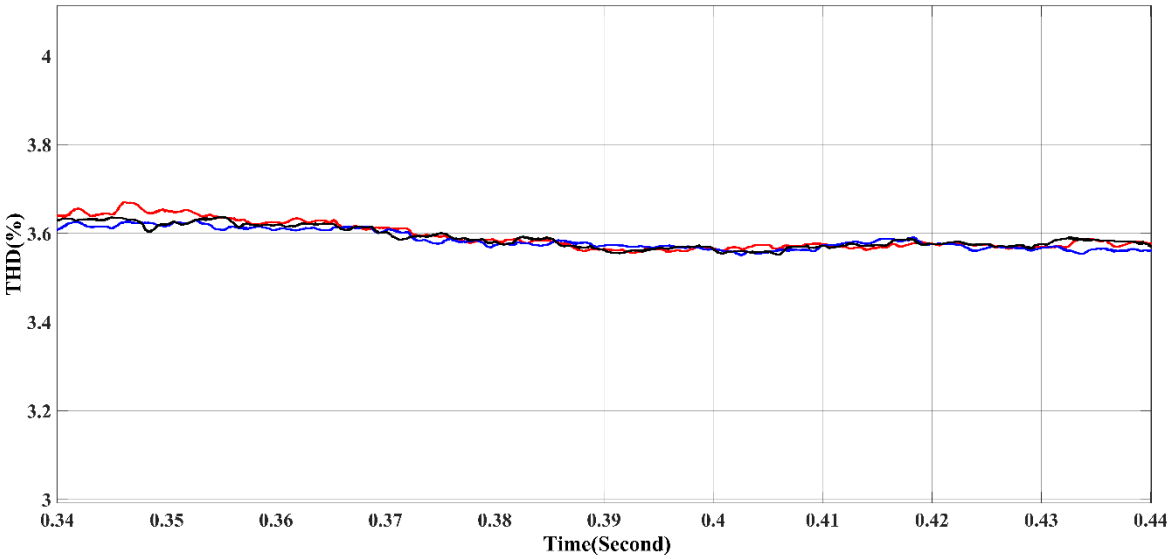


Figure 4.24. The THD of Daytime Mode LCL Filter with INC at 800 W/m^2

Figure 4.25 shows the THD values at the level of 800 irradiance with the INC MPPT method of two mode LCL circuit applied for both daytime and nighttime mode. As can be seen in the graph, there is no produced PV energy at night, and all nighttime mode THDs are located in the 3.2% band.

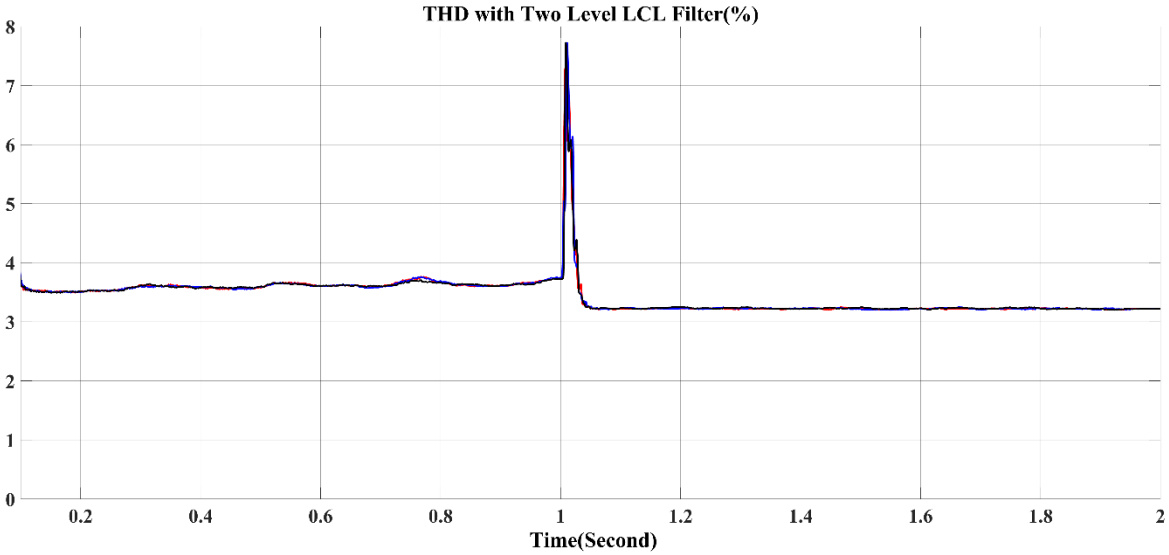


Figure 4.25. The THD of Two Mode LCL Filter with INC at 800 W/m^2

4.6. Simulation Outcomes at 800 W/m^2 with ANN

In this stage, the test results of ANN MPPT method are examined at 800 irradiance. As can be seen in the figure 4.26 and figure 4.11 in the ANN algorithm, the output graphs of inverter current and voltage are closer to the sine waveform. Thanks to these obtained graphs, it can be determined that the artificial intelligence method gives smoother results at low level irradiation. According to the outcome of this design, the inverter outputs are given below.

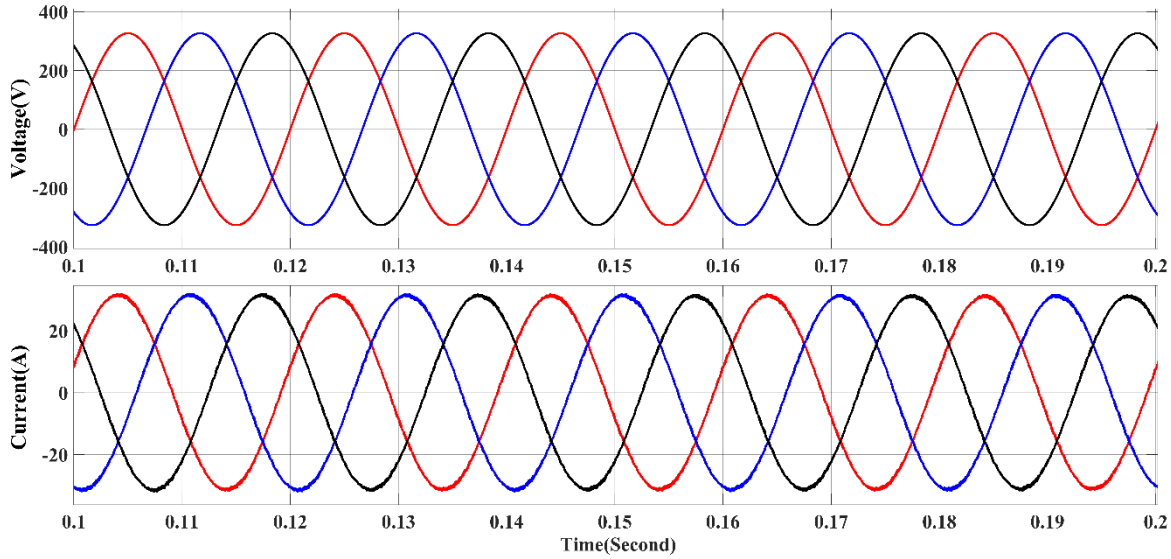


Figure 4.26. The Inverter Output Voltage and Current Waveform at 800 W/m^2 with ANN

The battery results are seen in figure 4.27. According to these outcomes, the battery discharge is 10.43A, as in other stages. The battery voltage is equal to 455V which is taken as the designed set value for charging controller. In addition, the DC link voltage gave a more uniform output than traditional methods. It approaches to the pure dc form. Ripples have been quite decreased with ANN MPPT.

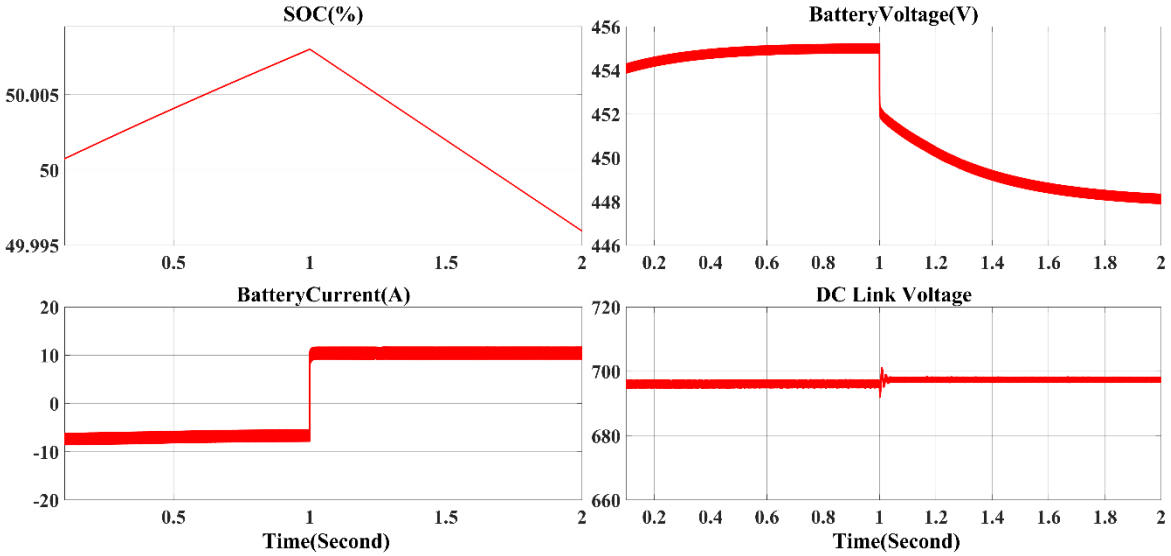


Figure 4.27. The Graphs of Battery Outcomes and DC Link Voltage with ANN at 800 W/m^2

In figure 4.28, the power efficiency of the ANN method was examined. In this part, the efficiency level rises above 97.5%. It is seen that the peak values have reached 98%. As a result of this output graphs, it was understood that the efficiency of intelligent method for 800 irradiance is higher than conventional methods.

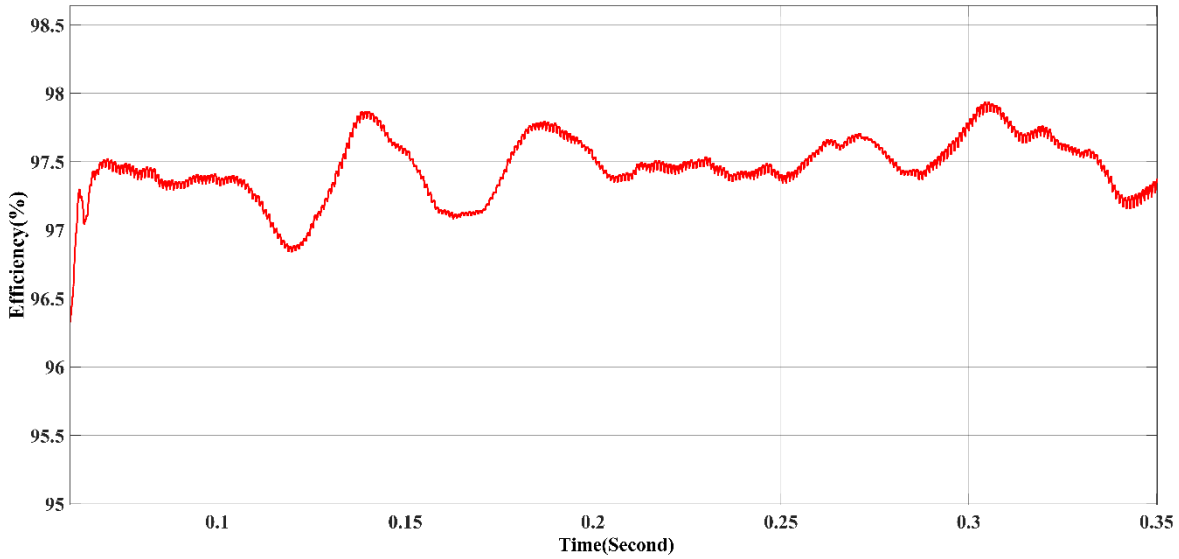


Figure 4.28. Efficiency of Power with ANN at 800 W/m^2

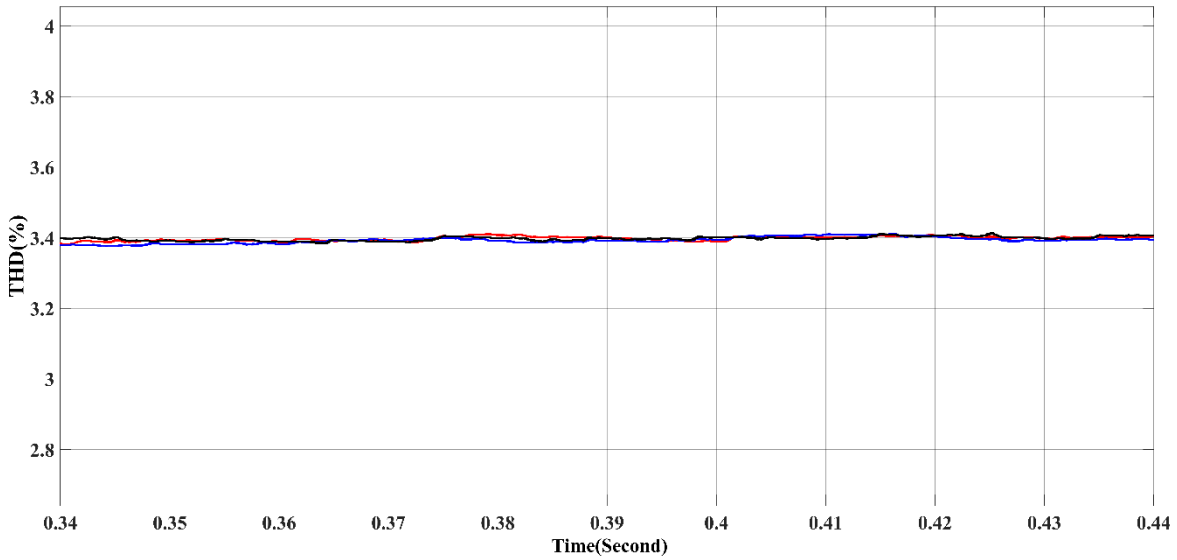


Figure 4.29. The THD of Daytime Mode LCL Filter with ANN at 800 W/m^2

The THD level of ANN intelligent MPPT method for 800 irradiance is indicated in the daytime mode in figure 4.29. According to this graph, the distortion level looks smoother than the other methods. It does not make any fluctuation interval and looks like a straight line. In addition, the output result has lower distortions than other conventional modes. In this mode, the THD level is acquired 3.4%.

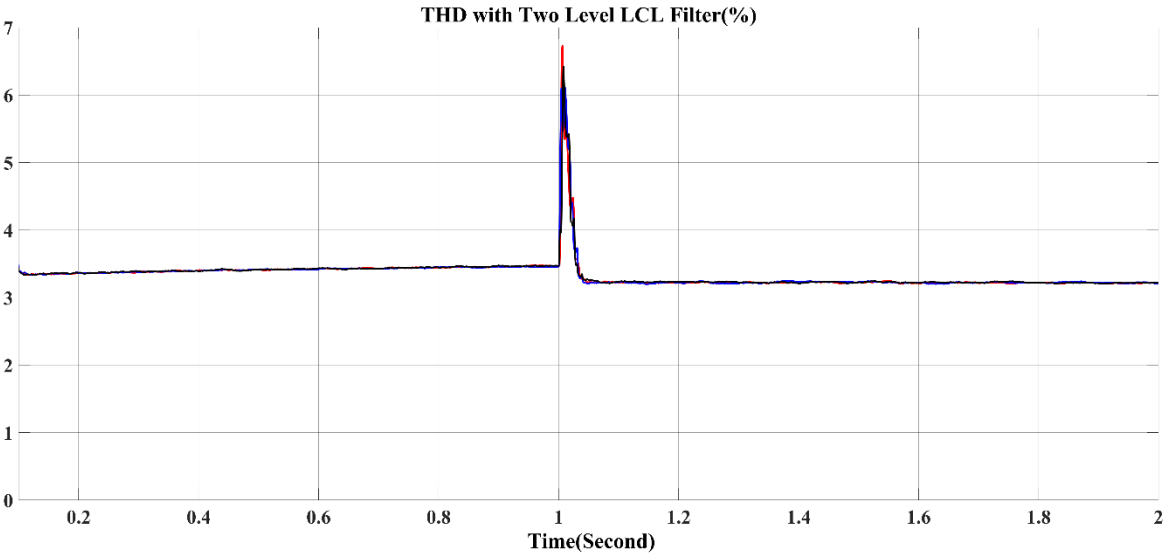


Figure 4.30. The THD of Two Mode LCL Filter with ANN at 800 W/m^2

In figure 4.30, the THD results of the double layer LCL filter structure which was used for both daytime and nighttime mode are given. As can be clearly seen in this structure, distortion is in a flat behavior in daytime and nighttime mode. It does not make any oscillation. The nighttime mode THD level resembles the others and seems to be 3.2%.

4.7. Simulation Outcomes at 600 W/m^2 with P&O

The test results obtained in this section were taken according to the P&O MPPT method at 600 irradiance. The first result is inverter output voltage-current graph and is shown n figure 4.31 below. It is also observed that there is no phase shift at low radiations. However, in the P&O method, as at other high level irradiance, there are minor distortions in the output current. As can be seen from the graph, this method is low in terms of performance test.

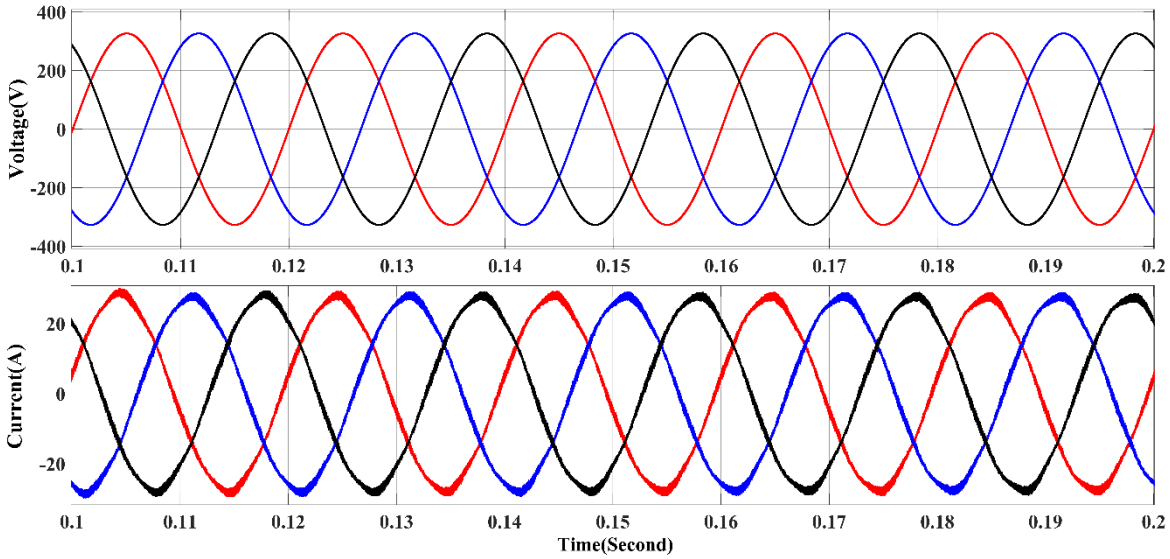


Figure 4.31. The Inverter Output Voltage and Current Waveform at 600 W/m^2 with P&O

The graphs of the battery parameters and DC link voltage are shown in figure 4.32. According to the specified values, the battery voltage and current have been properly output, the voltage for charging case is around 455V, the current for discharging case is around 10.43A. In addition, the DC link voltage includes high level ripples. It is clearly seen that this method generates unwanted ripples at 600 irradiance more than other algorithms.

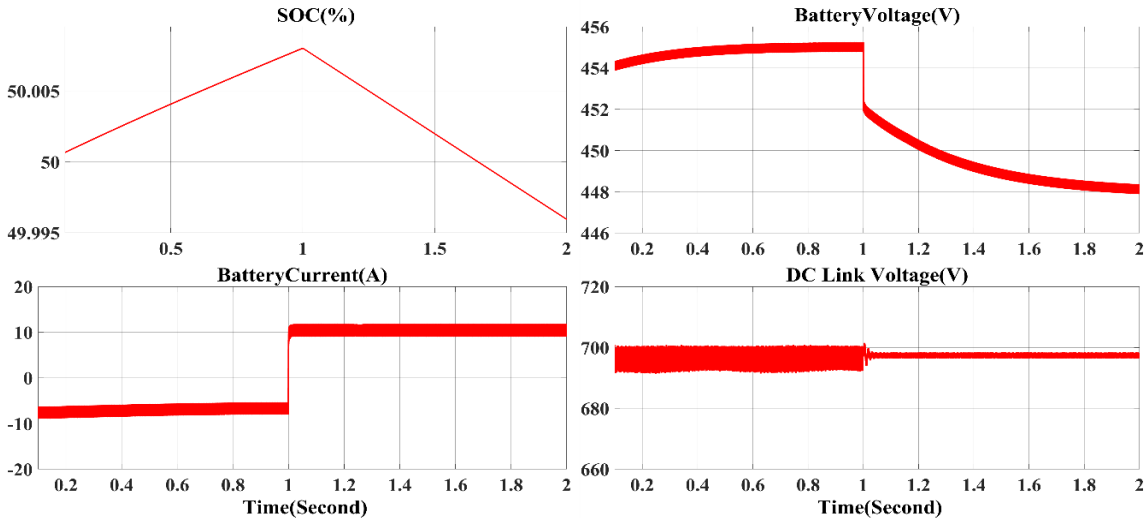


Figure 4.32. The Graphs of Battery Outcomes and DC Link Voltage with P&O at 600 W/m^2

In figure 4.33 shows the last power result is taken from the P&O simulation. The algorithm tested at 600 irradiance. It has given power efficiency result of about 95.5%.

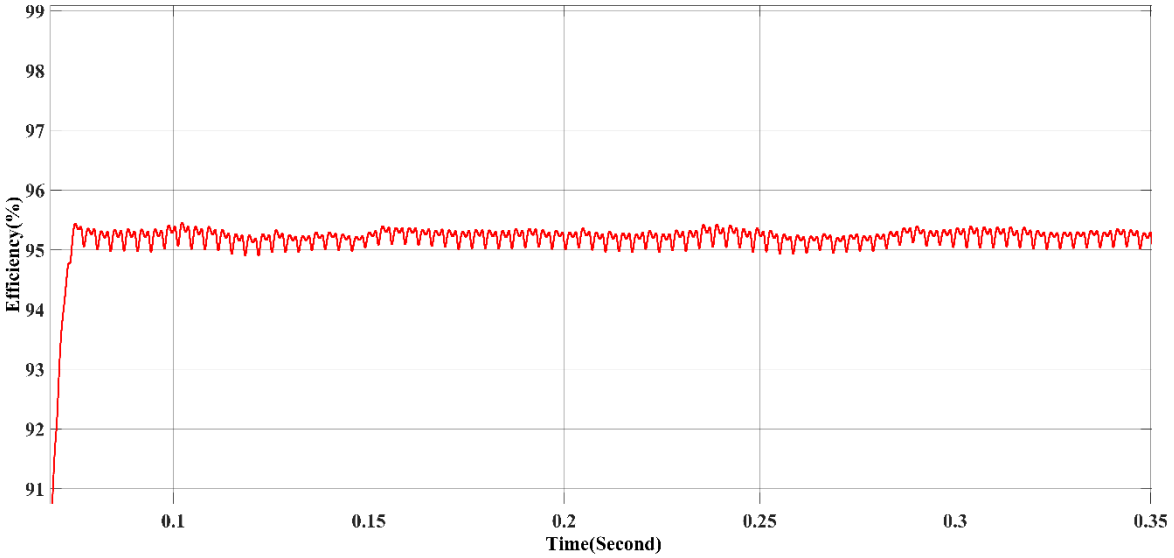


Figure 4.33. Efficiency of Power with P&O at 600 W/m^2

In this part, the THD result graph of the filter designed for daytime mode is indicated in figure 4.34 below. As it can be seen, the THD level varies between the 3.4% - 3.5%. When the THD results obtained by the P&O method with other irradiance levels are compared, it is seen that the lowest irradiance is acquired at 600 W/m^2.

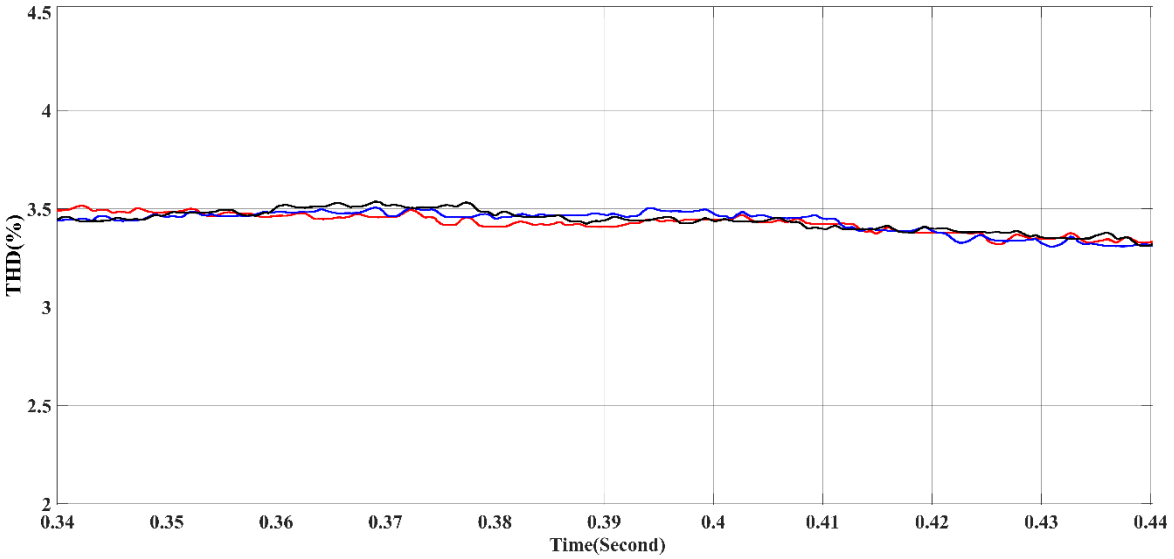


Figure 4.34. The THD of Daytime Mode LCL Filter with P&O at 600 W/m^2

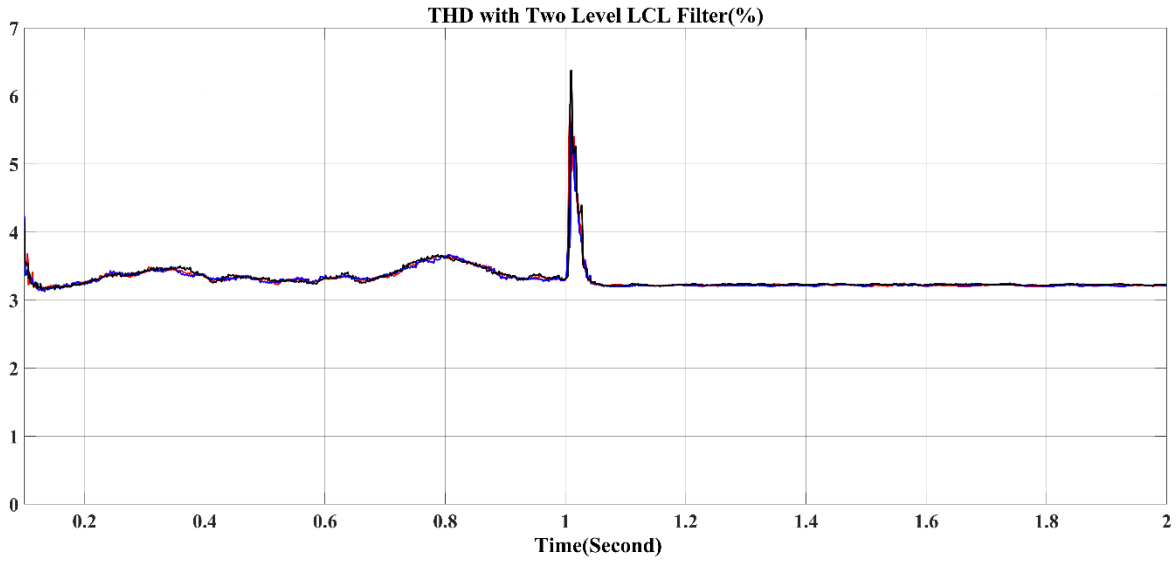


Figure 4.35. The THD of Two Mode LCL Filter with P&O at 600 W/m^2

When the daytime mode filter is also used in nighttime mode, THD level rises above 4.2%. In order to prevent this situation and suppress harmonic distortions, second LCL filter is applied only in nighttime mode. By using two mode LCL filter, THD of the system is reduced to 3.2%. The graph is also available in figure 4.35.

4.8. Simulation Outcomes at 600 W/m^2 with INC

The first simulation results of INC MPPT at 600 irradiance is inverter output graphs. These graphs contain voltage and current waveform. It is indicated in figure 4.36 below. When the figure is examined, it is seen that the waveform is closer to pure sinewave than the others. When the compared output of the INC method at three different radiations, it is clearly seen that 600 W/m^2 is the best waveform from the captured outputs.

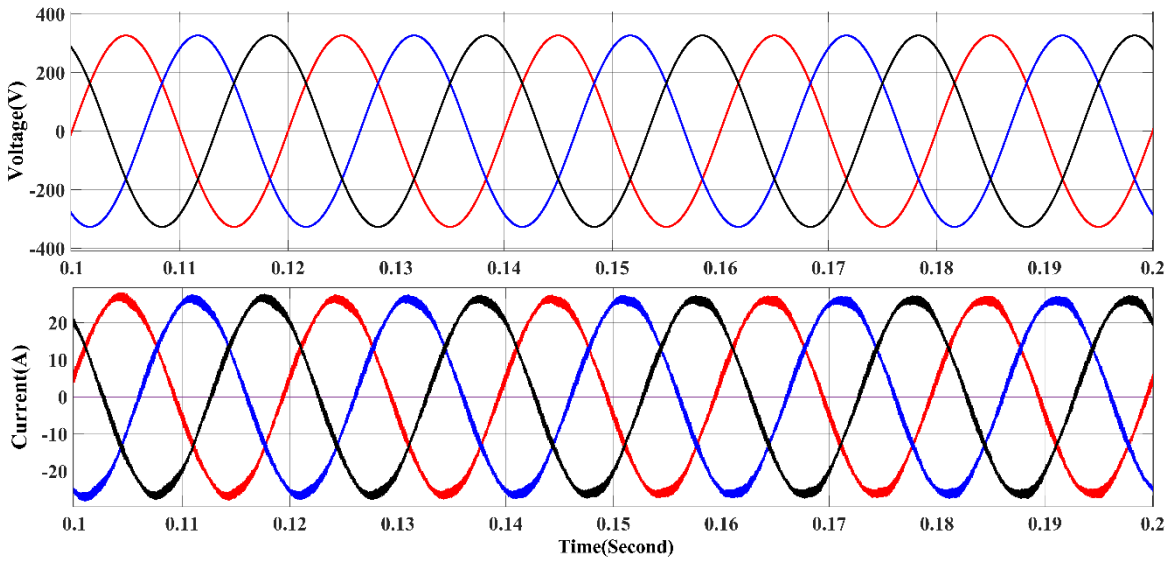


Figure 4.36. The Inverter Output Voltage and Current Waveform at 600 W/m^2 with INC

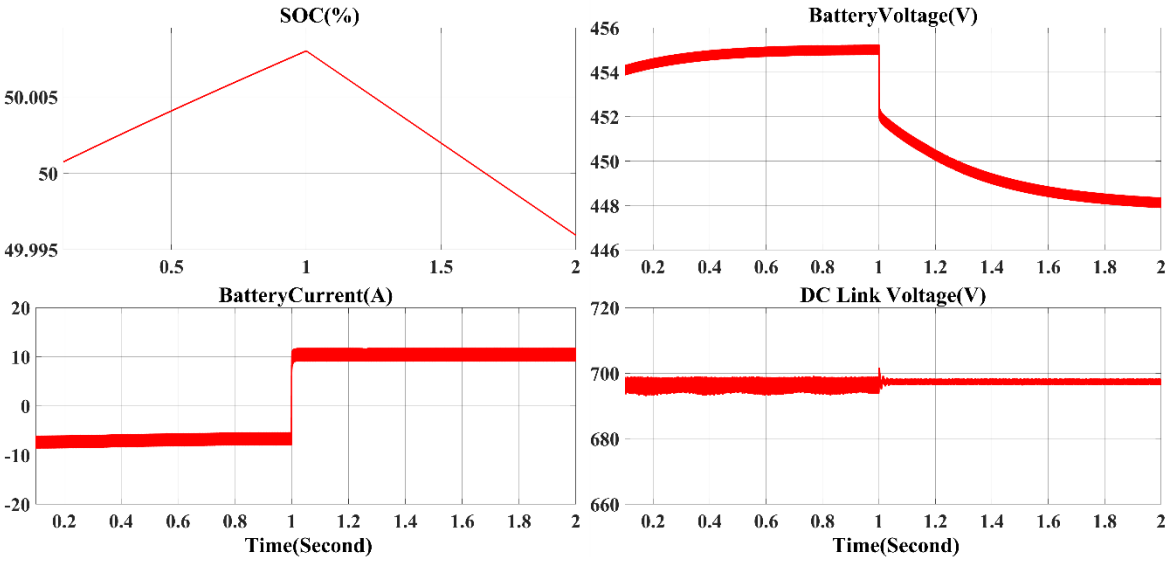


Figure 4.37. The Graphs of Battery Outcomes and DC Link Voltage with INC at 600 W/m^2

The battery results were specified in figure 4.37. The values in graphs are similar to the previous methods. For the INC algorithm, ripple level of DC link voltage appears to be less than P&O and more than the ANN method. Since ripples are undesirable, it can be said that the INC method DC link voltage becomes more smoothly than P&O. Compared to ANN, it is seemed to keep in the background.

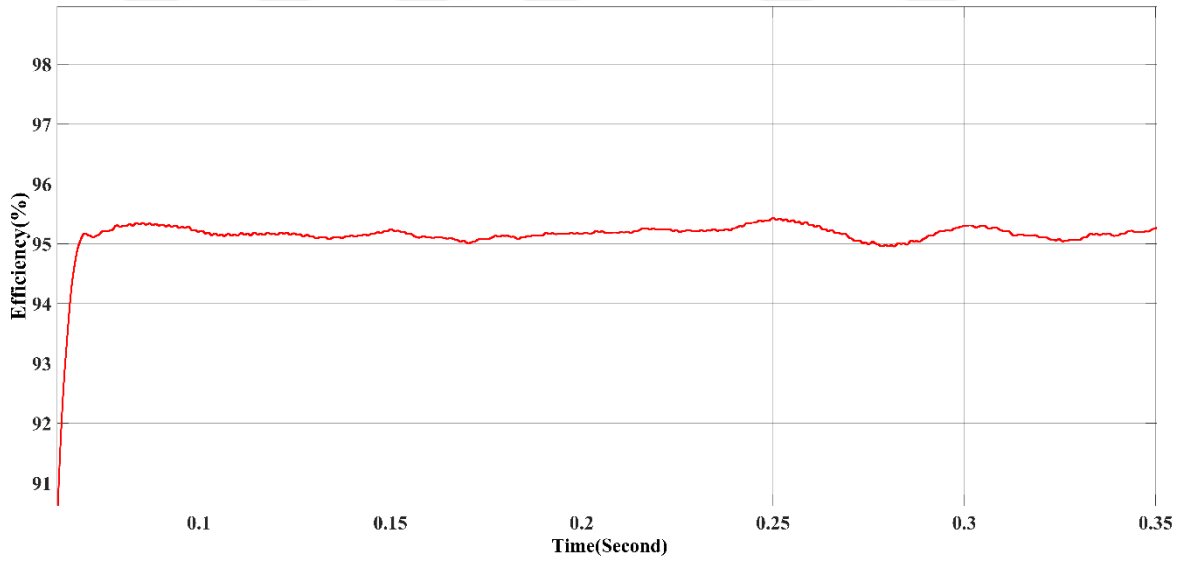


Figure 4.38. Efficiency of Power with INC at 600 W/m^2

Power efficiency was assessed by applying the 600 irradiance INC method at figure 4.38. As can be understood from the indicated chart, the efficiency level varies in the interval of 95%-95.25%.

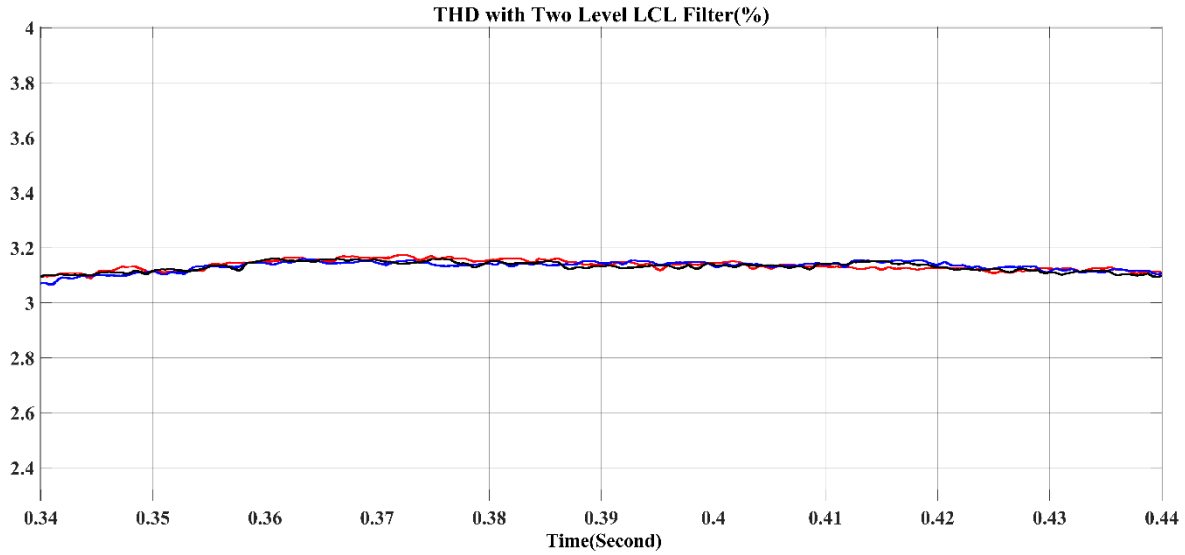


Figure 4.39. The THD of Daytime Mode LCL Filter with INC at 600 W/m^2

After the stages is performed, the THD of output current results were examined in figure 4.39 with only daytime mode LCL filter. As shown in this graph, the level of distortion has fallen significantly. It has reached the 3.1% band like straight line. When the INC method is compared with the other methods for THD outputs, the lowest THD output was acquired at the 600 W/m^2.

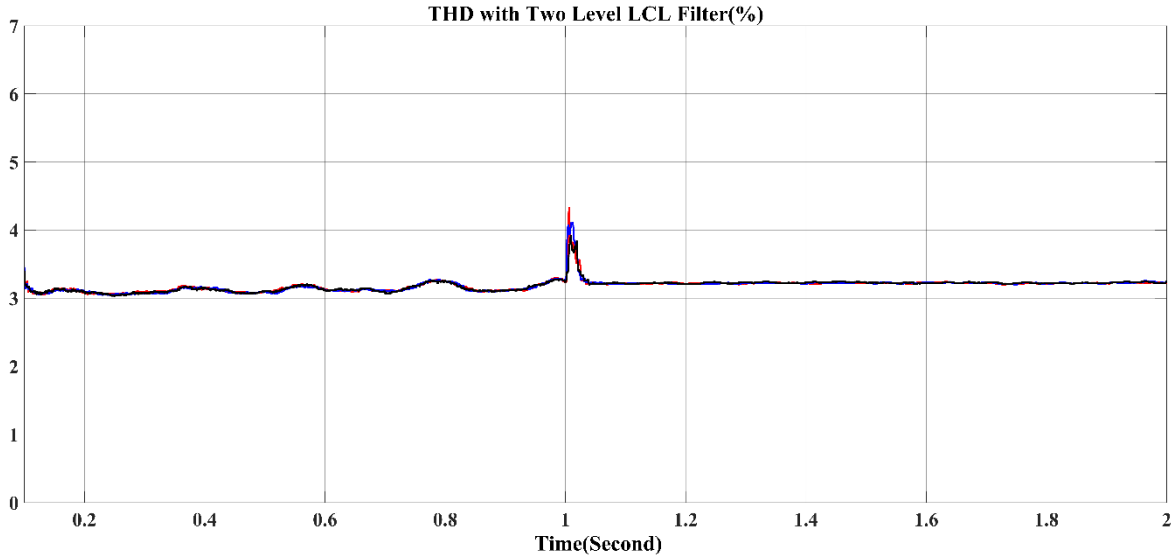


Figure 4.40. The THD of Two Mode LCL Filter with INC at 600 W/m^2

As in the previous outputs, the results of two level LCL filter application are indicated in figure 4.40. According to this chart, THD which continues in the 3.1% band in daytime mode, peaks up to 4%. When switching to nighttime mode filter, it is reduced to 3.2%. This indicates that successful results have been achieved with the two mode LCL filter design.

4.9. Simulation Outcomes at 600 W/m^2 with ANN

In the latest test simulation, the ANN tracking algorithm was examined in 600 irradiance. The first result is stated in figure 4.41 below. In this part, output of the current – voltage waveforms are displayed. In summary, compared with the ANN method and conventional algorithms which are called as P&O and INC, it seems that the ANN method gives much smoother inverter output graphs than others. Harmonic distortions are quite low in the inverter output current waveform with ANN supported system.

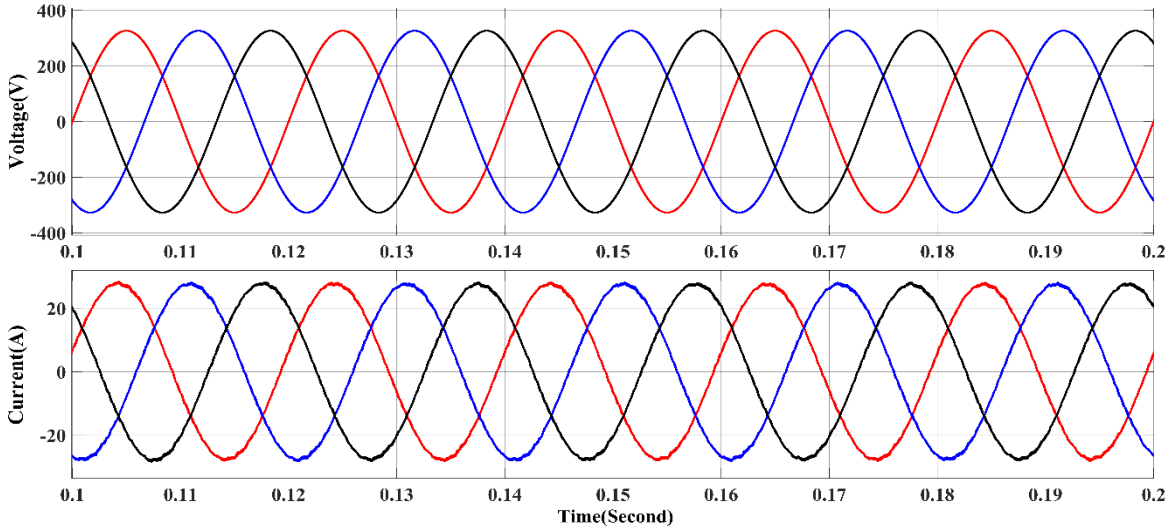


Figure 4.41. The Inverter Output Voltage and Current Waveform at 600 W/m^2 with ANN

After that, the battery output results are expressed in figure 4.42. The battery voltage- current and SOC values are similar in other irradiance levels. However, ANN algorithm has a greater effect on DC voltage generation than traditional methods. The smoothest shape of the DC bus voltage has been acquired in this section with using intelligent ANN tracking method.

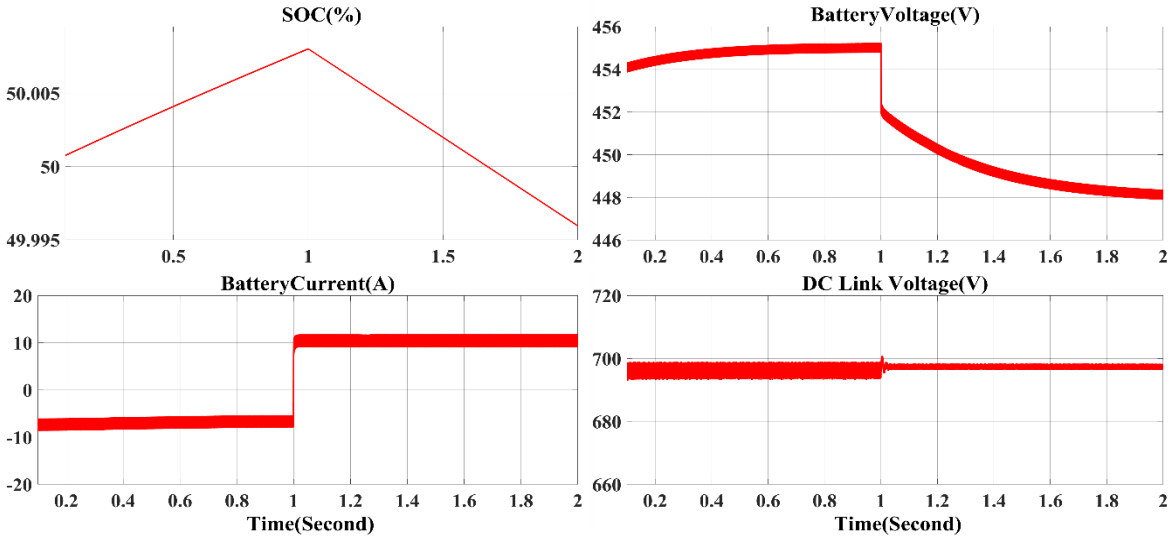


Figure 4.42. The Graphs of Battery Outcomes and DC Link Voltage with ANN at 600 W/m^2

System power efficiency at the level of 600 W/m^2, which is evaluated as low irradiance, is also available in figure 4.43 below. In this graph, it is seen that the power efficiency level is achieved around 97.5%. This result is the best outcome achieved at low radiation. For this reason, when the performance criteria are evaluated, it has been found that the ANN tracing method gives more efficient results at low radiation.

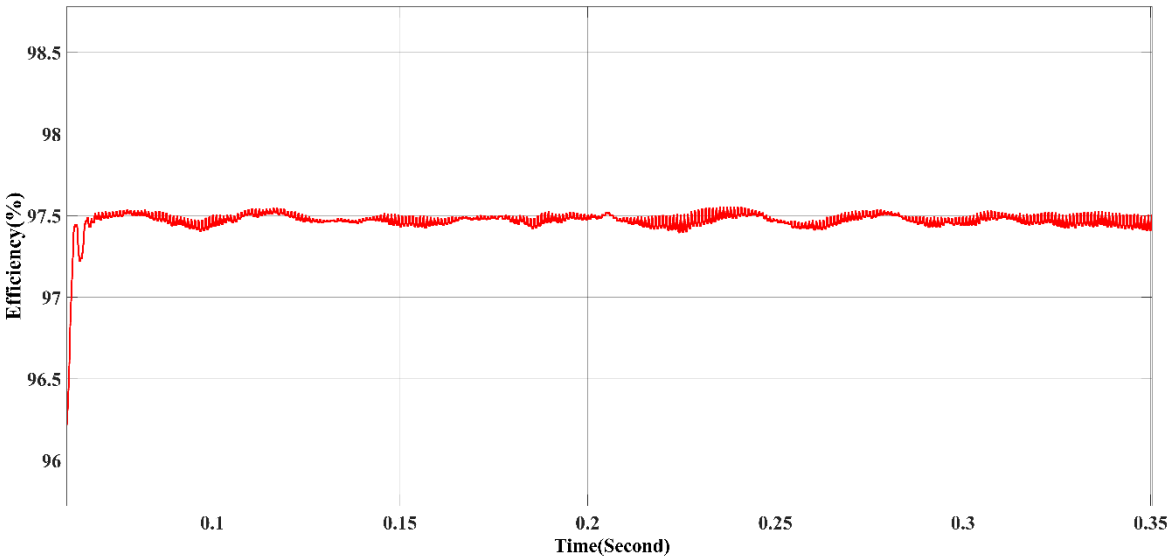


Figure 4.43. Efficiency of Power with ANN at 600 W/m^2

After the efficiency and inverter output graphs are evaluated, the THD level was examined in figure 4.44. The best outcomes continue here as well. As can be seen in figures 4.43 and 4.42. The best THD performance results were obtained by using the ANN algorithm in low irradiance. The distortion grade worked in daytime ode appears to be between 2.95% - 3.05%. These values are the best THD values acquired in daytime mode.

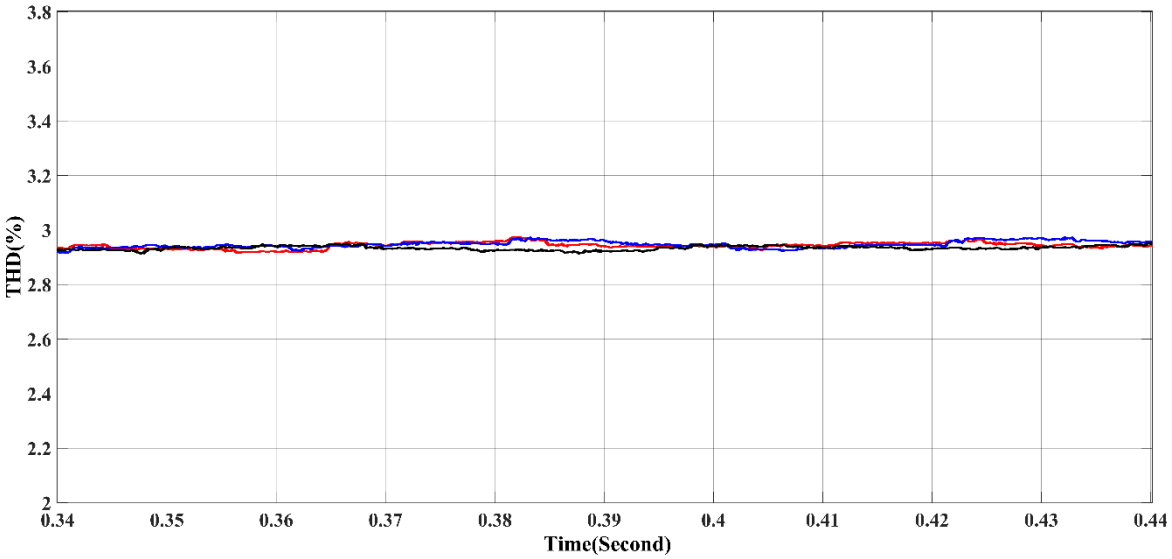


Figure 4.44. The THD of Daytime Mode LCL Filter with ANN at 600 W/m^2

The values acquired quite well in daytime mode, go up to the 4% band at nighttime. The second filter is activated to reduce this rising THD level. Thanks to the nighttime mode filter, it seems that the THD has reached 3.2%. The stated results are shown in figure 4.45 below. All the graphs are investigated, the ANN method shows very successful performance in terms of all criteria at 600 W/m^2.

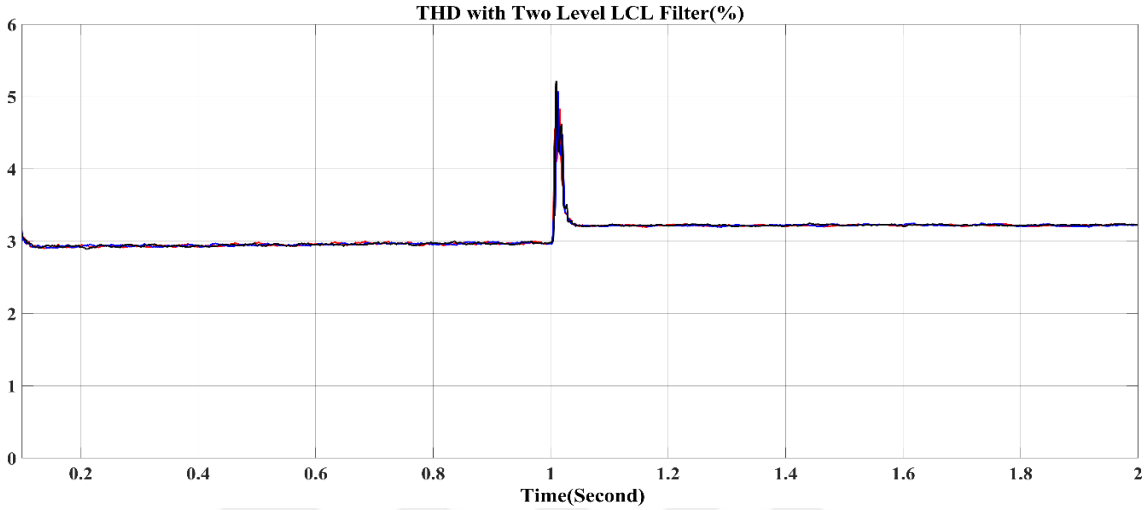


Figure 4.45. The THD of Two Mode LCL Filter with ANN at 600 W/m^2

4.10. Recommended Model: Using Hybrid Mode MPPT to Increase Efficiency

The most important parameter in power electronics applications is efficiency. If high efficiency is achieved in a study, the more meaningful to implement the study. When successful research is examined, it is seen that mostly intended to increase power efficiency. Therefore, in this thesis study, a hybrid method is proposed in which the most efficient results are combined to enhance efficiency. An important condition that must be in order to perform the hybrid method is to provide varying irradiance levels. Firstly, all the previous simulation results were evaluated and efficiency levels were studied. The percentage of efficiency offered by each method is different according to the specific irradiance. For this reason, the percentage of efficiency provided by each stage has been observed deeply.

The created graph for specific irradiance is also available in figure 4.46 below. As indicated in the graph, the values alter from 1000 W/m^2 to 0 W/m^2. These value changes occur in the interval of 0-1 second. Foremost, the irradiance parameter has been started as 1000 W/m^2. It decreases to 800 W/m^2 at 0.2 seconds. After a selected MPPT method between 0.2 to 0.4 seconds, the radiation level brings down from 800 W/m^2 to 600 W/m^2 at 0.4 second. Then, the efficiency percentage of an MPPT method is determined for 600 W/m^2 are observed between 0.4 to 0.6 seconds. When the simulation time reaches 0.6 seconds, the irradiance level is reduced to 400 W/m^2. The selected MPPT for 400 W/m^2 is executed for 0.2 seconds. Then, when the simulation time reaches 0.8, the radiation level is decreased to 200 W/m^2.

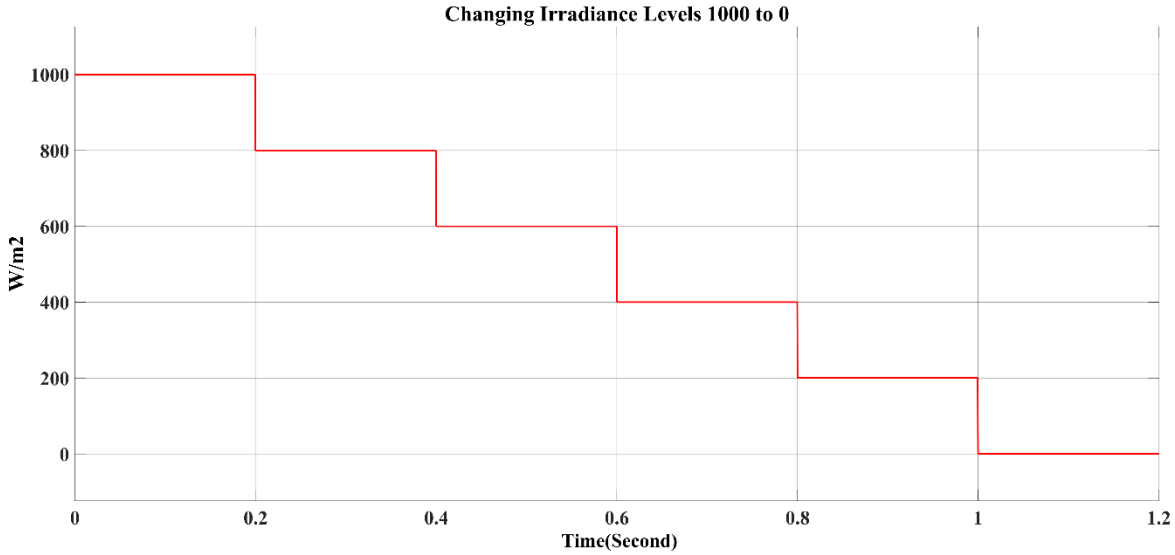


Figure 4.46. Irradiance Level for Hybrid Mode MPPT

According to the changing radiation values, MPPT algorithms with the most efficient results is determined respectively. In the applied Hybrid PWM algorithm, the PWMs generated by the most efficient MPPT types are handled. In this proposed method, PWM produced by P&O MPPT is used at 1000 W/m^2. When the radiation level reached 800 W/m^2, all algorithms are compared and it is observed that the most efficient method is INC. For this reason, PWM produced by the INC MPPT method is used at 800 W/m^2. After that, all the results for 600 W/m^2 is examined and it is determined that the most efficient method is ANN MPPT. For the 400 W/m^2 same like 600, ANN provided the most efficient result. Finally, at the 200 W/m^2 INC algorithm is ensured the best outcome.

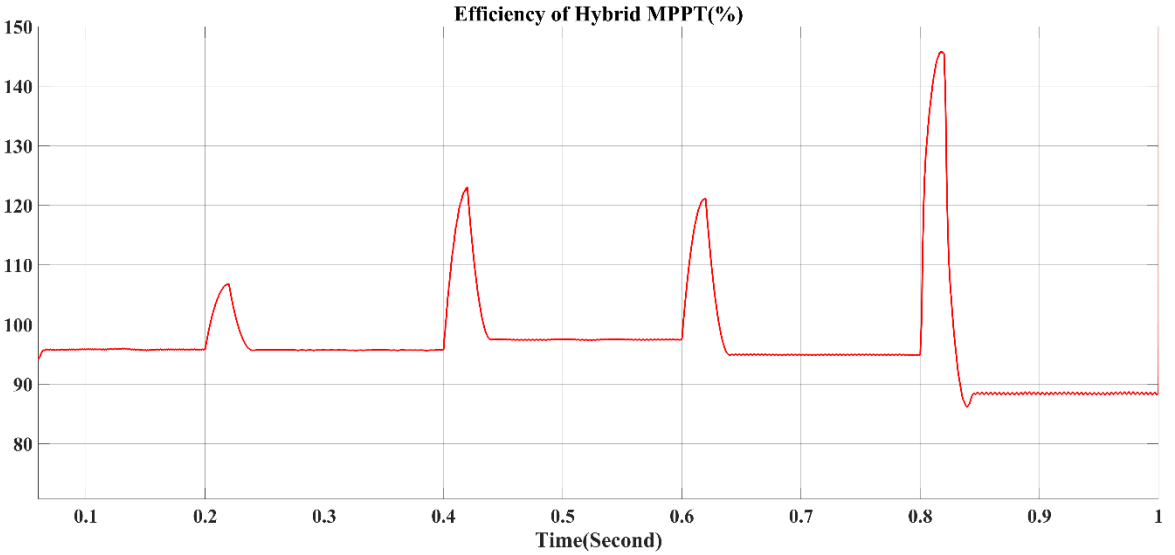


Figure 4.47. Efficiency Result of Hybrid Mode MPPT

4.11. Summary

In this section, simulation test of the project was carried out. The criterion parameters were taken as reference in these tests are the percentage of radiation and the type of tracking algorithm. Firstly, the radiation values were taken for 1000-800-600-400-200 W/m^2, but only for 1000-800-600, a detailed examination was made and expressed in this section. The efficiency of 400 and 200 W/m^2 parameters was examined and contributed to the development of the hybrid tracking algorithm. Although the proposed algorithm is a hybrid method, P&O, INC and ANN algorithms have also been used in the system. The proposed method was obtained by determining the most efficient cases of these three different algorithms and then combining them in the design. Thanks to the Hybrid MPPT method, high efficiency has been achieved at low power levels.

Besides the tracking methods and efficiencies, there are also different parameters that are examined. These are the DC bus voltage, the SOC parameter of the battery, the battery voltage and current, the THD values in daytime mode, 24-hour THD values both daytime and nighttime. The smoothest version of the DC bus voltage has been acquired by the ANN algorithm. Since the battery control algorithm used in each method is the same, the battery parameter values quite resemble to each other. The THD percentages, which was studied in daytime mode, increase due to the power difference between PV with battery when switching to night mode. For this reason, two mode LCL filter design has been made. With the implementation of this new architecture, the percentage of THD has been reduced at nighttime mode.

Finally, all the values obtained from the test results are available in table 4.1 below. There are several the painted cells in P&O, INC and ANN algorithms. These painted cells show that the method specified in the radiation level is also utilized for Hybrid MPPT. The algorithms used in the radiation state change are clearly seen in the table. These have been executed with P&O, INC, ANN, ANN, INC respectively.

Table 4.1. Summary of Simulation Results

General Simulation Outcomes of Thesis								
P&O			**INC**			**ANN**		
Irradiance	**THD**	**Efficiency**	**Irradiance**	**THD**	**Efficiency**	**Irradiance**	**THD**	**Efficiency**
1000	4.03%	95.87%	1000	4.11%	95.82%	1000	3.90%	96.00%
800	3.42%	95.50%	800	3.51%	95.70%	800	3.35%	97.60%
600	2.95%	95.21%	600	3.08%	95.25%	600	2.93%	97.4%
400	3.01%	93.52%	400	2.76%	93.78%	400	2.57%	94.97%
200	2.54%	87.47%	200	2.42%	88.55%	200	2.30%	86.73%

5. CONCLUSIONS

In this thesis, a battery supported PV to grid system is developed. The main reason for choosing this system is the demand for renewable energy sources. The studies and technological developments carried out in this field are increasing day by day. This topic was chosen because it is a current topic and can be improved in the future. In general, this thesis study focused on boost converter application, PV panel selection, LCL filter design in two modes, battery application and control algorithm, bidirectional buck boost converter development, grid-connected three phase inverter design and control, PLL circuit.

The fundamental purpose of this design is to determine the algorithm that will keep the energy obtained from sunlight at the maximum level with the most efficient way. Four algorithms were examined in this study. Two of them are P&O and INC tracking methods which are called as conventional methods. The other one is ANN method, which is referred as intelligent algorithm. The last method used is Hybrid MPPT. Apart from these algorithms, battery circuit is used to ensure power continuity at night. The battery, which is charged during the day thanks to the energy coming from the PV, goes into discharge at night and feeds the system. The power generated by PV panel in the developed circuit has been studied at three radiation levels as 1000 W/m^2,800 W/m^2 and 600 W/m^2. These irradiances have been worked with three different MPPT methods apart from hybrid type. In the hybrid method, radiation levels have been deployed 1000 W/m^2 to 200 W/m^2. The most efficient methods have been determined at each state change and a hybrid method has been created by combining all of changes. Additionally, the simulation time was assumed to be two seconds. The system operates in daytime mode between 0-1 seconds. In this time interval, PV feeds the battery and transfers power to the grid. After that, in the time interval 1-2 seconds, the PV goes into the cut off state and the battery goes to the discharging position and feeds the system.

In this thesis, a detailed literature review has been conducted. It has been tried to make a contribution to the academic community and to make a novelty. For this reason, the first designed LCL filter as a single mode gave high THD results in the transition from daytime to nighttime, so it is focused on solving this issue. High THD rate is due to the difference between the power produced by PV and the battery power. This academic contribution is to progress a two modes LCL filter that works separately for daytime and nighttime. When PV is active, the first mode filter works and the second mode filter is off position. When PV is inactive region, the first filter becomes off and the second filter becomes active.

Thanks to this new improvement for LCL filter, percentages of THD have been reduced from 5% to 3.2%. In addition to these results, the most efficient MPPT method has been identified. It was determined the algorithm that gives the best results in low level radiations is the Hybrid MPPT method. In this tracking algorithm, PWM is generated with ANN in low level radiations. At high

irradiance levels, conventional methods were used to create PWM. A maximum efficiency has been achieved around 97.5% - 97.7% with using the ANN algorithm.

In the future, with the increasing demand of renewable energy, such academic works will become even more important. By focusing on power electronic switching circuits, MPPT efficiency will increase to over 99%. Additionally, the great competition in this sector for more efficient PV panel production will continue to increase in the future. New and more agile tracking control algorithms will be developed for a safe and stable transition to renewable energy.

REFERENCES

Abbe, G., and Smith, H., 2016. Technological Development Trends in Solar-Powered Aircraft Systems. Renewable and Sustainable Energy Reviews, 60(1): 770-783. https://doi.org/10.1016/j.rser.2016.01.053

Abd-Elhady, M. S., Fouad, M. M., and Khalil, T., 2016. Improving the Efficiency of Photovoltaic (PV) Panels by Oil Coating. Energy Conversion and Management, 115(1): 1-7. https://doi.org/10.1016/j.enconman.2016.02.040

Abdelwahab, S. A. M., and Hamada A., 2020. Comparative Analysis of the Modified Perturb & Observe with Different MPPT Techniques for Grid Connected Systems. International Journal of Renewable Energy Research. 10(1)): 155-164.

Adams, W. G., and Day, R. E., 1877. The Action of Light on Selenium. Proceedings of the Royal Society, vol. A25, pp. 113.

Adnan, M. F., Oninda, M. A. M., Nishat, M. M., and Islam, N., 2017. Design and Simulation of a DC-DC Boost Converter with PID Controller for Enhanced Performance. International Journal of Engineering Research & Technology (IJERT), 6(9):1-6.

Alik, R., Jusoh, A., and Sutikno, T., 2015. A Review on Perturb and Observe Maximum Power Point Tracking in Photovoltaic System. TELEKOMNIKA, 13(3): 745-751. http://doi.org/10.12928/telkomnika.v13i3.1439

Alrubaie, A. J., Talib, S. H., Al-khaykan, A., Mousa, M. I., Malik, R. Q., and Kadhim, A. M., 2022. Review on MPPT Techniques in Solar System. 2022 8th International Engineering Conference on Sustainable Technology and Development (IEC), Erbil, Iraq. https://doi.org/10.1109/IEC54822.2022.9807500

Aman, M. M., Solangi, K. H., Hossain, M. S., Badarudin, A., Jasmon, G. B., Mokhlis, H., Bakar, A. H. A., and Kazi, S. N., 2015. A Review of Safety, Health and Environmental (SHE) Issues of Solar Energy System. Renewable and Sustainable Energy Reviews, 41(1): 1190-1204. https://doi.org/10.1016/j.rser.2014.08.086

Anonymous 1: https://wisevoter.com/country-rankings/renewable-energy-by-country/#turkey [accessed: 24.12.2023].

Anonymous 2: https://understandsolar.com/advantagesvs-disadvantages-solar-power/ [accessed: 24.12.2023].

Bagnall, D. M., and Boreland, M., 2008. Photovoltaic Technologies. Energy Policy, 36(12): 4390-4396. https://doi.org/10.1016/j.enpol.2008.09.070

Bozkurt, H., 2022. Optimal Design of a Hybrid PV-Battery System for On-Grid Applications. MSc Thesis, Çukurova University, Adana, pp. 214.

Britt, J., and Ferekides, C., 1993. Thin-Film CdS/CdTe Solar Cell with 15.8% Efficiency, Applied Physics Lettters, 62(22): 2851-2852. https://doi.org/10.1063/1.109629

Casaro, M. M., and Martins, D. C., 2009. Grid- Connected PV System Using a Three-Phase Modified Dual-Stage Inverter. 2009 Brazilian Power Electronics Conference, Bonito-Mato Grosso do Sul, Brazil. https://doi.org/10.1109/COBEP.2009.5347762

Catalano, A., Daiello R. V., Dresner, J., Faughnan, B., Firester, A., Kane, J., Schade, H., Smith, Z. E., Swartz, G., and Triano, A., 1982. Attainment of 10 Percent Conversion Efficiency in Amorphous Silicon Solar Cells. 16th Photovoltaic Specialists Conference, San Diego, USA.

Chapin, D. M., Fuller, C. S., and Pearson, G. L., 1954. A New Silicon P-N Juntion Photocell for Converting Solar Radiation into Electrical Power. Journal of Applied Physics, 25(5): 676-677 https://doi.org/10.1063/1.1721711

Chorfi, J., Zazi, M., Mansori, M., 2018. A New Intelligent MPPT Based on ANN Algorithm for Photovoltaic System. 2018 6th International Renewable and Sustainable Energy Conference (IRSEC). Rabat, Morocco. https://doi.org/10.1109/IRSEC.2018.8702858

Çelik, Ö., 2015. A Novel Hybrid MPPT Method for Grid Connected Photovoltaic Systems with Partial Shading Conditions. MSc Thesis, Çukurova University, Adana, pp. 151.

Dhillon, J., Unni, A., and Singh, N., 2022. Design and Simulation of a PV System with Battery Storage Using Bidirectional DC-DC Converter Using Matlab Simulink. 2022 1st International Conference on Sustainable Technology for Power and Energy Systems (STPES), Srinagar, India. https://doi.org/10.1109/STPES54845.2022.10006623

Dunlap-Shohl, W. A., Zhou, Y., Padture, N. P., and Mitzi, D. B., 2019. Synthetic Approaches for Halide Perovskite Thin Films. Chemical Reviews, 119(5): 3193-3295. https://doi.org/10.1021/acs.chemrev.8b00318

Dursun, M., and Döşoğlu, M. K., 2018. LCL Filter Design for Grid Connected Three-Phase Inverter. 2018 Second International Symposium on Multidisciplinary Studies and Innovative Technologies (ISMSIT). https://doi.org/10.1109/ISMSIT.2018.8567054

Easton, R. L., and Votaw M. J., 1959. Vanguard I IGY Satellite (1958 Beta). Review of Scientific Instruments. 30(1): 70-75. https://doi.org/10.1063/1.1716492

Eldessouky, A. S., Mahmoud, I. M., and Abdel-Salam, T. S., 2023. MPPT Based on a Novel Load Segmentations Structure for PV applications. Ain Shams Engineering Journal, 14(4): 101937-101949. https://doi.org/10.1016/j.asej.2022.101937

Elgendy, M. A., Zahawi, B., Atkinson, D. J., 2012. Evaluation of Perturb and Observe MPPT Algorithm Implementation Techniques. 6th IET International Conference on Power Electronics, Machines and Drives (PEMD 2012), Bristol, England. https://doi.org/10.1049/cp.2012.0156

Elobaid, L. M., Abdelsalam, A. K., and Zakzouk, E. E., 2015. Artificial Neural Network-Based Photovoltaic Maximum Power Point Tracking Techniques: ASurvey, 9(8): 1043-1063. https://doi.org/10.1049/iet-rpg.2014.0359

EMBER, 2023. Global Electricity Review 2023. Clean Energy Policy and Data, 762–769. https://doi.org/https://doi.org/10.1016/j.solener.2018.09.024

EMRA, 2023. Electric Network Regulation Report. Turkish Energy Market Regulation Association.

Fernandez, L., 2023. New Investment in Renewable Energy Worlwide from 2004 o 2022 2023. Statista.

Fritts, C. E., 1883. On a New Form of Selenium Cell, and Some Electrical Discoveries Made by Its Use. American Journal of Science, 156(1): 465-472. https://doi.org/10.2475/ajs.s3-26.156.465

Ghosh, S., and Yadav, R., 2021. Sustainable Energy Technologies and Assessments, 47(1): 101410. https://doi.org/10.1016/j.seta.2021.101410

Giannakopoulos, C., Sager, P. L., Bindi, M., Moriondo, M., Kostopoulou, E., and Goodess, C. M., 2009. Climatic Changes and Associated Impacts in the Mediterranean Resulting from a 2°C global warming. Global and Planetary Change, 68(3): 209-224. https://doi.org/10.1016/j.gloplacha.2009.06.001

Golestan, S., Guerrero, J. M., Vasquez, J. C., 2017. Three-Phase PLLs: A Review of Recent Advances, 32(3): 1894-1907. https://doi.org/10.1109/TPEL.2016.2565642

Gopi, A., and Saravanakumar, R., 2014. High Step-up Isolated Efficient Single Switch DC-DC Converter for Renewable Energy Source. Ain Shams Engineering Journal, 5(19): 1115-1127 http://dx.doi.org/10.1016/j.asej.2014.05.001

Gopi, R. R., and Sreejith, S., 2018. Converter Topologies in Photovoltaic Applications – A review. Renewable and Sustainable Energy Reviews, 94(1):1-14. https://doi.org/10.1016/j.rser.2018.05.047

Gorji, S. A., Sahebi, H. G., Ektesabi, M., and Rad, A. B., 2019. Topologies and Control Schemes of Bidirectional DC-DC Power Converters: An Overview. IEEE Access, 7(1): 117997-118019. https://doi.org/10.1109/ACCESS.2019.2937239

Green, M. A., 2001. Third Generation Photovoltaics: Ultra-High Conversion Efficiency at Low Cost. Progress in Photovoltaics: Research and Applications, 9(2): 123-135. https://doi.org/10.1002/pip.360

Guangul, F. M., and Chala, G. T., 2019. Solar Energy as Renewable Energy Source: SWOT Analysis. 2019 4th MEC International Conference on Big Data and Smart City (ICBDSC), Muscat, Umman. https://doi.org/10.1109/ICBDSC.2019.8645580

Gupta, A. K., Pachauri, R. K., Maity, T., Chauhan, Y. K., Mahela, O. P., Khan, B., and Gupta, P. K., 2021. Effect of Various Incremental Conductance MPPT Methods on the Charging of Battery Load Feed by Solar Panel. IEEE Access, 9(1): 90977-90988. https://doi.org/10.1109/ACCESS.2021.3091502

Gurkaynak, Y., Li, Z., and Khaligh, A., 2009. A Novel Grid-Tied, Solar Powered Residential Home with Plug-in Hybrid Electric Vehicle (PHEV) Loads, 2009 IEEE Vehicle Power and Propulsion Conference, Dearborn, MI, USA. https://doi.org/10.1109/VPPC.2009.5289765

Hajare, M. S., Patil, S. D., Madake, R. B., and Mulla, A. M., 2020. Control of Grid Connected PV Array Using P&O MPPT Algorithm. International Journal of Engineering Research & Technology (IJERT), 9(3): 673-676. https://doi.org/10.17577/IJERTV9IS030555

Humada, A. M., Hojabri, M., Mekhilef, S., 2016. Solar Cell Parameters Extraction Based on Single and Double-Diode Models: A Review. Renewable and Sustainable Energy Reviews, 56(1): 494-509. https://doi.org/10.1016/j.rser.2015.11.051

IEA, 2023. Net Zero Emissions by 2050 Scenario (NZE). International Energy Agency

IRENA, 2023. Renewable Capacity Statistics. International Renewable Energy Agency.

Jacobo, J. T., 2022. Fraunhofer ISE Claims 47.6% Solar Cell Efficiency Record https://www.pv-tech.org/fraunhofer-ise-four-junction-solar-cell-claims-47-point-6-percent-efficiency-record/ [accessed: 24.12.2023].

Jyothy, L. P. N., and Sindhu, M. R., 2018. An Artificial Neural Network Based MPPT Algorithm for Solar PV System. 2018 4th International Conference on Electrical Energy Systems (ICEES), Chennai, India. https://doi.org/10.1109/ICEES.2018.8443277

Kabir, E., Kumar, P., Kumar, S., Adelodun, A. A., and Kim, K., 2018. Solar Energy: Potential and Future Prospects. Renewable and Sustainable Energy Reviews, 82(1): 894-900. https://doi.org/10.1016/j.rser.2017.09.094

Karami, N., Moubayed, N., and Outbib, R., 2017. General Review and Classification of Different MPPT Techniques. Renewable and Sustainable Energy Reviews, 68(1): 1-18. https://doi.org/10.1016/j.rser.2016.09.132

Kaura, V., and Blasko, V., 1997. Operation of a Phase Locked Loop System Under Distorted Utility Conditions. IEEE Transactions on Industry Applications, 33(1): 58-63. https://doi.org/10.1109/28.567077

Khan, J., and Arsalan, H. M., 2016. Solar Power Technologies. Renewable and Sustainable Energy Reviews, 55(1): 414-425. https://doi.org/10.1016/j.rser.2015.10.135

Khan, M. A., Ahmed, A., Husain, I., Sozer, Y., and Badawy, M., 2015. Performance Analysis of Bidirectional DC-DC Converters for Electric Vehicles. IEEE Transactions on Industry Applications, 51(4): 3442-3452. https://doi.org/10.1109/TIA.2015.2388862

Khan, M. Y. A., Liu, H., Yang, Z., and Yuan, X., 2020. A Comprehensive Review on Grid Connected Photovoltaic Inverters, Their Modulation Techniques, and Control Strategies, 13(16): 4185-4225. https://doi.org/10.3390/en13164185

Kolantla, D., Mikkili, S., Pendem, S. R., and Desai, A. A., 2020. Critical Review on Various Inverter Topologies for PV System Architectures. The Institution of Engineering of Technology Journals(IET)RenewablePower Generation, 14(17): 3418-3438. https://doi.org/10.1049/iet-rpg.2020.0317

Kumar, A., Gupta, N., and Gupta, V., 2017. A Comprehensive Review on Grid-Tied Solar Photovoltaic System. Journal of Green Engineering, 7(1):213-254. https://doi.org/10.13052/JGE1904-4720.71210

Lameirinhas, R. A. M., Torres, J. P., and Cunha, J. P. M., 2022. A Photovoltaic Technology Review: History, Fundamentals and Applications. Solar Energy and Photovoltaic Systems, 15(5): 1823-1867. https://doi.org/10.3390/en15051823

Liu, D., and Li, H., 2006. A ZVS Bi-Directional DC-DC Converter for Multiple Energy Storage Elements. IEEE Transactions on Power Electronics, 21(5):1513-1517. https://doi.org/10.1109/TPEL.2006.882450

Macit, R., 2023. Design of a Hybrid PV-Fuel Cell System with Active Reactive Power Control Capabilities. MSc Thesis, Çukurova University, Adana, pp. 95.

Mishra, A. K., and Singh, B., 2018. Design of Solar-Powered Agriculture Pump Using New Configuration of Dual-Output Buck-Boost Converter. IET Renewable Power Generation, 12(14): 1640-1650. https://doi.org/10.1049/iet-rpg.2018.5258

Moharram, K. A., Abd-Elhady, M. S., Kandil, H. A., and El-Sherif, H., 2013. Enhancing the Performance of Photovoltaic Panels by Water Cooling. Ain Shams Engineering Journal, 4(4): 869-877. https://doi.org/10.1016/j.asej.2013.03.005

Mollick, R. A., 2023. Why It's Crucial to Understand the Fill Factor of Solar Cell? How It's Affecting the Efficiency of PV Cells? https://ecowowlife.com/fill-factor-of-solar-cell/ [accessed: 24.12.2023].

Mughal, S., Sood, Y. R., and Jarial R. K., 2018. A Review on Solar Photovoltaic Technology and Future Trends. International Journal of Scientific Research in Computer Science, Engineering and Information Technology (IJSRCSEIT). 4(1): 2456-3307.

Mumtaz, F., Yahaya, N. Z., Meraj, S. T., Singh, B., Kannan, R., and Ibrahim, O., 2021. Review on Non-Isolated DC-DC Converters and Their Control Techniques for Renewable Energy Applications, 12(4): 3747-3763. https://doi.org/10.1016/j.asej.2021.03.022

Naayagi, R. T., Forsyth, A. J., and Shuttleworth, R., 2012. High-Power Bidirectional DC-DC Converter for Aerospace Applications. IEEE Transactions on Power Electronics, 27(11): 4366-4379. https://doi.org/10.1109/TPEL.2012.2184771

Nandukar, S. R., Rajeev, M., 2012. Design and Simulation of Three Phase Inverter for Grid Connected Photovoltaic Systems. Proceedings of Third Biennial National Conference (NCTE).

Navamani, J. D., Vijayakumar, K., and Jegatheesan, R., 2018. Non-Isolated High Gain DC-DC Converter by Quadratic Boost Converter and Voltage Multiplier Cell. Ain Shams Engineering Journal, 9(4): 1397-1406. https://doi.org/10.1016/j.asej.2016.09.007

Nguyen-Duc, T., Nguyen-Duc, H., Le-Viet, T., and Takano, H., 2020. Single- Diode Models of PV Modules: A Comparison of Conventional Approaches and Proposal of a Novel Model. Photovoltaic Modules, 13(6): 1296-1318. https://doi.org/10.3390/en13061296

Olabi, A. G., and Abdelkareem, M. A., 2022. Renewable Energy and Climate Change. Renewable and Sustainable Energy Reviews, 158(1): 1-7. https://doi.org/10.1016/j.rser.2022.112111

Onar, O., Kobayashi, J., Erb, D. C., and Khaligh, A., 2012. A Bidirectional High-Power-Quality Grid Interface with a Novel Bidirectional Noninverted Buck-Boost Converter for PHEVS. IEEE Transactions on Vehicular Technology, 61(5): 2018-2032. https://doi.org/10.1109/TVT.2012.2192459

Özkan, Z., and Hava, A. M., 2014. Three-Phase Inverter Topologies for Grid-Connected Photovoltaic Systems. 2014 International Power Electronics Conference (IPEC-Hiroshima 2014-ECCE Asia), Hiroshima, Japan. https://doi.org/10.1109/IPEC.2014.6869630

Padhee, S., Pati U. C., Mahapatra, K., 2016a. Modelling Switched Mode DC-DC Converter Using System Identification Techniques: A Review. 2016 IEEE Students' Conference on Electrical, Electronics and Computer Science (SCEECS), Bhopal, India. https://doi.org/10.1109/SCEECS.2016.7509303

Padhee, S., Pati, U. C., and Mahapatra, K., 2016b. Design of Photovoltaic MPPT Based Charger for Lead-Acid Batteries. 2016 IEEE International Conference on Emerging Technologies and Innovative Bussiness Practices for the Transformation of Societies (EmergiTech), Balaclava, Mauritius. https://doi.org/10.1109/EmergiTech.2016.7737365

Pastuszak, J., and Wegierek, P., 2022. Photovoltaic Cell Generations and Current Research Directions for Their Development. Advances in Photovoltaic Materials, 15(16): 5542-5572 https://doi.org/10.3390/ma15165542

Radjai, T., Rahmani, L., Mekhilef, S., and Gaubert, J. P., 2014. Implementation of a Modified Incremental Conductance MPPT Algorithm with Direct Control Based on a Fuzzy Duty Cycle Change Estimator Using dSPACE. Solar Energy(ELSEVIER), 110(1): 325-337. https://doi.org/10.1016/j.solener.2014.09.014

Raghavendra K. V. G., Zeb, K., Muthusamy A., Krishna, T. N. V., Kumar, S. V. S. V. P., Kim, D. H., Kim, M. S., 2020. A Comprehensive Review of DC-DC Converter Topologies and Modulation Strategies with Recent Advances in Solar Photovoltaic Systems. Advances in Power Electronics Technologies for Renewable Energy Systems, 9(1)- 72. https://doi.org/10.3390/electronics9010031

Randelovic, M. P., Kocic, N., and Randelovic, B. S., 2020. The Importance of Renewable Energy Sources for Sustainable Development. Economics and Sustainable Development, 4(2): 15-24. https://doi.org/10.5937/esd2002016p

Ravi, A., Manoharan, P. S., and Anand, J. V., 2011. Modeling and Simulation of Three Phase Multilevel Inverter for Grid Connected Photovoltaic Systems, 85(11): 2811-2818. https://doi.org/10.1016/j.solener.2011.08.020

Reisi, A. R., Moradi, M. H., and Jamasb, S., 2013. Classification and Comparison of Maximum Power Point Tracking Techniques for Photovoltaic System: A review. Renewable and Sustainable Energy Reviews, 19(1): 433-443. https://doi.org/10.1016/j.rser.2012.11.052

Republic of Türkiye Ministry of Energy and Natural Resources, 2023. https://enerji.gov.tr/info-bank-investors-guide-for-electricity [accessed: 24.12.2023].

Roy, R. B., Rokonuzzaman, Md., Amin, N., Mishu, M. K., Alahakoon, S., Rahman, S., Mithulananthan, N., Rahman, K. S., Shakeri, M., and Pasupuleti, J., 2021. A Comparative Performance Analysis of ANN Algorithms for MPPT Energy Harvesting in Solar PV System. IEEE Access, 9(1): 102137-102152. https://doi.org/10.1109/ACCESS.2021.3096864

Salam, Z., Ahmed, J., and Merugu, B. S., 2013. The Application of Soft Computing Methods for MPPT of PV System: A Technological and Status Review. Applied Energy, 107(1): 135-148.
https://doi.org/10.1016/j.apenergy.2013.02.008

Sansaniwal, S. K., Sharma, V., and Mathur, J., 2018. Energy and Exergy Analyses of Various Typical Solar Energy Applications: A Comprehensive Review. Renewable and Sustainable Energy Reviews, 82(1): 1576-1601. https://doi.org/10.1016/j.rser.2017.07.003

Sarr, A., Soro, Y. M., Tossa, A. K., and Diop, L., 2023. Agrivoltaic, a Synergistic Co-Location of Agricultural and Energy Production in Perpetual Mutation: A Comprehensive Review. Solar Energy for Sustainable Agriculture, 11(3): 948-975.
https://doi.org/https://doi.org/10.1016/j.rser.2022.112125

Schonardie, M. F., Coelho, R. F., Schweitzer, R., and Martins, D. C., 2012. Control of the Active and Reactive Power Using dq0 Transformation in a Three-Phase Grid-Connected PV System. 2012 IEEE International Symposium on Industrial Electronics, Hangzhou, China.
https://doi.org/10.1109/ISIE.2012.6237095

Shahin, A., Hinaje, M., Martin, J. P., Pierfederici, S., and Rael, S., 2010. High Voltage Ratio DC-DC Converter for Fuel-Cell Applications, IEEE Transactions on Industrial Electronics 57(12): 3944-3955. https://doi.org/10.1109/TIE.2010.2045996

Shang, L., Guo, H., and Zhu, W., 2020. An Improved MPPT Control Strategy Based on Incremental Conductance Algorithm. Protection and Control of Modern Power Systems, 5(14): 1-8. https://doi.org/10.1186/s41601-020-00161-z

Singh, A. K., Hussain, I., and Singh, B., 2016. An Improved P&O MPPT Algorithm for Single Stage Three-Phase Grid Integrated Solar PV System. 2016 IEEE 7th Power India International Conference (PIICON), Bikaner, India. https://doi.org/10.1109/POWERI.2016.8077402

Stephen, A. A., Musasa, K., and Davidson, I. E., 2022. Modelling of Solar PV under Varying Condition with an Improved Incremental Conductance and Integral Regulator. ENERGIES, 15(1): 2405-2427. http://dx.doi.org/10.3390/en15072405

Suman, Sharma, P., and Goyal, P., 2020. Evolution of PV Technology from Conventional to Nano-Materials. International Conference on Aspects of Materials Science and Engineering, 28(3): 1593-1597. https://doi.org/10.1016/j.matpr.2020.04.846

Sun, D., Ge, B., Peng, F. Z., Haitham, A. R., Bi, D., and Liu, Y., 2012. A New Grid-Connected PV System Based on Cascaded H-Bridge Quasi-Z Source Inverter. 2012 IEEE International Symposium on Industrial Electronics, Hangzhou, China. https://doi.org/10.1109/ISIE.2012.6237218

Teke, A., 2011. Unified Power Quality Conditioner: Design, Simulation and Experimental Analysis. PhD Thesis, Çukurova University, Adana, pp. 226. 2008.

Triki, Y., Triki A., Bechouche A., Abdelslam, D. O., and Porumb, R., 2022. An Efficient Battery-Charging Algorithm with ANN Based MPPT Method for Off-Grid PV Systems. 2022 IEEE 21st International Conference on Sciences and Techniques of Automatic Control and Computer Engineering (STA), Sousse, Tunisia. https://doi.org/10.1109/STA56120.2022.10019093

Viswanatha, V., 2022. Closed Loop Control of Bidirectional Buck-Boost Converter for Battery Management in Automotive Systems. International Journal of Advanced Science and Technology, 29(10): 8568-8580.

Vo, T. T. E., Ko, H., Huh, J., and Park, N., 2021. Overview of Solar Energy for Aquaculture: The Potential and Future Trends. Energies, 14(21): 6923-6943. https://doi.org/10.3390/en14216923

Weldekidan, H., Strezov, V., and Town, G., 2018. Review of Solar Energy for Biofuel Extraction. Renewable and Sustainable Energy Reviews, 88(1):184-192. https://doi.org/10.1016/j.rser.2018.02.027

Wu, C., Wang K., Batmunkh, M., Bati, A. S. R., Yang, D., Jiang, Y., Hou Y., Shapter, J. G., and Priya, S., 2020. Multifunctional Nanostructured Materials for Next Generation Photovoltaics. Nano Energy, 70(1): 104480. https://doi.org/10.1016/j.nanoen.2020.104480

Xiao, B., Hang, L., and Tolbert, L. M., 2013. Control of Three-Phase Cascaded Voltage Source Inverter for Grid-Connected Photovoltaic Systems. 2013 28th Annual IEEE Applied Power Electronics Conference and Exposition (APEC), Long Beach, CA, USA. https://doi.org/10.1109/APEC.2013.6520223

Xu, J., and Han, K., 2016. The Single-Phase Inverter Design for Photovoltaic System. 2016 International Symposium on Computer, Consumer and Control (IS3C), Xi'an, China. https://doi.org/10.1109/IS3C.2016.95

Yu, N., Yang, J., Chen, S., and Ye M., 2014. Design of LCL-Filter Based Three-Level Active Power Filters. Indonesian Journal of Electrical Engineering, 12(1): 48-56. http://doi.org/10.11591/telkomnika.v12i1.3441

Zeb, K., Uddin, W., Khan, M. A., Ali, Zunaib., Ali, M. U., Christofides, N., and Kim, H. J., 2018. A Comprehensive Review on Inverter Topologies and Control Strategies for Grid Connected Photovoltaic System. Renewable and Sustainable Energy Reviews, 94(1): 1120-1141. https://doi.org/10.1016/j.rser.2018.06.053

Zebraoui, O., and Bouzi, M., 2020. Improved MPPT Controls for a Standalone PV/Wind/Battery Hybrid Energy System. International Jounal of Power Electronics and Drive System (IJPEDS), 11(22): 988-1001. http://doi.org/10.11591/ijpeds.v11.i2.pp988-1001

Zhang, Z., and Chau, K. T., 2017. Pulse-Width-Modulation-Based Electromagnetic Interference Mitigation of Bidirectional Grid-Connected Converters for Electric Vehicles. IEEE Transactions on Smart Grid, 8(6): 2803-2812. https://doi.org/10.1109/TSG.2016.2541163

CURRICULUM VITAE

Personal Information

Surname, Name : Güzey, Batuhan

Education

Degree	Institution	Graduation Year
Master	Çukurova University	2023
Undergraduate	Dokuz Eylül University	2020
High School		

Experience

Year	Workplace	Title
2022-Present	Sasa Polyester Sanayi A.Ş.	Maintenance Engineer
2021-2022	Temsa Skoda Sabancı A.Ş.	Purchasing Engineer